MASTER THESIS

ADDITIVE MANUFACTURING WITH FRICTION SURFACE CLADDING

Frederik H.J. Deunk

FACULTY OF ENGINEERING TECHNOLOGY
MECHANICAL ENGINEERING
CHAIR OF PRODUCTION TECHNOLOGY

EXAMINATION COMMITTEE
Prof. dr. ir. R. Akkerman
Dr. ir. T.C. Bor
Dr. ir. H.J.M. Geijselaers
L. Shaojie Lui, MSc

DOCUMENT NUMBER
CTW-PT – 15-1405

UNIVERSITY OF TWENTE.

27-08-2015

Author: F.H.J. Deunk

Supervision: dr. ir. T.C. Bor
L. Shaojie Liu, MSc

Faculty of Engineering Technology, Chair of production technology

Master Thesis, Univeristy of Twente, Enschede, the Netherlands
August 2015

Cover: Standardized format University of Twente

Summery

In the recent years the interest in Additive Manufacturing (AM), also known as 3D-printing, has grown. One of the challenges still remaining in the field of AM is the printing with aluminum. The Chair of Production Technology at the University of Twente (UTwente) is active in the research of Friction Surface Cladding (FSC). This solid state forming process is based on the metal joining technique of Friction Stir Welding (FSW), but uses it to clad a thin layer of pure aluminum. The research uses FSC as a start for AM. The research is split into three parts to answer the feasibility question of FSC for AM. The first part analyzes the cladding of commercially pure aluminum (AA1050) regarding multiple layers and different surface geometries. Thereafter cladding hard aluminum (AA2024-T351) on itself and the design of a continuous cladding tool are investigated.

The process of cladding a single layer of commercially pure aluminum on a hard aluminum substrate is extended to multiple cladding process. Layers of AA1050 are successfully clad in parallel and overlap configuration. With parallel cladding there is a small ridge detectable between two parallel layers, but this small ridge won't cause problems when overlapping cladding these parallel layers. The process has the possibility to cope with small irregular surface geometries, especially at high temperatures (>400 [°C]). Cladding over voids, previous layers and other irregularities is preferably on the advancing side of the new layer, because this side has less defects due to flow pattern. Cladding bigger irregularities is more problematic. The filling of the irregularities is worse and there is the risks of stopping the process by losing control of force and temperature. Higher temperature and supply rate reduce the amount of voids and risk of destabilizing, but increase the risk of intermixing between added layers and the substrate.

Multiple cladding of the hard AA2024 aluminum alloy is proven possible. A stable process window is found with a tool temperature of 400 [°C]. Within this window the layers are smooth, constant and regular. Multiple cladding with the hard AA2024 also produces good results, both for parallel and overlapping layers. The process results in a reduction in hardness of 15 to 30%. The hard aluminum is more demanding for the clad setup than the soft pure aluminum, this is clearly visible in the higher process forces during the cladding with the AA2024. The cladding rod can be heat treated to reduce the forces in the setup and increase the stability of the process. The heat treatment dissolves the participates in the rod, thus softening the clad material. An advantage of the cladding with AA2024 compared to the cladding with AA1050 is that no aluminum sticks to the cladding tool. The successful cladding of the hard A2024 alloy opens possibilities for other aluminums alloys, like the aluminum 2000, 6000 and 7000 series, which are researched for their FSW capabilities in other research.

The main challenge for AM with FSC is the design of a continuous cladding devise. The current friction surface cladding process is a single layer process. To apply the AM technique in industry, the process should be a continuous or a batch process. Based on experiments with different support block and transporting screws, the cladding behavior of the aluminum is analyzed. A simple 6 [mm] threaded bolt provides a well delivery mechanism, as it generates temperature, pressure and rotation. Pressure build-up and heat generation are well within the support block, but there is no bonding to the substrate. The use of hard AA6262-T9 aluminum in the tool instead of the soft aluminum generates more difficulties with the cladding pin and the pressure build-up.

The difficulties for the continues cladding process are just above substrate. Heat and movement of the aluminum are relative low at the cladding point, due to a stationary block edge and the heat generation in the support block. Suggested solutions are in moving the tool over the delivered material to finalize the clad layer, or a more complex support block with a rotating edge.

The conclusion of this research is that the use of FSC as an AM process appears promising. Multiple cladding is realized by parallel and overlap cladding, while it is also possible to fill and correct surface irregularities. The cladding of AA2024 on itself is stable and gives good results. The main challenge in using FSC for AM is in change from a single run experimental setup to a continuous AM process.

Table of Contents

1 Introduction

The chapter introduces the proposed Additive Manufacturing (AM) process. The chapter starts with an introduction of the technique and the setup of the report. After the introduction the research question is proposed and explained. The chapter ends with a review of the current state of research at the university and the test setup in Hengelo.

1.1 The additive manufacturing process

In the recent years the interest in Additive Manufacturing (AM), better known as 3D-printing, has grown. AM works well with various production processes, such as metal powder sintering, sand-casting and polymer techniques[2]. This research explores a new technique of AM based on a solid state forming technique. The Chair of Production Technology at the University of Twente (UTwente) is active in the research of Friction Surface Cladding (FSC).

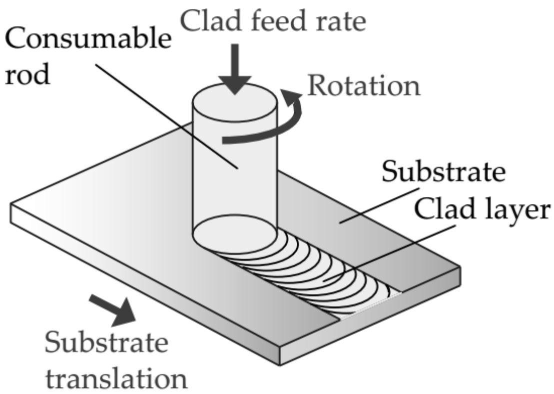

Figure 1.1: Schematic friction surfacing process, the figure is from the research of van der Stelt[1].

FSC is a friction surfacing (FS) technique with the adding of a tool around the consumable rod for a better controlled process. FS is developed based on friction stir welding (FSW) and intends to clad a thin layer on a substrate. The principle of FS is shown in figure 1.1. Heat is generated by moving a consumable cladding rod with a certain rotation speed over a substrate-plate. This heat in combination with pressure and deformation produces a small clad layer. The aim of this research is to test if the process of FSC is feasible for AM.

The technique has two interesting properties for AM. First the material supply rate is relatively high compared to other additive manufacturing techniques. Secondly the material does not melt, thus the process has less thermal influence on the substrate and feed material. The process enables the modification and strengthening of otherwise flat plates, without TIG-welding joining dis-advantages[3], while has much less material waste than a traditional removal based approach. The process would enable an AM printing method with the relative hard 2000, 6000 and 7000 aluminum series. Researchers are investigating comparable techniques, with various materials[4], but not with aluminum. The current cladding set-up at the UTwente uses a high strength aluminum (AA2024-T351) as substrate material and clad a layer of ductile commercially pure aluminum (AA1050) on top.

The research is split into three sections. The first section is an experimental research on the AA1050 AM process. This parts builds further on the work of van der Stelt[1]. Multiple cladding and irregular surface experiments are combined with literature research for an insight of the feasibility of the technique. The second section reviews the FSC process with AA2024 as clad material, the same material as the substrate. As the process is new, it extrapolates from the known AA1050 FSC process. The third part of the report aims to design a new printing head for the 3D printing process. The current process is based on an experimental setup with a preparation time of about one hour, hence the process is unpractical for industrial production. The design is based on the current experiences combined with literature. It will aim to develop a proof of principle and give suggestions for further development.

1.2 Research question

The feasibility research of the AM method is approached with a main research question with three sub questions. The research builds on the PhD research of van der Stelt[1], the cladding of a single layer AA1050 on a AA2024 substrate. If single cladding is possible, multiple cladding for AM should also be possible. This has resulted in the following research question:

Is it feasible to use friction surface cladding as an additive manufacturing process with aluminum?

To answers this question, the question is split into 3 sub-questions. Each section reviews a different part for the AM method.

What are the influencing factors when building layers with FSC?
The first question is based on the relatively known cladding of AA1050 on an AA2024 substrate. The known stable process window is further reviewed with new features. First parallel and overlapping layers are clad to test the cladding of multiple connecting layers. Secondly different surface irregularities are reviewed for the process, for an insight in the stability when printing patterns.

Is it possible to clad AA2024 on a substrate of AA2024?
The process of cladding AA2024 on AA2024 is new and a stable process window is sought in this section. The influencing factors on the process are reviewed. Based on these first results the parallel and overlap cladding of layers is tested.

How can the FSC process be changed into a (semi-) continuous process?
The current friction surface cladding process is a single strip process. For industrial process the AM method needs a continuous or batch process. A first tool design is produced and reviewed by experiments and modeling. These are compared for a better insight in the design and to retrieve guidelines for further development.

1.3 State of research

The FSC cladding process is developed at the University of Twente with the support of M2i, NLR and Fokker Aerostructures. Research started with the PhD research of van der Stelt[1] and is currently followed up by Shaojie Liu MSc., under the supervision of dr. ir. Bor. The technique of friction surfacing (FS) is based on the FSW solid state welding process. A combination of stretch, heat and pressure creates a solid state bond, at relative low temperatures. The FSW process applies a rotating pin to generate heat and mix the material together. The FS process rotates a consumable rod on top of a substrate. The rotating rod delivers the material, adds pressure and generates the heat[4].

The addition of the FSC to FS is a cladding tool, see figure 1.2. The tool improves the stability and smoothness of the process, by regulating the pressure and preventing the forming of a revolving flash formation around the supply rod. The flash formation is a problems in FS techniques[4] without at tool. The tool furthermore enables better control of the thickness and monitoring of the temperature in a constant way near the substrate surface. In the research commercially pure aluminum (AA1050) is selected as clad material and hard aluminum (AA2024-T351) as substrate material. The AA1050 is relative easily deformed and corrosion resistant, while the AA2024 is relative strong and corrosion-sensitive.

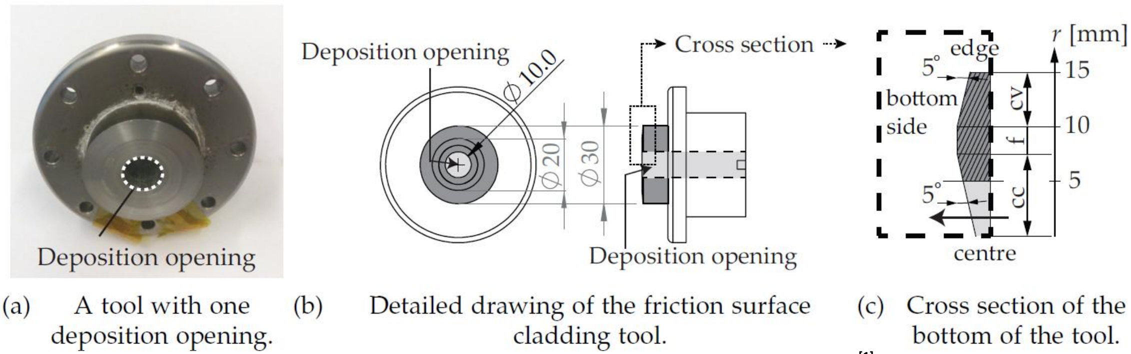

Figure 1.2: Schematic view of the cladding process, the figure is from the research of van der Stelt[1].

By rotating the tool while pressing a consumable rod against the substrate three requirements for the process are fulfilled: sufficient deformations, pressure and heat at the interface for the cladding process. The temperature is correlated to the rotation speed, so the required speed is determined by the heat demand. A difficulty is the self reinforcing effect in the heat generation process. More heat creates a wider clad layer, so the friction area increases, thus increasing the heat generation. The current results suggest a measured cladding tool temperature between 200 [°C] and 400 [°C]. Temperature has a major effect on the process and the results. A higher temperature results in a more viscous supply material, thus lowering forces and pressure. However, material properties degrade though the higher temperature by dissolving of the participates in the AA2024, which decreases the hardness[5] of the substrate.

Generally a lower temperature is better for the material properties. A risk with high temperatures and especially combined with high forces is intermixing. Intermixing is unwanted for the cladding, but there is no principle problem for additive manufacturing. A lager tool-force creates a thicker intermixing layer. It is furthermore suggested that the risk of aluminum sticking to the tool is smaller at a lower temperatures. However, lower temperatures result in less reduction of the yield strength, which increases the forces required for the process, thus creating a lower limit for the temperature. The process of FSC is capable of producing thin clad layers, with a thickness of 0.2 up to 0.8 [mm] and a clad feed rate of about 250 [mm^3/min]. Contact between the cladding-tool and the substrate material should be avoided, as contact creates further intermixing.

1.3.1 Experimental setup

The experiments are preformed at the test facility in Hengelo. A modified planer machine is used for the friction surface cladding process, see figure 1.3. For the rotating movement of the FSC process a 13 [kW] Siemens electromotor is used. The motor allows for rotation speeds Ω between 300 and 1500 [rpm]. The motor is fixed in all directions and the table with the substrate moves under the motor. The translation speed of the substrate while cladding is from 0 up to 500 [mm/min].

Figure 1.3: The modified planer machine for friction surface cladding[1].

The cladding process is performed with a supply rod in a cladding tool. The tool has a Ø10 [mm] center hole in the middle and slopes forward with an angle of 5° to Ø15 [mm]. From Ø15 to Ø20 [mm] the bottom surface of the tool is flat, while the tool slopes backwards with a angle of 5° from Ø20 to Ø30 [mm], as shown in figure 1.2. To monitor the process a thermocouples is placed inside the tool. The maximal normal force F_t of the tool is 50 [kN] and the tilt angle ϕ can be varied between -10° and 10°.

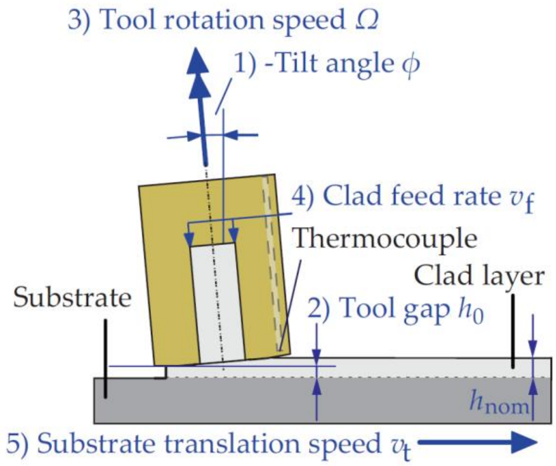

Figure 1.4: Schematic of the cladding tool and the parameters for the experiments[1].

A substrate plate is mounted on the planer table under the FSC tool and is fixed with clamps and three M13 holes. The substrate is an AA2024 plate of 181 [mm] wide, 300 [mm] long and 4 [mm] thick. Five K-type thermocouples are inserted along the length direction of the substrate, with a distance of 40 [mm] between each other. The first thermocouple is located 45 [mm] from the substrate edge with a depth of 16 [mm]. The cladding process starts at this point. The other thermocouples are placed at regular distance of 40 [mm], also under the center of the cladding layer. Specifications of the substrate plate are in Appendix A. Before the cladding process starts the substrate plate is grinded with sand paper and cleaned with ethanol.

Table 1.1 - Reference parameters for the experiments.

Reference parameters		
Tilt angle	ϕ	1 [°]
Tool rotation speed	Ω	300 [rpm]
Tool gap	h_0	0.2 [mm]
Clad feed rate	v_f	3.0 [mm/min]
Substrate translation speed	v_t	60 [mm/min]

During the cladding process there are five main parameters to control, shown in figure 1.4. The reference setup of these parameters is shown in table 1.1. The tilt angle ϕ influences the smoothness and pressure distribution in the clad layer. The angle is set constant at 1[°]. The tool gap h_0 influences the layer thickness and the force required, typically it is set between 0.1 and 0.4 [mm]. The tool rotation speed Ω contributes to the clad material being spread, the required stretch and the heat generation. The Ω is typically between 300 and 600 [rpm]. The clad feed rate v_f and substrate translation speed v_t control the material delivery. The v_f controlled indirectly by the pumping speed of the hydraulic pressure pump and is set to be around 3.0 [mm/min]. The v_t is controlled by the planer machine and is adjusted directly. All the experiments start with a substrate translation speed of 60 [mm/min].

2 Analysis of the additive process: AA1050 on AA2024

The current setup with AA1050 as clad material is the basis for a first investigation of the possibility to use FSC as an AM process. The concept of AM is reviewed with multi-cladding attempts, combined with various types of holes and surface irregularities. The chapter starts with an introduction about literature and earlier research, followed by the experimental setup. The setup is reviewed in the third part, which is followed by the conclusion.

2.1 Introduction

To start the research of AM with AA1050 the FSC process is introduced. The topic of FS is researched in many places around the world with various metals, the use of a tool is rare. The research focuses on the material properties after the FSW or FS process. The effect of temperature and other process variables are extensively reviewed in papers[6-9]. The influence of surface irregularities to the process are unknown. Furthermore a previous experiment is shown as a reference experiment for single layer cladding with AA1050 on AA2024.

2.1.1 Relation between grain structure, hardness and strength

The heat influence on the micro structure of the substrate is described by various researchers, both for AA2024 and AA1050. The research of Jones et al[6] about the relation between the microstructure and micro-hardness in a friction stir welded 2024 aluminum alloy describes the hardness pattern in the AA2024 substrate. The center of the weld has a very fine equiaxed grain size. Just under weld zone, the AA2024 has over aged or dissolved participates, while the grain structure has been coarsened. The region next to the over aged precipitates has less aged small precipitates and less or no coarsening. The most outer region of the heat affected zone has not much coarsening, but there is some dissolution of the precipitates due to the lower cooling rate farther from the tool. Regarding the cladding of AA1050 the research of Yadav et al.[7] reviews the microstructure of clad pure aluminum. The effect of the process is a strong grain refinement in the weld zone, from roughly 84 [µm] to 3 [µm] grains. The yield strength improved due to the grain refinement. The ductility of the clad material remained comparable to before the processing.

The change in grain structure and precipitates has a major influence on the hardness of the aluminum. The effect of the different micro structures on hardness is reviewed by Khodir et. al[8] and Genevois et al[9]. The hardness of the weld zone remained nearly the same as base material. In the heat affected zone just next to the weld with the over aged participates the hardness is at its low point. Even with the best test result this still meant a decrease of 10% of the hardness compared to the base material. The region with the less aged precipitates has a hardness close to the base material. The outer region of the heat affected zone with the dissolved precipices has a drop in hardness again. Furthermore it is noted that higher and longer peak temperatures and a gradual cooling all contributed to a lower hardness.

The correlation between the hardness and yield strength of a material is recognized by Khodir[8]. The material with the highest hardness, also has the best yield strength and vice versa. The relationship between hardness and tensile strength is further described by Zhang et al[10], in his research about the general relationship between strength and hardness. The empirical relationship is known in work-hardened metals and bulk metal glasses. With ultra fine or coarse metals there are some irregularities in this relation, but the trend remains. The use of this relation for aluminum 7010 is further researched by Tiryakioglu et al.[11]. In his research a 0.383 factor plus a constant relates the hardness to the maximum yield stress. A 0.247 factor relationship plus a constant is determined between the hardness and the tensile strength.

2.1.2 Reference experiment

The result of a successful experiment will serve as a reference for this research. The parameters of this experiment are a benchmark for the multiple cladding experiments and are shown in table 2.1.

Table 2.1: Settings and results of reference experiment 0.

Parameters			**Results**		Median	Maximum
Tilt angle	[°]	1	Temperature	[°C]	310	330
Tool rotation speed	[rpm]	300	Force pump	[kN]	9	6
Tool gap	[mm]	0.2	Force tool	[kN]	9	4
Clad feed rate	[mm/min]	3.1	Hardness in clad layer	[HV]	28	35
Substrate translation speed	[mm/min]	60	Hardness in substrate	[HV]	123	144

The result of the reference experiment is shown in table 2.1 and fig 2.1. The clad layer is smooth and has a constant width. The temperature during the cladding is just under 300 [°C] in the cladding tool. The tool force is around 4 [kN] after an peak of 9 [kN]. In figure 2.1 an influence of the process parameters is visible. Due to the rotating of the tool and the tool angle a distinctive surface pattern occurs. The upper side is called the retreating side (RS), the bottom side is called the advancing side (AS). The RS has more problems with the layer smoothness at the edge. The side shows traces of the small fluctuations in material supply. The internal and external flow patterns of FSW materials are explained by Krishan et al[12].

The process heat influences the hardness. This is shown in figure 2.2 and 2.3. The harness of the clad layer is about 28 [HV], ~40% of the starting value. The hardness just under the cladding layer (zone A) is decreased by ~15% to 123 [HV]. At the bottom of the substrate and to the side of the clad layer (zone B) the hardness remained roughly constant at 135 [HV]. The second hardness dip (125 [HV]) described by Khodir[8] is in zone C, while zone D (~140 [HV]) is unaffected by the clad process.

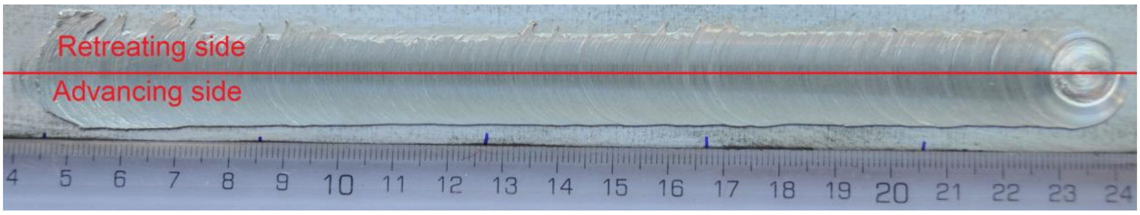

Figure 2.1: Result of the single clad layer.

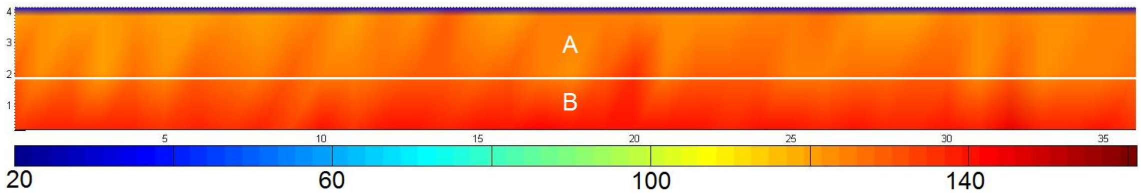

Figure 2.2: A hardness profile in [HV] alongside the red line in figure 2.1.

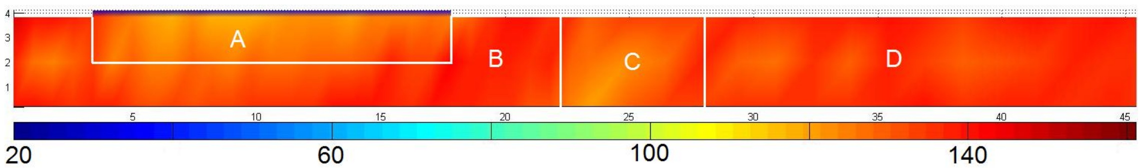

Figure 2.3: A hardness profile in [HV] perpendicular to the red line in figure 2.1.

2.2 Experimental setup

For a better understanding of the cladding behavior of AA1050 on AA2024 different cladding configurations with overlap and irregularities are tested. The cladding of a single layer is demonstrated in chapter 2.1.2. The planned multiple and irregular surface cladding experiments are explained in this chapter. The testing of the cladding behavior is divided into two series, with the second series designed based on the results of the first series. The first series consist of five experiments, while the second series consists of three.

2.2.1 Series 1

The experiment starts with two multiple cladding experiments. These are followed by three experiments over surface irregularities. All experiments are described and have a schematic view to further explain the setup.

Experiment 1.1

The first experiment is an overlap cladding experiment. Two layers of AA1050 are clad on top of each other, as shown in figure 2.4. The experiment uses the reference settings and standard substrate plate. The aim is to test the possibility of stapling layers with AA1050.

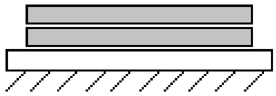

Figure 2.4: Schematic view of experiment 1.1.

Experiment 1.2

The second test for AM are parallel clad layers, as depicted in figure 2.5. The second clad layer is partially in overlap with the first clad layer to have a continuous bond. This overlap is at the retreating side of the fist layer, to cover the rough edge of the first layer. The substrate plate has an increased width of 181 [mm] to facilitate the second clad layer.

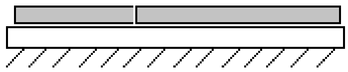

Figure 2.5: Schematic view of experiment 1.2.

Experiment 1.3

Experiment three is designed to simulate the cladding between two layers. A 0.5 [mm] lowered trench is milled in the substrate plate. The trench starts with a width of 8 [mm], and widens to 10 and 12 [mm], as shown in figure 2.6. As more material and heat is required due to the trench, the clad feed rate and subsequent rotation speed are increased. The aim of the experiment is to completely fill the trench.

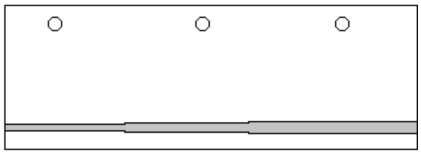

Figure 2.6: Schematic view of the substrate plate of experiment 1.3. The grey part is lowered 0.5 [mm] and widens from 8 to 10 to 12 [mm].

Experiment 1.4

Experiment four simulates the over-cladding of half a layer by a small ridge in the middle of the cladding layer. The ridge is produced by milling the top surface of the substrate 0.1, 0.2 and 0.3 [mm] down, as shown in figure 2.7. The clad feed rate and rotation speed are increased to compensate for the higher material demand. A successful experiment has a smooth cover with no voids at the edges.

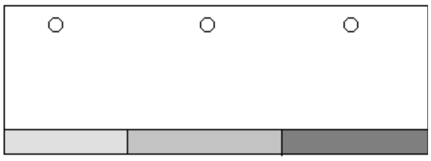

Figure 2.7: Schematic view of the substrate of experiment 1.4. The darker grey the part, the more section is lowered relative to the plate.

Experiment 1.5

The last experiment tests the behavior of a cladding layer over a series of holes. The experiment tests the filling of a hollow structure. The experiment uses four holes of Ø 5 [mm] through the plate. Three of these four holes have an lowered outer ring with of Ø 10 [mm] with a depth of 0.5, 1.0 and 1.5 [mm]. The aim is to fill the holes entirely without any void or defects to the top of the clad layer.

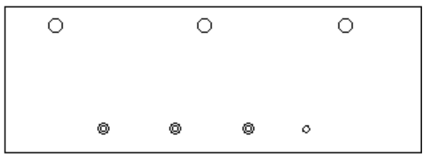

Figure 2.8: Schematic view of the substrate plate of experiment 1.5.

2.2.2 Series 2

The second series of tests is an update of the first series. In the first series of experiments the surface irregularities proved challenging, especially in experiment 1.3 and 1.5. The descriptions are in section 1.3.3 and 1.3.5. To improve the results and understanding of the process, experiments 1.3 and 1.5 are re-examined with a tweaked setup.

Experiment 1.3-a

Experiment 1.3-a re-examines the cladding in a trench. The trench is only lowered 0.2 [mm] instead of the 0.5 [mm] in experiment 1.3. The process starts with a normal flat substrate. After 30 [mm] a trench of 2 [mm] wide and 0.2 [mm] deep starts. This trench is widened 2 [mm] each 30 [mm], to a final with of 12 [mm], as shown in figure 2.9. The flat start-up place is to develop a stable startup. The widening will show the influence of the width of the trench on the filling.

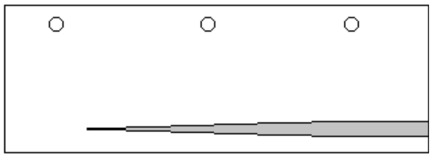

Figure 2.9: Schematic view of the substrate of experiment 1.3-a. The grey part is lowered 0.2 [mm].

Experiment 1.3-b

The second variation based on experiment 1.3 is the opposite of the previous experiment. The experiment starts in a trench wider than a clad layer and the trench contracts 2 [mm] every 30 [mm] in the cladding direction, as shown in figure 2.10. The trench begins with a width of 20 [mm] and contracts to 10 [mm]. This shrinking is to review the same effect as in experiment 1.3-a, but from the opposite side.

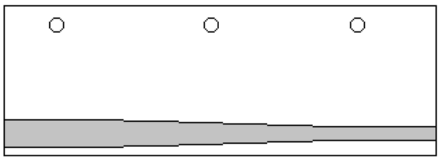

Figure 2.10: Schematic view of the substrate experiment 1.3-b. The grey part is lowered 0.2 [mm].

Experiment 1.5-a

Experiment 1.5-a tests the process stability of cladding small holes and their filling. The previous experiment 1.5 has rather big holes and only two are partially filled. The diameters of the holes increase from Ø 1 [mm] to Ø 4.5 [mm], with steps of 0.5 [mm]. The holes are 20 [mm] away from each other. The aim is to evaluate the filling of the holes.

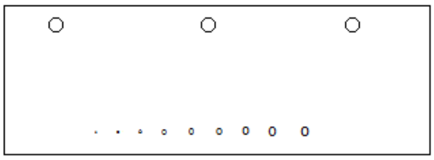

Figure 2.11: Schematic view of the substrate of experiment 1. 5-b.

Review of the experiments

To review the experiments, the temperature in the tool and the substrate, the pressing force and the normal force are recorded. The clad substrates are stored at room temperature for more than two weeks to allow for ageing. The samples are picked afterwards for further analysis like microstructure observation and hardness measurement. All the picked samples are grinded with silicon paper up to grade 4000, polished to 1 [µm] and etched with 50% NaOH at 70 [°C] for 20-30 [s].

2.3 Results and discussion

The results of the experiments described in section 2.2 are reviewed and discussed with respect to AM in this section. A review starts with the pre-experiment settings of each experiment, followed by a description of the process result. Finally, cross sections are reviewed for grain structure and hardness. All the data is available in Appendix C-J.

2.3.1 Experiment 1.1

The first experiment is the multiple cladding of one layer on top of another. Both layers are reviewed separately. The results of the first layer are shown in table 2.2 and figure 2.12 and of the second in table 2.3 and figure 16. The first layers starts with the same settings as the reference experiment. Due to the increasing force and temperature at the start, the substrate translation speed is increased to 80 [mm/min] early in the process.

Table 2.2: Settings and results of experiment 1, first layer.

Parameters			Results		Median	Maximum
Tilt angle	[°]	1	Temperature	[°C]	300	390
Tool rotation speed	[rpm]	300	Pump force	[kN]	19	19
Tool gap	[mm]	0.2	Tool force	[kN]	4.5	11
Clad feed rate	[mm/min]	0.9	Hardness in clad layer	[HV]	30	32
Substrate translation speed	[mm/min]	60->80	Hardness in substrate	[HV]	105	144

Figure 2.12: The first layer of experiment 1.1.

The first cladding strip shows an irregular performance, as shown in figure 15. The tool temperature is around 300° [C], with a peak temperature of nearly 400° [C] at the start and end of the process. The tool force settles around 5 [kN], after a peak of 10 [kN]. The pump force is much higher, nearly 20 [kN]. The irregular clad pattern in figure 2.12 indicates a lack of material supply as the low feed rate shows in table 2.2. The clad feed rate is much lower than in the reference experiment. The substrate is partially covered with a clad layer, so the result is usable for a multiple cladding experiment.

In the second experiment the substrate translation speed remains at 60 [mm/min] and the tool rotation speed stays at the 300 [rpm]. The tool is placed 0.4 [mm] above the plate, thus 0.2 [mm] above the previous clad layer. To compensate for the lack of material in first layer, the feed rate of the clad material is increased for a more stable process.

Table 2.3: Settings and results of experiment 1, second layer.

Parameters			Results		Median	Maximum
Tilt angle	[°]	1	Tool temperature	[°C]	350	420
Tool rotation speed	[rpm]	300	Pump force	[kN]	9	7
Tool gap	[mm]	0.2+0.2	Tool force	[kN]	10	5
Clad feed rate	[mm/min]	4.6	Hardness in clad layer	[HV]	30	32
Substrate translation speed	[mm/min]	60	Hardness in substrate	[HV]	105	144

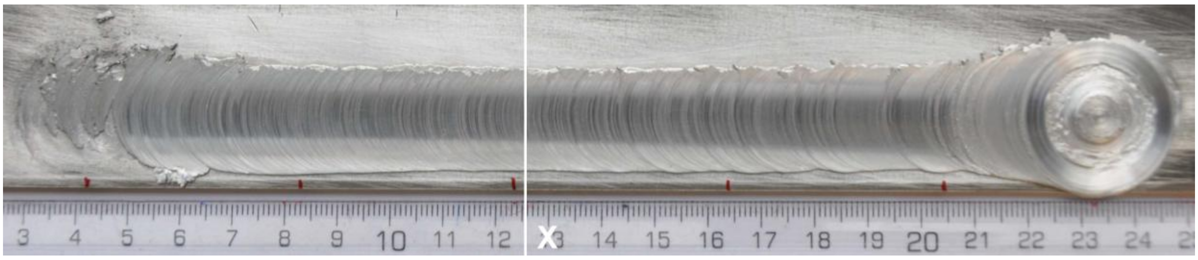

Figure 2.13 : The second row of experiment 1.1, the white line X indicates the place of the cross section.

The second layer of the multiple cladding experiment results in a smooth layer, visible in figure 2.13. The tool force starts with a short peak of 10 [kN], but decreases to a stable force around 5 [kN]. The pump force is around 7 [kN]. The temperature begins at 300 [°C] and gradually increased to over 400 [°C]. The higher temperature of 400 [°C] produces a smooth layer, but will further decrease the hardness of the substrate material.

The regular cladding of second clad layer over the first layer is a positive indication for AM. The second layer covers the first layer entirely and there is a good connection between the two layers, as shown in figure 2.13 and 2.14. The border between the two layers is only visible at the left side of the clad layer in figure 2.14. So, not only does the second layer cover the first one, the second layer even repairs the irregularities of the first layer.

Figure 2.14 : The cross section of experiment 1.1, a layer of AA1050 on the AA2024 substrate, taken at line X of figure 2.13.

The hardness profile of at the cross section is shown in figure 2.15. The hardness of the clad material, is around 30 [HV], which is comparable to the hardness of the single reference clad layer. The hardness of the substrate just under the cladding layer (A) is lower compared to the reference. The lowest hardness is just above the 100 [HV], which is lower than the 123 [HV] of the reference experiment. This is probably due to the repeated heating and the higher peak temperature. The influence of a higher peak is already noted by van der Stelt[1], while the influence of the repeated heating is mentioned by Genevois[9]. The rest of the hardness profile shows the expected values. In zone B the hardness increases to nearly full hardness (135 [HV]), zone C has a dip in hardness (110 [HV]) and in zone D the hardness is at the basis value (~140 [HV]).

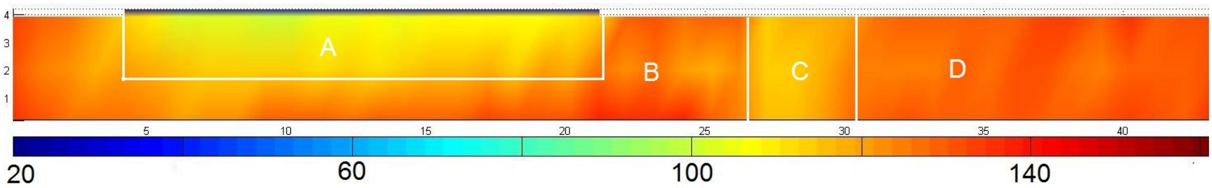

Figure 2.15: The hardness in [HV] of experiment 1.1, taken at line X of figure 2.13.

2.3.2 Experiment 1.2

The second experiment is the cladding of two parallel layers. To accommodate the second layer the substrate plate is prepared with a width of 181 [mm] instead of 141 [mm]. The first layer is clad close to the edge of the substrate, on top of the thermocouples. The second layer is clad next to the first, partially covering the rough retreating side of the first clad layer. The settings are the same as those in the second attempt of experiment 1.1. The first experiment starts with a substrate translation speed 60 [mm/min], which is increased to 70 [mm/min] after a quarter of the process.

Table 2.4: Settings and results of experiment 1.2, first layer.

Parameters			**Results**		Median	Maximum
Tilt angle	[°]	1	Tool temperature	[°C]	400	410
Tool rotation speed	[rpm]	300	Pump force	[kN]	8	17
Tool gap	[mm]	0.2	Tool force	[kN]	8	10
Clad feed rate	[mm/min]	4.1	Hardness in clad layer	[HV]	26	28
Substrate translation speed	[mm/min]	60->70	Hardness in substrate	[HV]	83	144

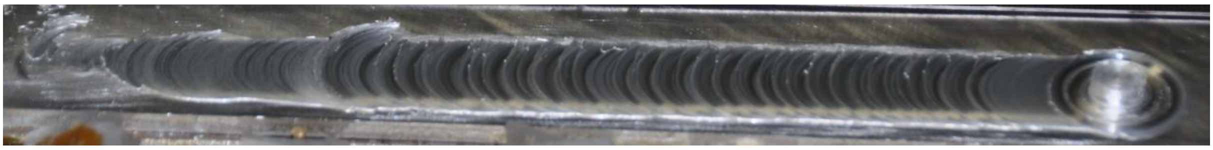

Figure 2.16 : Picture of first layer of experiment 1.2.

The first cladding run produced a constant layer over most of the clad layer length, see figure 2.16. The process has a low temperature at the start of process. This low temperature explains the irregularities and force build-up at the start of the process. The increase of translation speed is to prevent surplus of clad material and force build-up. Thereafter the process ran smoothly with a temperature around 400 [°C] in the tool. The normal force is about 8 [kN], while the pump force gradually goes down to 6 [kN], after a peak of 16 [kN].

Table 2.5: Settings and results of experiment 1.2, second layer.

Parameters			**Results**		Median	Maximum
Tilt angle	[°]	1	Tool temperature	[°C]	400	410
Tool rotation speed	[rpm]	300	Pump force	[kN]	7	14
Tool gap	[mm]	0.2	Tool force	[kN]	5	9
Clad feed rate	[mm/min]	4.6	Hardness in clad layer	[HV]	30	34
Substrate translation speed	[mm/min]	60	Hardness in substrate	[HV]	98	144

The performance of the second layer is shown in figure 2.17. The process is stable and produces a constant and smooth layer. The second clad process has about the same tool temperature as the first experiment. The temperature measured by the thermocouples in the substrate plate is lower, due to the layer distance to the thermocouples. The tool force drops to 5 [kN] after a peak of 8 [kN]. The pump force settles at 7 [kN] after a top of 14 [kN].

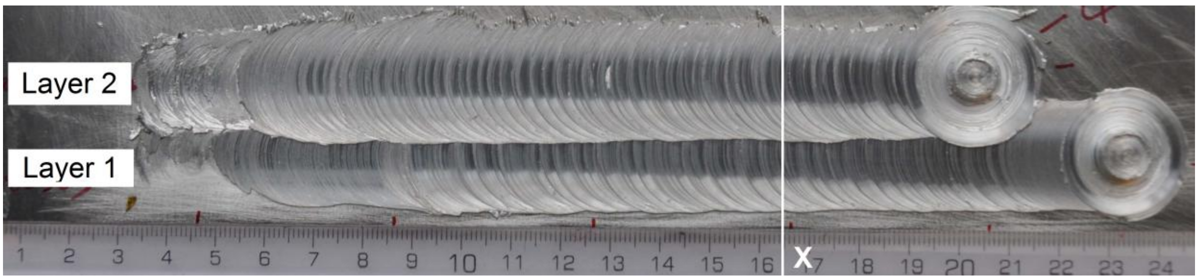

Figure 2.17: First and second row experiment 1.2, the white line X indicates the place of the cross section.

The result shown in figure 2.17 and 2.18 are positive for AM. The two clad layers have a stable overlap without voids. There is a small border edge detectable between the layers, but the cover is complete. The process parameters of the second clad layer are not much influenced by the first layer. The cross section in figure 2.18 does not have distinguishable traces of a boundary between the first and second clad layer, except for the clear height difference between the layers.

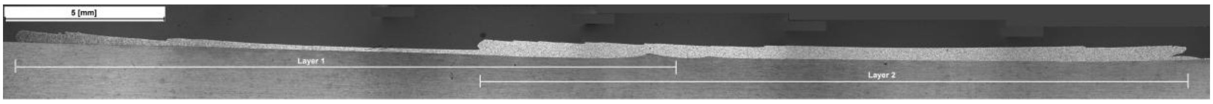

Figure 2.18 : The cross section of experiment 1.2, two parallel layers of AA1050 on AA2024, made at line X in figure 2.16.

The hardness measurement of the cross section in figure 2.19 shows relative worse results compared to the reference experiment. A substrate hardness of 81 [HV] is measured under the first layer (A), a 44% hardness drop. The hardness of the clad layer is 28 [HV]. The hardness under the second clad layer (B) is between 90 and 100 [HV], still a strong reduction compared to the reference experiment. In zone C the hardness starts to increase again to ~120 [HV]. The relative low hardness is due to the high temperature during the cladding. Furthermore, the second clad process appears to further decrease the hardness under the first clad layer. This is in line with the hardness profile of Khodir[8].

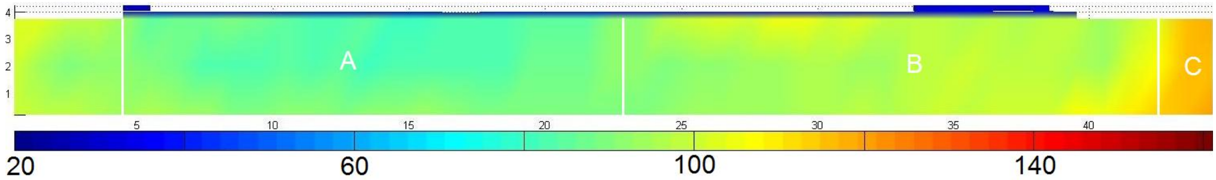

Figure 2.19: The hardness in [HV] of experiment 1.2, made at the line X in figure 2.16.

2.3.3 Experiment 1.3

Experiment 1.3 has a lowered trench with a depth of 0.5 [mm] in the substrate. The width of the trench increases in two steps from 8 [mm] to 12 [mm]. The third experiment is performed in two attempts, due to startup problems. The first attempt used the standard parameters, including the cladding speed of 60 [mm/min] and a clad feed rate of 4.5 [mm/min]. The pre-experiment settings are in table 2.6.

Table 2.6: Settings and results of experiment 3, first attempt.

Parameters			**Results**		Median	Maximum
Tilt angle	[°]	1	Tool temperature	[°C]	180	240
Tool rotation speed	[rpm]	300	Pump force	[kN]	8	18
Tool gap	[mm]	0.2	Tool force	[kN]	5	8
Clad feed rate	[mm/min]	4.5	Hardness in clad layer	[HV]	58	60
Substrate translation speed	[mm/min]	60	Hardness in substrate	[HV]	130	144

The clad layer only partially filled the trench and is stopped before the end of the trench. Shortage of clad material prevented enough heat build-up. The tool temperature has a peak of 240 [°C], but never stabilizes above 200 [°C]. This resulted in high pump forces (18 [kN]), hence the process is stopped several times. The partial filled trench is showed at the left side of the red line in figure 2.20.

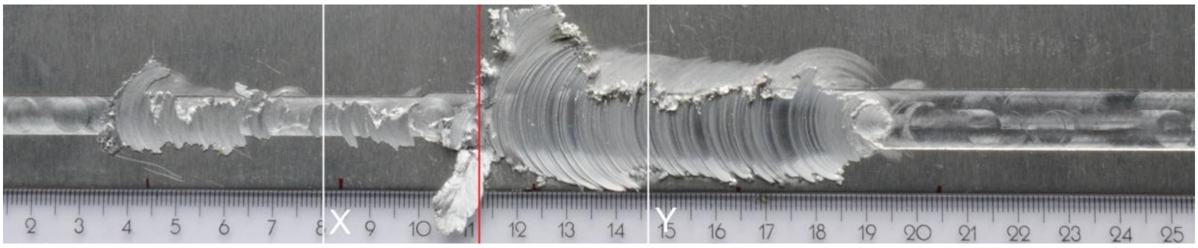

Figure 2.20: First and second cladding attempt for experiment 1.3, the red line divides the two attempts. The lines X and Y indicate the places of the cross sections and hardness measurements.

Figure 2.21 and 2.22 show the microstructure and hardness profile at cross section line X in figure 2.20. The trench is only partially filled, but no voids are visible. The hardness is well compared to other experiments, a hardness of 58 [HV] in the cladding layer and a minimum of 130 [HV] in the substrate. This is only 10 % under the original hardness and the best results yet. These results are comparable with the best FSW results of Khodir[8]. It is probable that even lower temperatures and higher forces could result in better material properties, a trend recognized by van de Stelt[1].

Figure 2.21: The cross section of experiment 1.3, first attempt, perpendicular to the cladding direction, made at line X.

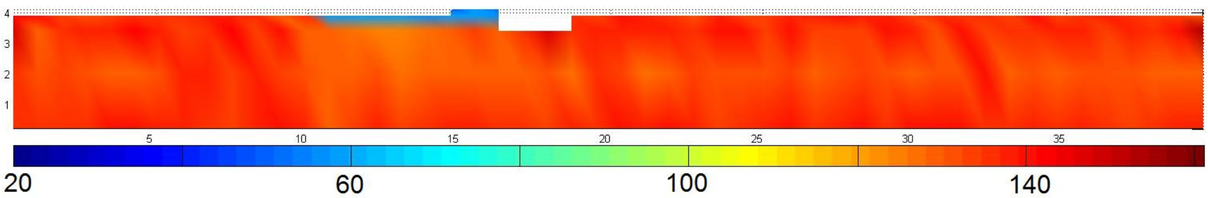

Figure 2.22: The hardness in [HV] of experiment 1.3, first attempt, perpendicular to the cladding direction, made at line X.

The substrate is reused for a second experiment, as it is only partially clad. In the second experiment the cladding speed is reduced and the rotation speed is increased. Thereby the temperature is higher and there is more supply material per length of the clad layer. The settings are shown in table 2.7.

Table 2.7: Settings and results of experiment 3, second attempt.

Parameters			Results		Median	Maximum
Tilt angle	[°]	1	Tool temperature	[°C]	400	410
Tool rotation speed	[rpm]	450	Pump force	[kN]	8	11
Tool gap	[mm]	0.2	Tool force	[kN]	7	9
Clad feed rate	[mm/min]	5.1	Hardness in clad layer	[HV]	38	35
Substrate translation speed	[mm/min]	30	Hardness in substrate	[HV]	95	144

The second attempt fills the trench with more clad material than the first attempt, as visible in figure 2.20. The adjusted settings result in a lower pump force and more material to fill the trench. The material flow is excessive, especially at the start of the process. The peak pump force is 11 [kN] and the peak tool temperature is 410 [°C]. Figure 2.24 shows the hardness profile of the second cladding attempt. The hardness is 35 [HV] in the clad layer and 100 [HV] under the clad layer in substrate (A). To the right (B) the hardness increases again up to 135 [HV] and the second smaller drop in hardness is in zone C (~120[HV]).

A problem for AM manufacturing is shown by cross-section depicted in figure 2.23. There is a void (L) hidden under the right side of the clad layer. The void is not directly visible from the top view of the clad layer in figure 2.20, so there is a risk of hidden voids when filling lager irregularities. At the left side of figure 2.23 the edge (K) of the substrate has intermixed with the clad layer. The sharp corner visible in figure 2.21 is not visible in figure 2.23. Intermixing is in unwanted for cladding, but allowable for AM.

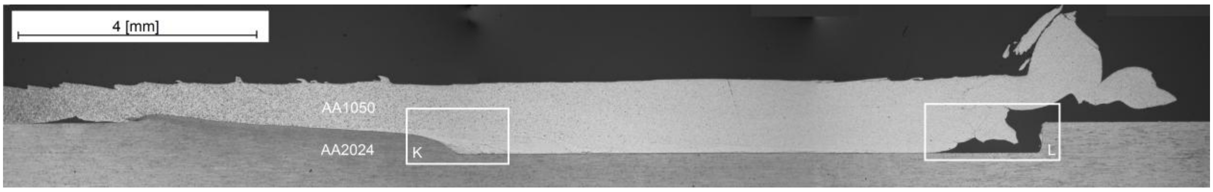

Figure 2.23: The cross section of experiment 1.3, second attempt, taken at the line Y in figure 2.19.

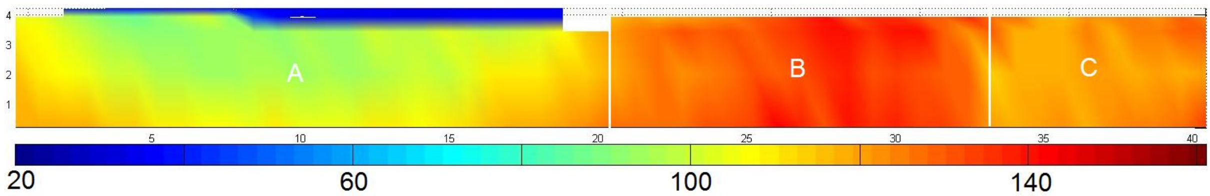

Figure 2.24: The hardness in [HV] of experiment 1.3, second attempt, taken at line Y in figure 2.19.

2.3.4 Experiment 1.4

Experiment 1.4 is the cladding over a small edge. The edge is located in the middle of the clad layer and is created by milling one side of the substrate 0.1, 0.2 and 0.3 [mm] lower. The tool gap of 0.2 [mm] is relative to the base level of the substrate, so the lowered side has a 0.3, 0.4 and 0.5 [mm] tool gap. The setup uses a higher clad feet rate to accommodate the edge. The rotation speed is raised to facilitate extra heat generation to ensure a stable process.

Table 2.8: Settings and results of experiment 1.4, second attempt.

Parameters			**Results**		Median	Maximum
Tilt angle	[°]	1	Tool temperature	[°C]	320	360
Tool rotation speed	[rpm]	450	Pump force	[kN]	5	8
Tool gap	[mm]	0.2	Tool force	[kN]	2.5	8
Clad feed rate	[mm/min]	4.5	Hardness in clad layer	[HV]	30	35
Substrate translation speed	[mm/min]	60	Hardness in substrate	[HV]	110	144

The result of the cladding is visible in table 2.8 and figure 2.25. The edge has an effect on the process development. In experiments without an edge and with constant rotation speed the temperature gradually increases during the clad process. The increase of the edge height in this experiment requires more material, thus reducing the layer width. The small reduction in layer width combined with the higher material demand, result in a stable temperature during the entire clad process. The tool and pump force both remained relative low at 5 and 2.5 [kN]. The layer appears smooth over the entire stretch, both at the top surface and at the edges.

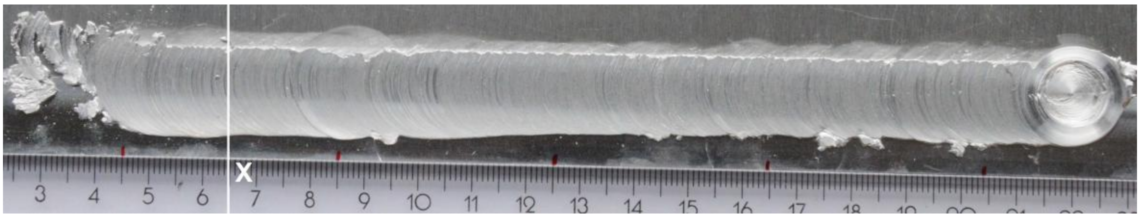

Figure 2.25: Result of the single clad layer over a small edge, the line X indicate the place of the cross section.

The relative low temperature and force have a positive effect on the hardness of the material, especially at the last part of the cladding in figure 2.25. The clad layer has a hardness of 30 [HV], with a peak of 35 [HV]. The substrate has quite predictable findings, a mean hardness of 110 [HV] under the clad layer(A). In the zone B and D it increases to above 130 [HV], while in zone C the hardness is around 110 [HV].

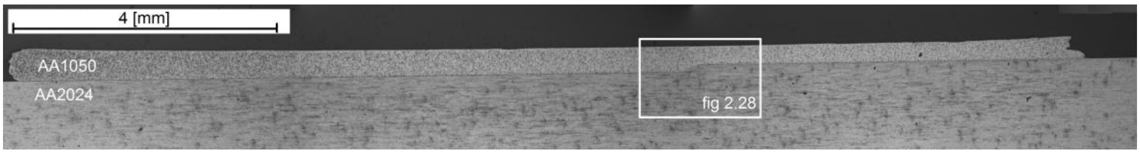

Figure 2.26: Cross section the single clad layer over a small edge, taken at line X in figure2.25.

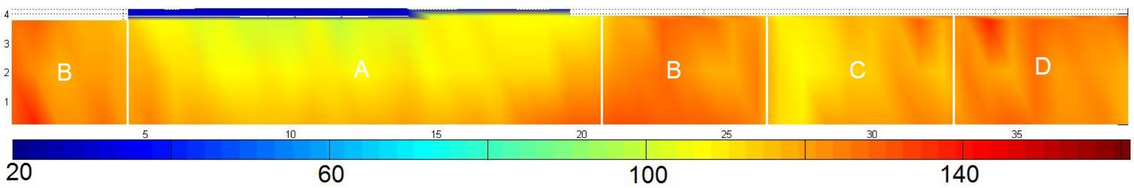

Figure 2.27: Hardness result in [HV] of the single clad layer over a small edge, taken at line X in figure2.25.

The result of the cross section is in figure 2.26. The clad layer appears well and the cover is complete without any voids. However, figure 2.28a shows a void (Z). The other round black points are indents made during the hardness measurement. After the hardness measurement the sample is re-polished to remove the indents and to make a fresh cross section for etching. However, the voids hidden beneath the clad layer are also polished away (figure 2.26 and 2.28b), which indicate that the void is small. Therefore, when cladding over an edge's, there is still a risk of creating a small void at the edge. This removal of voids is seen at all edge heights, not only the 0.1 [mm] shown in figure 2.28. The voids are smaller for a smaller height differences and all are smaller as experiment 1.3.

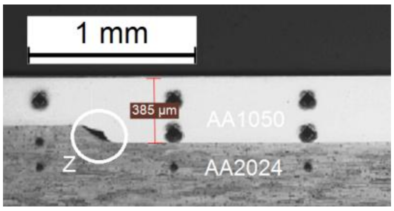

figure 2.28a: Cross section at line X. The round black holes are due to the hardness measurement.

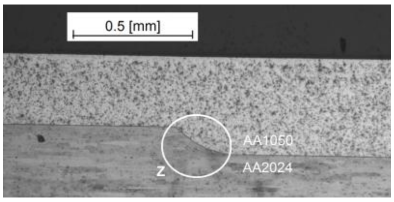

figure 2.28b: Cross section at line X. The same place as 2.27 after a re-polish.

Based on experiment 1.3 and this experiment, cladding edges and trenches can create small voids, especially at the retreating side. Voids beneath the cladding layer are unwanted for an AM process. A possible solution is to clad with more force and heat. This will cause intermixing and more deterioration of the substrate material, both unwanted but allowable for an additive manufacturing process. Another possible solution is the placement of the edge relative to the clad layer, the advancing side has no voids in experiment 1.3. The placement of the edge is further reviewed in experiment 1.3-a.

2.3.5 Experiment 1.5

The fifth experiment observes cladding over a series of holes. The holes are placed along the cladding path in line with the tool axis, starting with a diameter of Ø 5 [mm]. Hole 1-3 have a Ø 10 [mm] second circular lowering around this central hole, with a depth of 0.5, 1.0 and 1.5 [mm], see figure 2.11. The rotation speed, tool gap and clad feed rate are set at higher rates to accommodate the material supply demand.

Table 2.9: Settings and results of experiment 1.5

Parameters			**Results**		Median	Maximum
Tilt angle	[°]	1	Tool temperature	[°C]	350	430
Tool rotation speed	[rpm]	450	Pump force	[kN]	5	12
Tool gap	[mm]	0.4	Tool force	[kN]	3	7
Clad feed rate	[mm/min]	5.6	Hardness in clad layer	[HV]	25	30
Substrate translation speed	[mm/min]	60	Hardness in substrate	[HV]	105	144

A picture of the cladding over holes is in figure 2.29. During the cladding each hole causes a drop in pressure and temperature. This effect is especially strong with two biggest holes (2, 3). The force and temperature drop nearly stopped the process. The cladding went well for hole 4 and also quite well for hole 1. Both holes are probably filled completely in a multiple cladding attempt, as shown in experiment 1.1. Hole 2 and 3 have a bigger void and are hardly filled. The hardness profile (figure 2.30) of the fourth hole indicates more heat flow through the plate, as there is no relative hard zone (B) under the clad layer. The zone A has hardness around 105 [HV]. Zones B and D are above 130 [HV] while the hardness zone C is just under 120 [HV].

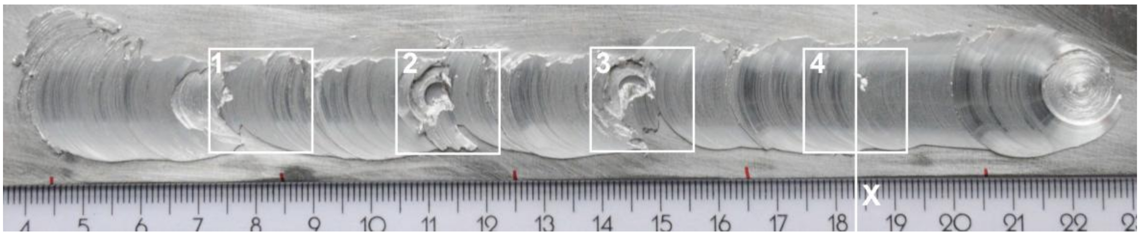

Figure 2.29: Result of the single clad layer over some holes. Number 1 to 4 indicate the holes, line X indicates the cross section.

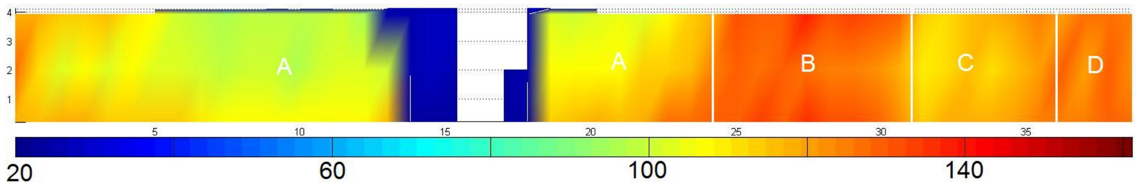

Figure 2.30: Hardness profile of the of the filled hole, taken at line X in figure 2.29

Hole 4 is further reviewed with a cross section (figure 2.31), made at line X in figure 2.29. The hole is filled about 90%, but not entirely. The higher temperature and smaller diameter appear to have a positive impact on the filling of the holes, hole 4 has the highest cladding temperature and smallest pressure drop. A possible influencing factor for the voids is trapped air inside the hole, as most voids are at the bottom.

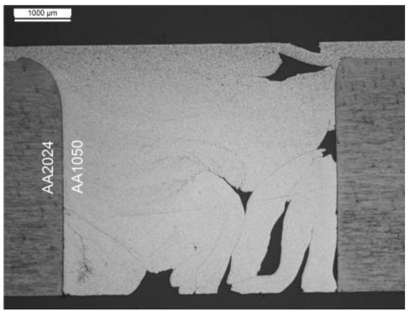

Figure 2.31 : Result of the single clad layer over the fourth hole. The cross section is made at line X in figure 2.29

For AM the filling of holes is challenging. Bigger holes cause process disruption, while smaller holes still have voids. A further review of the behavior regarding holes is in chapter 1.3.8, where a series of smaller holes is tested.

2.3.6 Experiment 1.3-a

Experiment 1.3-a is a re-approach of experiment 1.3 in chapter 1.3.3. Experiment 1.3-a has an uniform trench depth of 0.2 [mm]. The trench starts with a width of 0.2 [mm], thereafter it is widened by 0.2 [mm] at each 30 [mm] in the cladding direction, to a total width of 12 [mm], see figure 2.9. The rotation speed and clad feed rate are increased to accommodate the surface irregularities and the higher material demand.

Table 2.10: Settings and results of experiment 3-b

Parameters			Results		Median	Maximum
Tilt angle	[°]	1	Tool temperature	[°C]	410	420
Tool rotation speed	[rpm]	450	Pump force	[kN]	10	15
Tool gap	[mm]	0.2	Tool force	[kN]	5	8
Clad feed rate	[mm/min]	3.0	Hardness in clad layer	[HV]	38	42
Substrate translation speed	[mm/min]	60	Hardness in substrate	[HV]	100	144

The experiment produces a smooth clad layer covering the entire trench, as shown in figure 2.32. The tool temperature is above 400 [°C] and slightly increases during the cladding with a median of 410 [°C]. The influence of the widening gap probably holds the temperature constant. The tool force on the cladding plate stays roughly constant. The pump force increase is either due to the sticking of aluminum inside the tool or to the influence of the geometry.

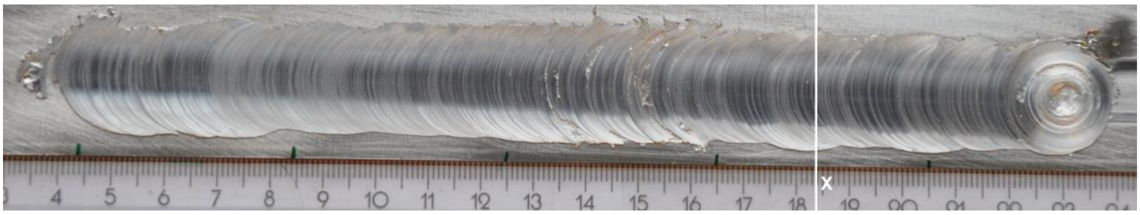

Figure 2.32: Result of the single clad over a widening trench, the white line X indicates the cross section.

The cross section in figure 2.33 shows intermixing between the two layers. The AA1050 layer is bonded well on the substrate, but the original corners of the trench are not visible in the cross section. Zoom A shows the intermixing pattern at the advancing side, while zoom B shows it at the retreating side. At the retreating side (B), the trench is smeared in the gutter, so the substrate is used as extra clad material. At the advancing side (A), the substrate material is heaped into two bumps, making place for AA1050. Both these intermixing patterns are probably due to the high temperature and force. The cross section at X and two other cross sections showed no voids.

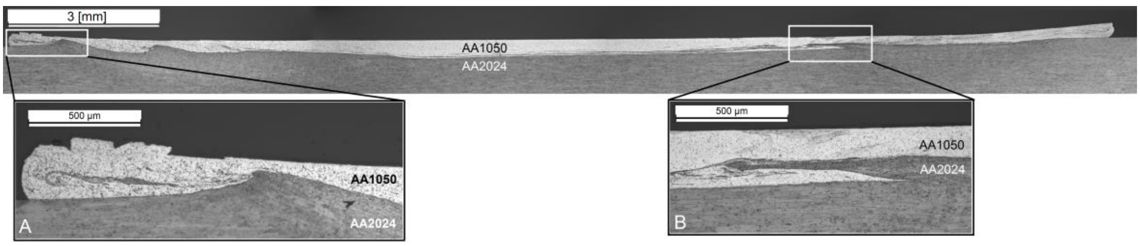

Figure 2.33: Cross section of the cladding in a trench, made at white line X in figure 2.32.

The influence of temperature and material supply on a clad layer over an edge is showed by comparing experiment 1.3, 1.4 and 1.3-a. Experiment 1.4 clad a layer at roughly 320 [°C]. The edge is still intact, but there are some voids at the edge (figure2.26-Z). Experiment 1.3 has a higher temperature of 400 [°C]. Intermixing is found between the substrate and the clad material at the AS (figure2.23-K), but there are no voids. At the retreating side there are voids due to material shortage (figure 2.23-L). Experiment 1.3-a shows good cover without voids when enough material and heat is supplied, though at the risk of intermixing.

2.3.7 Experiment 1.3-b

Experiment 1.3-b is similar to experiment 1.3-a, however the trench tightens instead of that it widens. The trench starts 20 [mm] wide and tightens 2 [mm] at each 30 [mm] in the cladding direction, see figure 2.10. The experimental settings have an elevated clad feed rate and rotation speed at the start to adjust for the relative high tool gap of 0.4 [mm] to the trench bottom.

Table 2.11: Setting and results of experiment 1.3-b

Parameters			**Results**		Median	Maximum
Tilt angle	[°]	1	Tool temperature	[°C]	420	450
Tool rotation speed	[rpm]	300-500	Pump force	[kN]	8	15
Tool gap	[mm]	0.2	Tool force	[kN]	5	8
Clad feed rate	[mm/min]	2.8-3.3				
Substrate translation speed	[mm/min]	60-40-60				

The result of experiment 1.3-b is shown figure 2.34. The experiment performed quite irregular. Due to the effective tool gap 0.4 [mm], the force and temperature did not build-up well. Therefore the rotation speed is increased during the process and the substrate translation speed is decreased to avoid lack of material. Halfway the cladding the substrate translation speed is raised to 60 [mm/min] again. The process stabilized halfway the trench. The temperature is high at 420 [°C] in the successful cladding part and results in a rough layer.

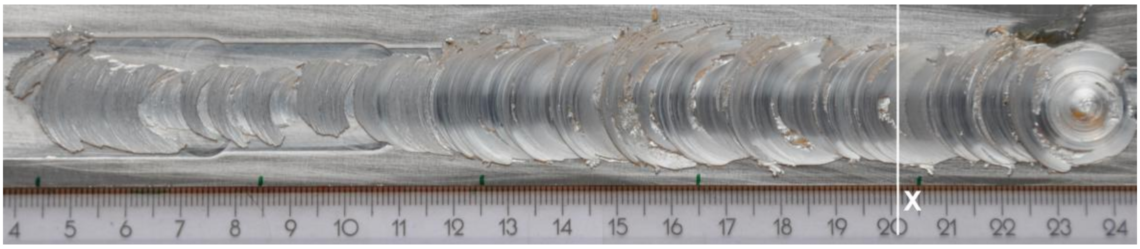

Figure 2.34: Result of the single clad layer in a tightening trench. The white line X indicates the place of the cross section.

The high temperature and irregular behavior of the cladding process have an influence on the cross section, shown in figure 2.35. There is intermixing and the original trench is not recognizable anymore. A small void is visible at position A. This void is probably due to the high temperature and force, which results in the irregular clad surface.

Figure 2.35: The cross section of experiment 1.3c, perpendicular to the cladding direction, made at red line in figure 2.33.

For AM with AA1050 a temperature higher than 420 [°C] for should be avoided, based on a comparison between experiment 1.3-a and 1.3-b. Experiment 1.3-a has less intermixing and the original trench is still retraceable. In 1.3-b the original substrate structure is not recognizable anymore. The high temperature does prevent voids at the edges, but the higher temperature 1.3-a did create a void (figure 2.35-A) in the middle of the clad layer.

2.3.8 Experiment 1.5-a

Experiment 1.5-a re-investigates the cladding over a series of holes. In experiment 1.5, the cladding of the smaller hole of Ø 5 [mm] diameter is reasonably successful, but the other holes gave problems. To test the clad behavior over smaller holes, a second attempt with smaller holes is performed. The series starts with a Ø 1.0 [mm] hole through the plate and increases with steps of 0.5 [mm] to a Ø 4.5 [mm] hole at the end of the substrate, see figure 2.14. A higher temperature and clad feed rate are used to accommodate the filling of holes.

Table 2.12: Settings and results of experiment 5-b.

Parameters			Results		Median	Maximum
Tilt angle	[°]	1	Tool temperature	[°C]	400	430
Tool rotation speed	[rpm]	450	Pump force	[kN]	8	12
Tool gap	[mm]	0.4	Tool force	[kN]	4	8
Clad feed rate	[mm/min]	5.6	Hardness in clad layer	[HV]		
Substrate translation speed	[mm/min]	60	Hardness in substrate	[HV]		

The result of the cladding in figure 2.36, the white squares indicate the places of the holes and their diameters. The influence of the holes is clearly visible in both the force and the temperature by a drop of about 0.5 [kN] and 10 [°C]. The drop of force and temperature increased with bigger holes. The result of the process is a smooth clad layer. Only with the bigger holes the location of the hole is still visible by a small indent. These small indents are unwanted, but will cause no problems for a second overlapping layer, as shown in experiment 1.1.

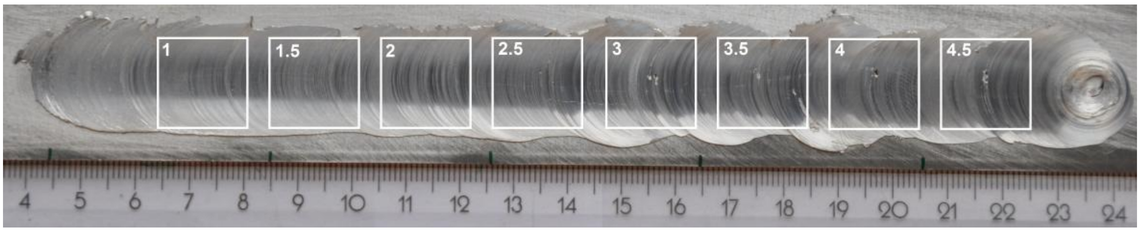

Figure 2.36: Result of the single clad layer over several holes, the place of the hole is indicated with a square, the number is the diameter.

Cross sections of experiment 1.5-a are made in the middle of the cladding layer, along the cladding direction. The results of the hole Ø 1.5, Ø 2.5. Ø 3.5 and Ø 4.5 [mm] are shown in figure 2.37 to 2.40. In the pictures the cladding direction is from the left to the right. This is visible in the cross section by the edge deformation of the hole: the left side flows over, while the right side is moved back.

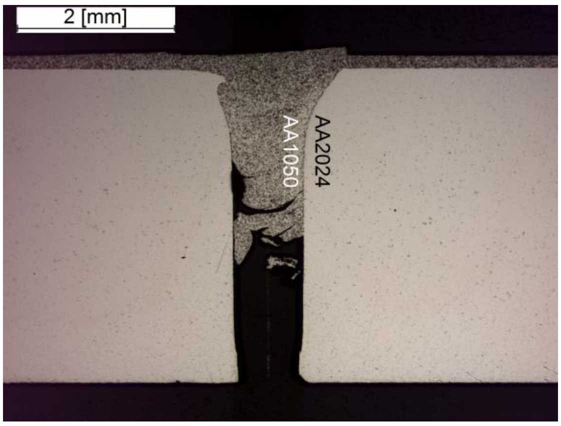

Figure 2.37: Cross section of the 1.5 [mm] hole.

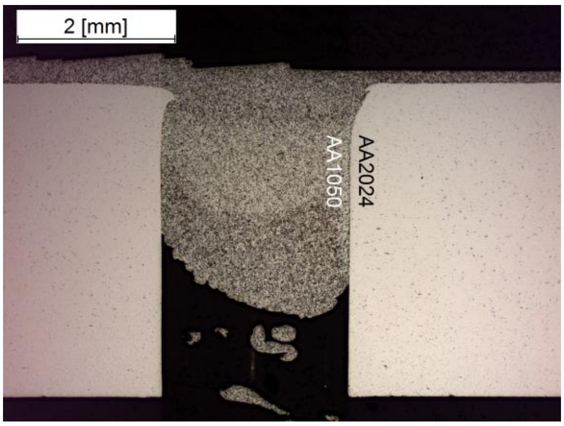

Figure 2.38: Cross section of the 2.5 [mm] cladding hole.

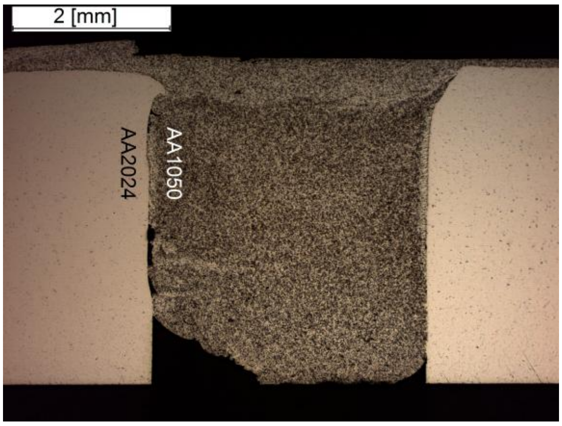

Figure 2.39: Cross section of the 3.5 [mm] hole.

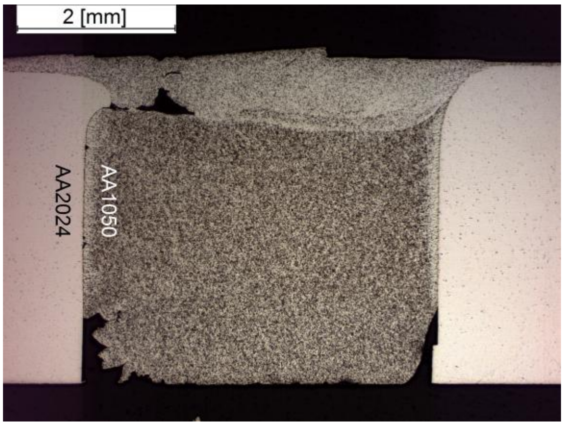

Figure 2.40: cross section of the 4.5 [mm] hole.

Generally the filling is well in the upper part of the holes, especially with the smaller holes. The bottom part of the hole is unfilled in the smaller holes, while the bottom part contains voids in bigger holes. The filling of the Ø 4.5 [mm] hole in figure 2.40 is better than the Ø 5 [mm] hole in figure 2.31. The higher temperature of experiment 1.5-a is the most reasonable explanation, as the cladding layer approaching the hole is smooth in both cases. The lighter color in the top of the hole in figure 2.39 and 2.40 is probably due to some intermixing. This is in line with the difference between experiment 1.4 and 1.3-a.

For AM the result indicates that FSC is reasonably well in filling holes. Small voids are hard to prevent, but with a higher temperature and material supply most holes are filled well up to a certain depth. The results also mean that creating hollow structures is a challenge. If internal structures are desirable, probably lower temperature, less material and a higher substrate translation speed could help. This approach has however the risk of destabilizing the FSC process.

2.4 Conclusion

The use of AA1050 for AM appears possible as the process is stable and generally produces good results. Both parallel and overlap cladding of layers work well, the basic handlings for AM. The second clad layers are well bonded and even compensated for small defects of the first clad layers. This will likewise happen with the small edge between two overlapping layers. The parameters stayed in the normal boundaries known for single layer cladding. The multiple cladding runs indicate that FSC can be used to repair aluminum surfaces, as the second clad layer perfectly covered and filled some irregularities of the first clad layer.

A trade-off between temperature and cover appears when comparing the influences of different surfaces. Lower temperatures (<300 [°C]) result in sharp edges and no intermixing. Yet, the forces are high and there is a tendency to get voids at irregularities and in small holes, especially at the retreating side. If the cover and material properties are good, small voids may be allowable for cladding. The voids are however highly unwanted for an AM method. A higher temperature of 400 [°C] is preferred for AM. The process runs smoothly and the filling of irregularities and smaller holes is well. The process is stable and hardly has any voids while the forces are relative low. The drawback is intermixing between the clad layer and the substrate, especially at edges of height differences under a clad layer. This is however not a fundamental problem for AM.

The influence of the temperature is also visible in the hardness measurements. A relative low temperature <300 [°C] and a higher forces result in substrate roughly 15% softer than before the cladding. Clad temperatures around 400 [°C] result in a 30% decrease in hardness of the substrate. Extremes temperatures in both directions cause problems. The hardness pattern of a multiple clad experiment is comparable to that of single layer cladding experiment, though the harness has reduced more. Too low temperatures result in high forces and an unstable process, while high temperatures increase the material degradation. The cladding process in the experiment is still in the startup phase. If the input parameters and the surface stay constant, there is a slow temperature increase.

3 Analysis of the additive process: AA2024 on AA2024

The second part of the report describes the cladding of AA2024 on AA2024. Cladding the same material on itself, specifically hard aluminum alloys, is not studied yet. FSC with AA2024 enables AM with AA2024. The section starts with an introduction and the experimental setup. These are followed by the review of the experiments. The section ends with a conclusion about the clad behavior of AA2024 with respect to AM.

3.1 Introduction

The experiments of cladding AA2024 on AA2024 are based on those of AA1050 on AA2024. The AA1050 process is a relative controllable process with predictable and understood results. The higher hardness of the aluminum AA2024 relative to the AA1050 will probably cause a higher force during the cladding process. This larger force can partially be compensated with a higher cladding temperature, as a higher temperatures reduces the strength of the clad material. The relative high hardness can have a favorable side affect. One of the problems with the softer AA1050 is the sticking of some clad material to the tool. The harder AA2024 may not have this problem.

The friction stir welding papers mentioned in the previous chapter are also relevant for the cladding of AA2024 on AA2024. The nugget zone of FSW is similar to the clad layer in FSC, so the same grain structure as studied by Jones[6] is expected. The cooling and heating in a FSC process will result in a hardness pattern as described by Khodir[8] and Genevois[9]. Fine grains and re-precipitation due to large plastic deformation at elevated temperature are expected in the layer. In the substrate coarsening of the grains and (over-) aged precipitates are expected. Coarsening and dissolution of participates are expected in the substrate near the clad layer. Grain coarsening and dissolution of participates leads to lower hardness, while grain refinement and re-precipitation recover hardness.

The cladding process of AA2024 on AA2024 is comparable to a pinless FSW process, as researched by Li et al.[13]. Li welded a AA2024 plate of 1.5 [mm] with a welding tool with involute grooves at the bottom. Li mentions the influences of increasing heat due to higher rotation speeds, which leads to a lower tensile strength. A higher welding speed influences the mixing, which increases the change of the failure mode at the retreating side. It is suggested that if this effect can be prevented, the higher cladding speed will produce a higher tensile strength.

Gandra et al. [14] used AA6082-T6 aluminum to FS a AA2024 substrate. They produced sound aluminum coatings, with limited intermetallic formation at the bonding interface. The lack of a cladding tool results in rougher layer and a revolving flash around the supply rod. The flash consumes about 70% of the clad material. The result of the experiments show a 15 % hardness decrease in the clad layer and 6% in the substrate plates. The axial force is critical for a good bonding, though excessive force will result in a concave shaped cross section.

Dilip et al[15] use mild steel rods to FS a structure on a steel substrate. Mild steel rods are clad with overlap into a pyramid structure. The rough surface of FS due to the lack of a cladding tool is compensated by milling the top surface of an added layer. Dilip's process gave successful results and has no unintended voids, while it is possible to deliberately create small voids. The clad layers are fine grained and heat affected, comparable to wrought steel.

3.2 Experimental setup

The experiments simulate the basic circumstances an AM process needs for a proof of principle. The experiments start with a single layer to research the possibility of cladding AA2024. Thereafter the multiple cladding experiments are similar to the previous experiments of AA1050.

Experiment 2.1

The first experiment is to clad of a layer of AA2024 on an AA2024 substrate. As the process is tried for the first time, the process window is unknown. The parameters for this experiment are based on the cladding of AA1050 on AA2024, with an elevated rotation speed for more heat generation to compensate for the harder AA2024. The aim of the experiment is to clad a regular and smooth clad layer, the parameters of the experiment will become the reference for the multiple cladding experiments.

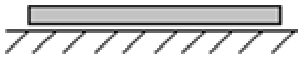

Figure 3.1: Schematic view of

Heat treatment of the cladding rods

One of the difficulties with experiment 2.1 is the force build-up in the startup. A proposed solution is to heat treat the cladding rods to reduce the hardness. Cladding rods are put in an oven of 350 [°C] for 18 hours. The heat treatment dissolves participates in AA2024, thus reducing the hardness from 144 [HV] to ~80 [HV]. As participates reform during the cladding process and by aging after the process, the effect in the end is presumed minimal. These heat treated cladding rods are used for the multiple cladding experiments.

Experiment 2.2

The second experiment is the overlap cladding of two layers of AA2024, based on the stable process window found in experiment 2.1. The process is performed twice over the same trajectory. For the second layer the cladding tool is placed 0.2 [mm] above the top surface of the first layer. The goal is to built a well overlapping and bonded layer.

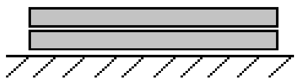

Figure 3.2: Schematic view of

Experiment 2.3

Beside overlap cladding, it is also needed to test the parallel cladding behavior for the AM process. The substrate is prepared with a width of 181 [mm] instead of the standard 141 [mm] since two parallel layers produce a wider clad layer. The second clad layer is deposited next to the first layer with a small overlap. This overlap is at the retreating side to clad the irregularities at that side and avoid voids between the layers.

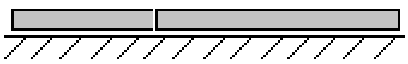

Figure 3.3: Schematic view of experiment 2.3.

Review of the experiments

As all the experiments performed previously, the temperature in the tool and the substrate, the pressing force and the normal force are recorded. The deposited substrates are stored at room temperature for more than two weeks to allow for ageing. Afterwards, samples are picked for further analysis, like microstructure observation and hardness measurement. All the samples are grinded with silicon paper up to grade 4000, polished to 1 [µm] and etched with 50% NaOH at 70 [°C] for 20-30 [s].

3.3 Results and discussion

The results of the experiments are analyzed and discussed in one subsection per experiment. The section reviews the experimental setup, the visible appearance, cross sections and hardness data. These reviews are in the light for AM. All results and the rotation speed development of experiment 2.2 and 2.3 can be found in the appendix K-M.

3.3.1 Experiment 2.1

Experiment 2.1 is the first attempt to clad AA2024 directly on an AA2024 substrate. This is a new field of cladding. The tool rotation speed is set at a relative high rate 450 [rpm] to generate more heat to soften the harder material. The other parameters are the same as those used in the cladding process of AA1050.

Table 3.1: Settings and results of experiment 2.1

Parameters			**Results**		Median	Maximum
Tilt angle	[°]	1	Tool temperature	[°C]	400	430
Tool rotation speed	[rpm]	450->600	Pump force	[kN]	15	18
Tool gap	[mm]	0.2	Tool force	[kN]	9	16
Clad feed rate	[mm/min]	2.7	Hardness in clad layer	[HV]	112	122
Substrate translation speed	[mm/min]	60-90	Hardness in substrate	[HV]	110	144

The result of the cladding is a smooth layer, visible in figure 3.4. The layer is smoother than comparable AA1050 experiments. The cladding process has troubles in the start-up phase, which might be due to a not or less rotating supply rod in the cladding tool. The lack of a layer in the startup results in insufficient heat generation and a major force build-up. To increase the heat generation, the tool rotation speed is increased to 600 [rpm] and the substrate movement is started. After these changes the process starts to run smoothly at a temperature of 400 [°C], though the high forces remain. To reduce the pump force, the translation speed is increased to 90 [mm/min], as this lowers material supply per section. Pump force still gradually accumulates with the cladding time. This results in the breaking of the oil seals in the pressure pump, thus ending the experiment.

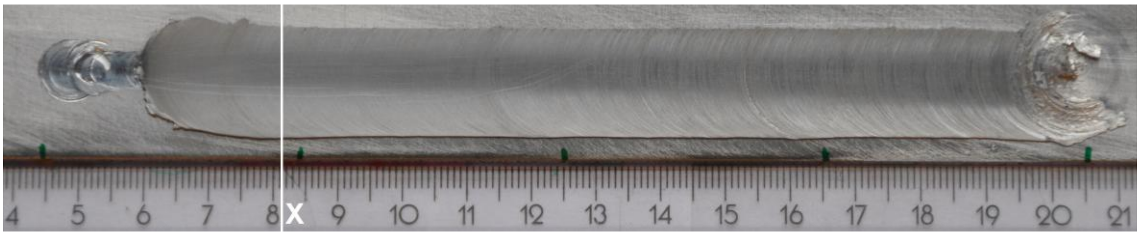

Figure 3.4: Result of the single clad of AA2024, the white line X indicates the place of the cross section.

The effect of the temperature on the hardness of the clad layer and substrate is shown in figure 3.5. The pattern is comparable with the results of the research of Jones[6] and the earlier AA1050 experiments at higher temperatures. The hardness varies in the clad zone between 108 and 122 [HV]. Zone A just under the clad layer is the softest area, with a hardness around 105 [HV] and extremes under 100 [HV]. To the right (B) the hardness increases to 140 [HV] with the usual small second dip (C). Entirely to the right (D) the hardness goes back to ~144 [HV], which is the hardness of the base material.

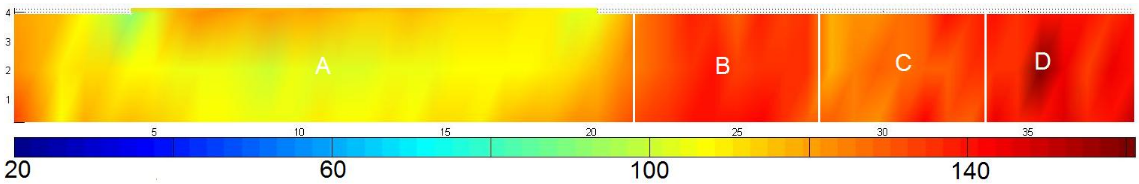

Figure 3.5: Hardness result in [HV] of the single clad of AA2024, the line X in figure 3.4 indicates the place of the cross section.

The cross section of cladding layer is shown in figure 3.6. There is a strong grain refinement and intermixing visible in the middle of the clad layer and substrate. At the outer edge the boundary between the substrate plate is still visible (K+L). The rest of the layer is mixed with the substrate and there is no clear boundary between the layers and the substrate. So, the material is well bonded without voids.

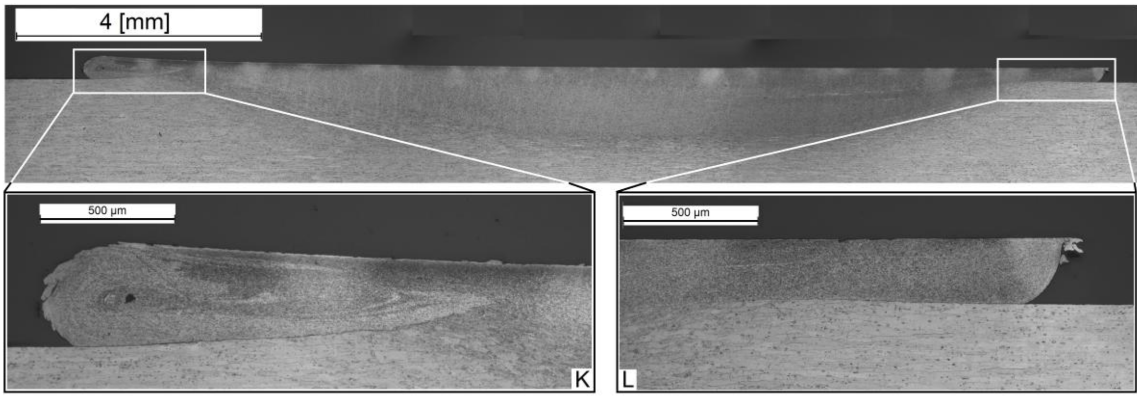

Figure 3.6: Cross section of the single clad of AA2024, the line X in figure 3.4 indicates the place of the cross section,

The first test with cladding AA2024 on AA2024 proves promising for AM. Cladding of AA2024 on AA2024 results in a good bond between the substrate and the clad layer. The test is successful up to the force build-up at the end. The main challenge for the process lies in avoiding the high forces in the setup.

3.3.2 Experiment 2.2

The second experiment is a multiple cladding experiment with overlapping layers. To prevent the problems with the startup, the AA2024 cladding rods are heat treated to reduce the hardness to ~80 [HV] from the basis hardness of 144[HV]. The experiment starts with a high rotation speed of 600 [rpm]. The rotation speed is slowly lowered to keep the tool temperature around 400 [°C]. The rotation speed ends at 524 [rpm] with the first layer and 470 [rpm] with the second. The tool gap is set at the standard 0.2 [mm] in the first experiment. For the second layer the tool is placed 0.2 [mm] above the top surface of the first layer, which meant a tool gap relative to the substrate of 0.56 [mm].

Table 3.3: Settings and results of experiment 2.2

Parameters first layer			**Results**		Median	Maximum
Tilt angle	[°]	1	Tool temperature	[°C]	400	410
Tool rotation speed	[rpm]	600-524	Pump force	[kN]	9	14
Tool gap	[mm]	0.2	Tool force	[kN]	8	10
Clad feed rate	[mm/min]	3.2	Hardness in clad layer	[HV]	115	122
Substrate translation speed	[mm/min]	60	Hardness in substrate	[HV]	100	144
Parameters second layer			**Results**		Median	Maximum
Tilt angle	[°]	1	Tool temperature	[°C]	400	415
Tool rotation speed	[rpm]	600-470	Pump force	[kN]	11	14
Tool gap	[mm]	0.56	Tool force	[kN]	8	11
Clad feed rate	[mm/min]	3.2	Hardness in clad layer	[HV]	115	122
Substrate translation speed	[mm/min]	60	Hardness in substrate	[HV]	100	144

The cladding of the first layer went smooth and the cladding of a second layer on the first went similar to cladding on a substrate. The fist layer is in figure 3.7 and the second is in figure 3.8. The second layer covers the first layer entirely. The layer appears well an smooth on visual inspection. Force and temperature developed similar during the experiments, a temperature around 400 [°C] and forces between of 8 and 10 [kN]. The heat treatment of the cladding rods positively influenced the cladding process. The startup phase went well and the forces remained relative low compared to experiment 2.1. With the current setup, a stable process window is found.

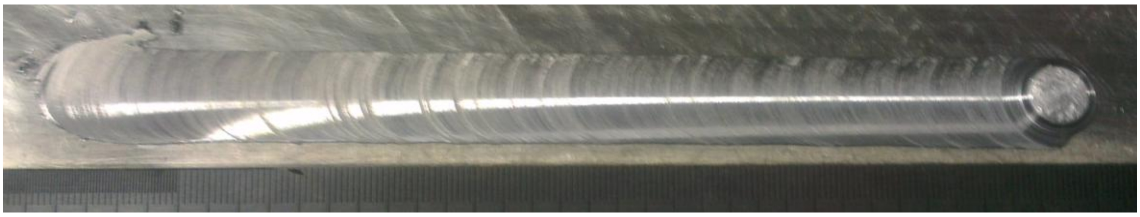

Figure 3.7: Result of the first clad layer of AA2024.

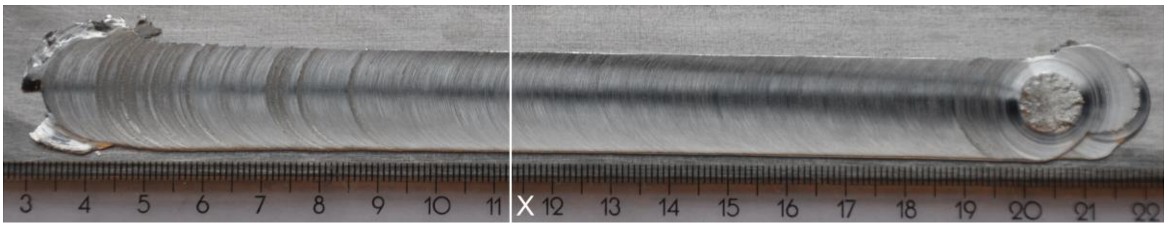

Figure 3.8: Result of the second clad layer, clad on top of the first layer, the white line X indicates the place of the cross section.

The hardness pattern of the clad layer is comparable to that of experiment 2.1, as shown in figure 3.9. The hardness in the clad layer is roughly 115 [HV]. Double heat exposure lowered the hardness of the substrate under the clad layer (A) to 100 [HV], which is in line with the research of Khodir[8]. The hardness increases to above 130 [HV] in zone B and goes back to ~144 [HV] in D, with a dip to 120 [HV] in C.

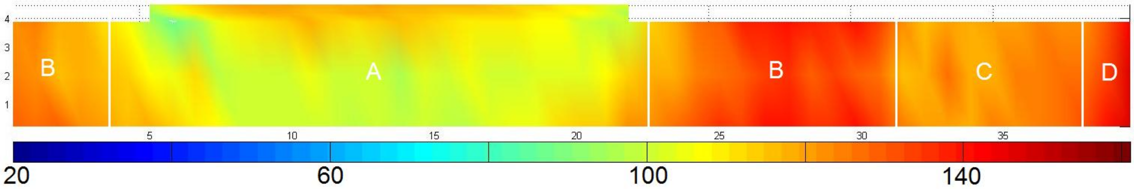

Figure 3.9: Hardness result in [HV] of the double clad layer of AA2024, made at the line X in figure 3.8.

The cross section of the two overlapping layers show a solid bond, as shown in figure 3.10. Near the edges the clad layer/substrate interface line is still visible (K+L), but the bond is well and without voids. In the middle of the clad layer the difference between the clad layers and the substrate is not recognizable. There is a fine grain structure and probably intermixing between the layers. The intermixing is not clearly visible, as the clad material is the same material as the substrate. This result is comparable with the results of multiple cladding with AA1050 in experiment 1.1.

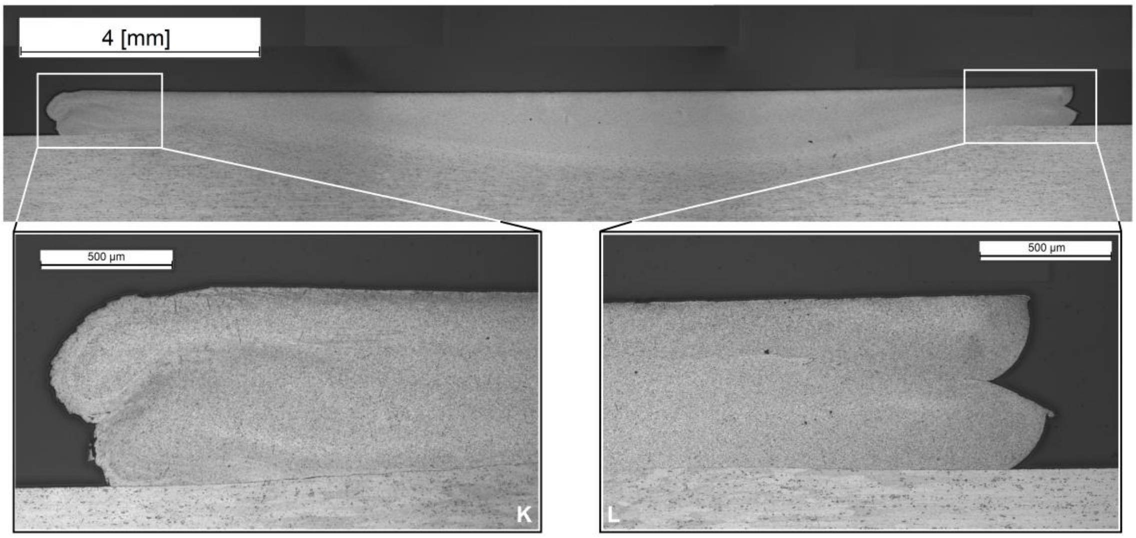

Figure 3.10: Cross section of the double clad layer of AA2024, taken at line X in figure 3.8.

The result of the overlap cladding experiment with AA2042 is positive for AM. The process with the heat treated cladding rod is much more stable than experiment 2.1. Furthermore the cladding of a second layer on top of the first layer gave no process problems and the bond between the layers is well. Based on the tool rotation speed development, the heat requirement of the second layer is lower than the fist layer. Two possible explanations for this are less heat deflection through the substrate and the relative short turnaround time between the cladding of the layers, which means there is still more residual heat in the setup.

3.3.3 Experiment 2.3

The third experiment is to clad of two parallel layers. To accommodate the second parallel layer, experiment 2.3 uses a wider substrate plate. Just as in experiment 2.2, the rotation speed starts at 600 [rpm] and is lowered during the cladding process to keep the temperature around 400 [°C] in the tool. With the first cladding track the rotation speed reduces to 580 [rpm] and in the second to 468 [rpm]. Because the cladding tool contacts the first layer when cladding the second layer, the tool is rotating when lowered into the position.

Table 2.4: Settings and results of experiment 2.3

Parameters first layer			**Results**		Median	Maximum
Tilt angle	[°]	1	Tool temperature	[°C]	400	410
Tool rotation speed	[rpm]	600-580	Pump force	[kN]	9	14
Tool gap	[mm]	0.2	Tool force	[kN]	7.5	10.5
Clad feed rate	[mm/min]	3.1	Hardness in clad layer	[HV]	110	118
Substrate translation speed	[mm/min]	60	Hardness in substrate	[HV]	100	144
Parameters second layer			**Results**		Median	Maximum
Tilt angle	[°]	1	Tool temperature	[°C]	410	420
Tool rotation speed	[rpm]	600-468	Pump force	[kN]	13	15
Tool gap	[mm]	0.2	Tool force	[kN]	10	12
Clad feed rate	[mm/min]	3.2	Hardness in clad layer	[HV]	118	122
Substrate translation speed	[mm/min]	60	Hardness in substrate	[HV]	100	144

The cladding process of both layers went smooth. The layers have overlap in 70 % of the cladding length, with an increasing overlap to the end, as shown in figure 3.11. The temperature remained around 400 [°C] in both experiments. The cladding process of the first layer is similar to that of the previous experiment. The pump and tool force are around 9 [kN] and 7.5 [kN] during the experiment. The contact of the tool with the first layer is visible by a higher tool force and the heating of the tool before force build-up of the pump force. The second experiment has a higher pump and tool force of 13 [kN] and 10 [kN].

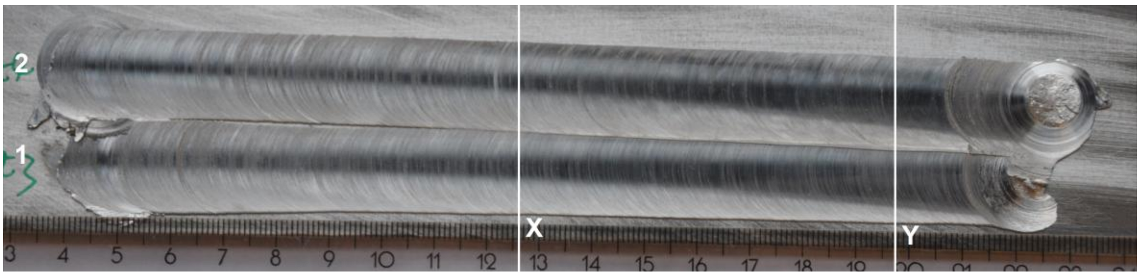

Figure 3.11: Result of the two parallel layers of AA2024, the bottom layer is the first layer, the top layer is the second layer. The white lines X and Y indicate the places of the cross sections.

The hardness is influenced by the double heat generation of the two clad layers, as depicted in figure 3.12. The second layer (above B) lays on the right side of the first layer (above A). The hardness in the first clad layer is around 110 [HV] (above A) while it is around 118 [HV] in the second layer (above B). The hardness of the substrate just under the first layer (A) is around 105 [HV], and 90 [HV] at the bottom of the substrate. The hardness of the substrate just under the second layer (B) is around 115 [HV], and 105 [HV] at the bottom. In zone C the hardness increases to above 120 [HV]. The heat of the second cladding process probably further coarsened the participates in the layer and substrate in zone A, thus reducing the hardness in zone A more than in zone B.

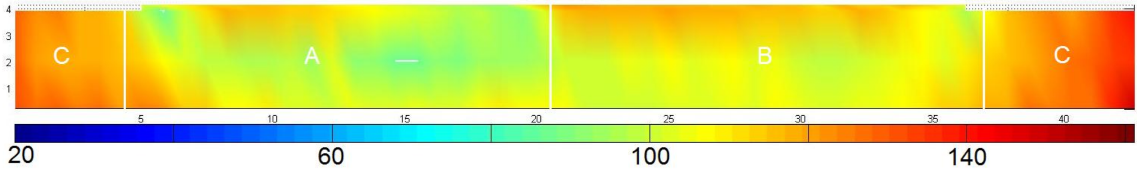

Figure 3.12 : Hardness result of the two parallel layers of AA2024, made at line Y. The first layer is clad at the left side (above A), the second layer on the right (above B).

The two cross sections, where the two layers overlap, are displayed in figure 3.13 and 3.14. The cross section in figure 3.13 is at the position the layers start to overlap (figure 3.11-X) , the cross section of figure 3.14 is taken at the end with more overlap (figure 3.11-Y). The extent of overlap between the layers is important for a defect free overlap. Cross section 3.13 has a small void (L) and the border between the two layers is visible, with a overlap of ~4% of the layer width. Cross section 3.14 has two perfectly bonded layers, only at the top of the layer the overlapping interface is visible (M), with a overlap of ~8% of the layer width. Assuming a relocation of the second clad layer by the width of the void in cross section 3.31 would create a defect free overlap, a ~5 % overlap is required.

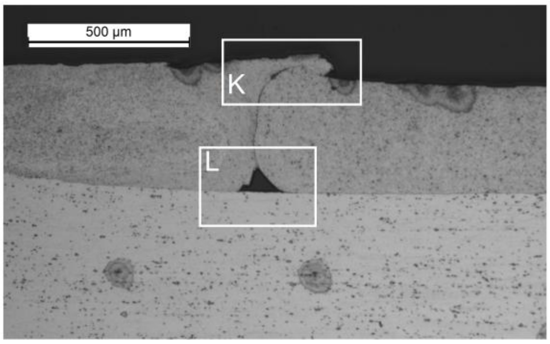

Figure 3.13: Result of the two parallel layers of AA2024 at 1

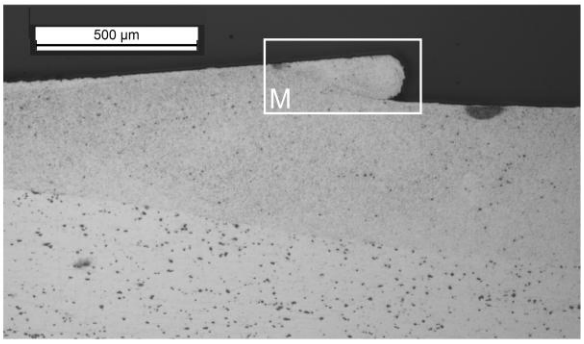

Figure 3.14: Result of the two parallel layers of AA2024 at 2

The result of the parallel cladding experiment are promising for AM. Parallel cladding is possible and a small overlap of >5 % is probably enough for a defect free cladding. The bonding properties are well and the cladding process is stable. The small edge seen between the two layers would cause no problem when parallel cladding is combined with overlap cladding.

3.4 Conclusion

Cladding AA2024 on AA2024 works well, as the results are good while the process is stable. Five layers of AA2024 are clad on a substrate in three different experiments. A stable process window is found at a tool temperature of around 400 [°C]. In this window the process is stable and controllable. Startup of the cladding process is greatly improved when the supply rod is heat treated to reduce the hardness before cladding. The bond between the clad layer and the substrate is good. The clad layer has a hardness reduction of 15% compared to the original value, while a 20% reduction in hardness is measured in the substrate.

Compared with the cladding process of AA1050 on AA2024, the current process of AA2024 on itself provides both advantages and disadvantages. The latter approach produces layers with a smoother top surfaces. Secondly, due to the high hardness of the clad material of AA2024, no clad material is found stuck in the tool after the cladding process. However, the harder clad material caused higher force build-up in the whole process, which is a risk for the current clad material supply system.

The technique of FSC with AA2024 appears promising for AM. The cladding process remains stable in both parallel and overlapping layers, with minor fluctuations in the resulting forces. Except for a part of the parallel cladding where the overlap is to small (<5%), the layers are connecting well and there are no voids or other imperfections in overlapping layers. Compared to single clad layers, the hardness in the substrate reduces more in the multiple cladding due to the reheating.

4 Development of a new printing tool

The process of friction surface cladding is currently in an experimental stage. The setup is designed for experiments and the process preparation time is long. For the industrial feasibility of friction surface cladding as an AM process, a continuous or batch process is required. Some first design guidelines for a new cladding tool are developed in this chapter. Several geometries are tested with experiments and further reviewed with a model.

4.1 Introduction

A cladding tool for continuous friction surface cladding is a combination between FSC and an aluminum extrusion process. The extrusion occurs inside the support block to heat and deliver the material, while the cladding process is on top of the substrate. The design starts from the process of cladding a layer of 6262 T9 aluminum (AA6262) or AA1050 on an AA2024 substrate. A solution should consider the following factors: a steady outflow of clad material, temperature and force build-up and rotation of the clad material close to the substrate.

The design of a flexible aluminum extrusion tool is described by A.J. Koopman[16] in his PhD thesis. The design process itself is described as a trial and error process, but there are various guidelines. Potential problems are in dead zones, force build-up, geometry and fittings of the extrusion block. The research of Li et al[13] reviews the pinless friction stir welding of AA2024-T3 joint and its failure modes. This pinless tool welding can be combined with an extrusion tool for printing research.

A model is built to compare the results of the design experiments with simulations. Based on the experiments and model the printing tool design is reviewed for feasibility. For the model the PhD thesis of Rituraj Nadan[17] about the computational modeling of heat transfer and visco-plastic flow in friction stir welding is a guideline. The printing process is a complex physical process with a non-Newtonian viscoplastic flow. Challenges are in the frictional heat, deformation heat and the stick-slip conditions at the contact interfaces. The relative large heat deflection of the substrate and tool is a further challenge.

The model is built in COMSOL multiphisics 4.4[18], based on two tutorials regarding fluid-structure interaction in aluminum extrusion[19] and friction stir welding[20]. The FSW tutorial studies the heat transformation and ductility of the aluminum in a FSW process. The aluminum extrusion model calculates the stress and heat generation based on the viscosity. The determined is simulated by the Zener-Holloman parameter. Data of this model[21] is compared with the research of Asthiani et al[22]. Asthiani uses the Zener-Holloman parameter to simulate the behavior of the commercially pure AA1070 aluminum. AA1070 is comparable to the commercially pure AA1050 aluminum used in this research. Asthiani mentioned the increased flow stress with higher strain rates and lower temperatures. Strain rate influences the constants of the Zener-Holloman equation. This effect is accounted for in the formula, to ensure a good fit between the predicted and experimental results.

4.2 Design analysis

The current setup for FSC produces a single strip and is relative stable and gives good results. The drawback is that the process is sequential and the preparation time is long. The preparation mainly consist of cleaning the cladding tool and re-installing the tool with a new cladding rod. For industrial purposes a (semi-) continuous process is required. Based on the research in chapter 2 the following influencing parameters are known: the normal force, rotation speed, temperature and supply rate. Unbalance between these parameters caused several problems during the experiments in section 2 and 3. The thesis of A.J. Koopman[16] about die casting of aluminum mentions various problems in the extrusion and transport of the aluminum. The combination of these two information sources gives some potential problems to be considered:

- Aluminum stuck to the tool
- A high force build-up
- Aluminum in the spacing of (rotating-) parts
- Dead zones in the aluminum flow process
- Irregular inflow and outflow of aluminum
- Start-up of the process
- Deformations of the support block or cladding tool due to pressure and temperature

4.2.1 Morphological scheme

Information from both experiments and literature already described in this report is applied for a morphological scheme. The scheme is in table 4.1 and describes various input geometries. The first two rows describe the supply material shape and diameter, followed by the supply direction and mechanism of the material. The rows with the heating, material delivery, pressure and guidance process describe parameters of the support block. The last row rotation/cladding tool chooses between a solid and a hollow rotating tool, comparable between the choice of a FSW welding pin or a FSC cladding tool. The morphological scheme is used for conceptual design on the next page.

Table 4.1: The morphological design scheme

Shape of the suply	○	□	▭	△
Diameter	5 mm	10 mm	15 mm	20 mm
Suply Direction	Side	Top	Bottom	
Suply mechanism	Suply line	Pressure	Roling wheels	Tread
Heating	Heating element	Laser	Friction	
Process style	Infinit	Serial	Piece	
Pressure	Hydraulic	Pneumatic	Mechanical	
Guidance	No guidance	Fixed	Flexible	
Rotation/Cladding tool	Hollow	Solid		

4.2.2 Concept design

Five concepts are designed based on the morphological scheme in part 4.2. These five concepts are presented and reviewed in this section, based on which a concept is chosen. Each concept has a schematic view, shown in figure 4.1.

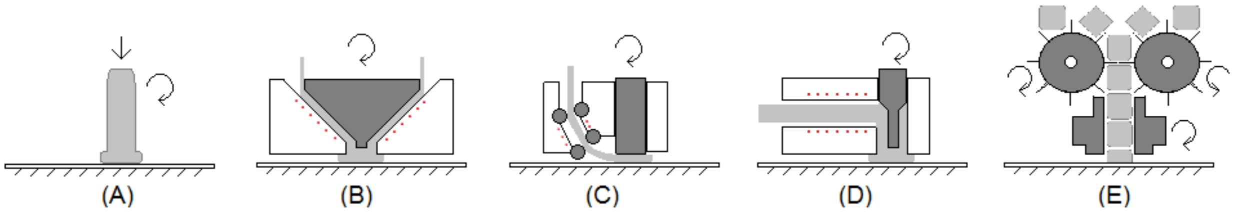

Figure 4.1: Five different concepts designs for a continuous cladding devise. In the schematic view the blank parts are the non-moving parts. The grey parts are the supply material and dark grey parts are the rotating parts. Arrows indicate a force or a rotation and the red dots indicate potential spots for heating elements.

Design 1

The first concept (figure 4.1-A) is a friction surfacing setup. In the concept a cladding rod rotates on the substrate. The concept does not use pre-heating of the material or a cladding rod. Parameters to controle the process are the downward force, rod diameter and the rotation speed. The advantage of the process is its simplicity. There are also some problems related to the continuity of the process and the surface finish. Dilip[15] improved the surface finish by milling the top surface of the clad layer.

Design 2

A threaded cone for rotating, heating and guiding the cladding material is used for the second concept, shown in figure 4.1-B. The process can use both aluminum wire and powder, which is supplied from the top in the spacing between the support block and the cladding tool. The side opposite to the cone could be heated to enhance the material flow. The concept advantage is the downward delivery and the pre-heating. Disadvantages are in the higher complexity of producing the thread on the cone and the maintaining the right spacing between the parts during the process.

Design 3

The third concept uses a strip of aluminum which is guided from the side towards the bottom of the cladding tool, see figure 4.1-C. The supply material is supplied through the support block and can be preheated before being delivered to the bottom of the tool. The rotating tool will clad the aluminum to the substrate. This process is a modified pinless FSW process. Guidance of the strip is driven by rollers and side supports to prevent unwanted movement. The advantage of the process is the simplicity of the concept and the continuous delivery mechanism. Furthermore the startup of the process is relative straightforward. Potential problems are in guiding the strip to the tool and in changing the cladding direction.

Design 4

The fourth concept (figure 4.1-D) delivers a supply rod from the side towards the cladding pin. Clad material can be pre-heated in the support block before contacting the cladding pin. The cladding pin will further heat and transport the aluminum to the substrate material. The advantage of the process is the simple delivery system and internal structure. Potential problems are in aluminum moving upwards and askew forces on the rotating cladding pin.

Design 5

The last concept tweaks the current cladding tool for a continuous delivery system. New supply rods are constantly supplied by the delivery system, while the system simultaneously applies downward force. The delivery system is based on two cogs. The system is designed based on the well-studied current process, which has good cladding results, while another advantage is the steady supply. Challenges are in the high complexity and controlling the downward force.

4.2.3 Concept choice for further development

From the five concepts one is selected for further development. The concept is selected by grading a four elements. The first element is the expected surface finish. The estimation is made based on earlier experiments and literature. Simplicity is defined as the amount of complex and tight fitting parts. Continuity gives an indication of the material supply flow and stability predicts constancy the cladding process. The final scores are in table 4.2.

The first concept has a relative straightforward process with a good stability. A disadvantage is the poor surface finish, which is expected due to the lack of a cladding tool or support block. Furthermore the continuality of the supply material is low, as the rod has to be replaced after depletion. This could be solved by a kind of extrusion process, but this will lower the simplicity of the concept.

The second concept probably produces a good surface finish due to the bottom of the support block. Continuality is also expected to be good. The challenge is to provide a stable delivery of clad material and pressure build-up of the material between the block and the cone. Controlling the heat production and pressure though the rotation speed is difficult during the process. These disadvantages result in the lower scores of stability and simplicity.

The third concept has the side delivery of a strip of aluminum under a rotating cladding tool. The advantage is a straightforward material supply system, and the surface finish should be good. However, it might be a challenge to guide of the supply material under the tool, this reduces the score on stability.

The fifth concept uses the current setup as a basis with an automated rod supply mechanism. The surface finish is expected to be best in this scenario due to the rotating tool edge. A challenge is to deliver the aluminum at a constant supply rate and with constant force. A second challenge is in the multiple rotating parts. These two factors result in a low score for simplicity and stability.

The fourth concept is the most promising concept among the five concepts. The design is straightforward to realize. There is a small risk of upward flow of material, but there are no complex parts. The heating can be performed with a heating element or by viscose heating. The concept is expected to perform relative well on all grading elements.

Table 4.2: Comparison of the concepts with test scores

	Surface finish	Simplicity	Continuality	Stability	Total
Concept 1	-	++	-	+	**+**
Concept 2	+	0	+	+	**+++**
Concept 3	+	+	+	0	**+++**
Concept 4	+	+	+	+	**++++**
Concept 5	++	-	+	-	**+**

Feasibility test

Concept four is further developed in section 4.3. The feasibility of this concept is tested by trying to clad a small point on a substrate. The concept is tested by a series of different printing blocks and transport pins. This pin is applied to transport, heat and rotate the aluminum on the substrate. The block is to confine the aluminum for transport and heat build-up.

4.3 Experimental setup

The concept is tested with three series of experiments, each containing of several tests. Various support block designs are combined with different cladding pins to find the best combination. The support blocks are produced in-house by milling, drilling and turning in the metal workshop of the Univeristy of Twente. The blocks are made of standard construction steel. The experimental design is kept simple. The cladding pin geometries are described first and they are followed by the support block designs and experimental setup. The second and third series are updated experiment series based on the results of previous experiments.

The first two series of the experiments are performed with a 5 [mm] 6262-T9 aluminum (AA6262) supply rod, instead of the 5 [mm] AA1050 rod as indented. AA6262 is harder than AA1050, which makes the process more difficult to start and get well flowing supply material. The results of the AA6262 experiment series will give a first insight in the cladding tool design for harder aluminums. The results are also evaluated for the design and the third experiment series, which is performed with A1050.

4.3.1 Cladding pins

In the three experiment series four different pin geometries are tested. The first series use one geometry, the second series use four different geometries and the third series use one geometry. The pin geometries and their clamps are described in an own section per experiment series. The different geometries are shown in figure 4.2.

Series 3.1

The first series uses a drill of Ø6 and Ø10 [mm]. The end of the drill is cut flat, as a flat bottom surface to clad the material to the plate, see figure 4.2-A. The drill is placed with the flat bottom just above the substrate. The groove of the drill is to transport the aluminum, warm up the material and build-up the required force. The flat bottom of the drill should clad the material to the substrate. The drill is clamped with a collet in a custom made collet chuck.

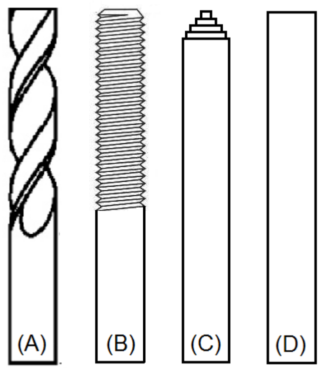

Figure 4.2: different clad-pin geometrics. A is at topped drill, B is a screw, C is a topped round pin and D is plain round pin.

Series 3.2

The second series uses four identical blocks with four different Ø6 [mm] cladding pins, shown in figure 4.2. Pin A is the same as in the first experiment series, a Ø6 [mm] drill with a flat bottom. The second pin (B) contains bolt thread to transport the aluminum downwards to the contact point. The third pin (C) is a cylinder with pointed tip, to allow for more material build-up close to the substrate. The fourth pin (D) is a simple cylindrical pin with a flat bottom. All pins are again clamped with a collet in a custom made collet chuck.

Series 3.3

The third experiment series use pin B in figure 4.2. The clamping of cladding pin with the collet is of the major problems during the previous experiment series. The cladding pin has the tendency to start rotating inside the collet. To prevent the slip of the cladding pin in the collet, the collet holder is changed to a Ø6 [mm] clamping tool. The clamping tool fixes the round pin on a flat side , which will prevent slip, so the pin will either rotate or break.

4.3.2 Support block

In all the experiment series seven different support block geometries are tested. The first series has four different geometries, the second series uses one geometry and the third series uses two support block geometries. The geometries of the support blocks are described in section per experiment series.

Series 3.1

The first test series uses a support block of 80*25*25 [mm]. A cross section of the first experimental setup is in figure 4.3. The horizontal Ø5 [mm] hole is to supply the clad material. The vertical Ø6 [mm] hole in the support block is for the cladding pin. The support block is designed with four different internal geometries. Two support block designs are tested for a Ø6 mm cladding pin. One block has a vertical hole of Ø6 [mm] trough block, the other block has a vertical hole of Ø6 [mm] in the upper section and a vertical Ø7 [mm] hole in the lower section. This wider lower section provides more space for the supply material. A similar configuration is produced with a vertical hole of Ø10 [mm] as a basis for a Ø10 [mm] cladding pin. One block design has a hole of Ø10 [mm] through block and the second has a widened bottom part of the hole of Ø11 [mm].

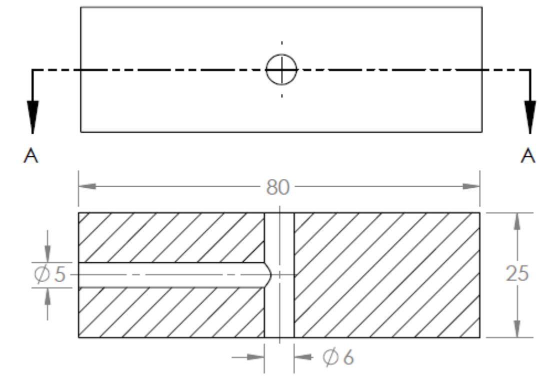

Figure 4.3: Schematic cross section of the first support block.

Series 3.2

The second series of tests has a slightly altered support block compared to the first series, as shown in figure 4.4. The block dimensions are 100*20*20 [mm]. The news support block contains a Ø13 [mm] hole at the end for fixing the block to the table. The Ø5 [mm] horizontal supply hole is drilled 5 [mm] above the bottom. This relocation of the horizontal hole is to supply the clad material closer to the substrate and generate the heat closer to the substrate. The vertical hole for the cladding pin is Ø6 [mm].

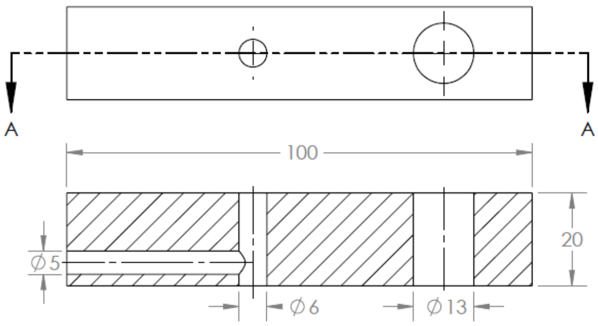

Figure 4.4: Schematic cross section of the second support block.

Series 3.3

In the third series of test has a different clamping tool is used and this tool is partial in the support block. Secondly an extra fixing hole of Ø13 [mm] is added for extra safety. To accommodate these both changes the block size is increased to 100*50*30 [mm]. The third series contains of two different support blocks.

The concept of support block 3a, as shown in fig 4.5, is similar to that of the experiment series 3.2. There is a horizontal supply hole on the left side. The aluminum is supplied from the side to the cladding pin. The pin hole is Ø6 [mm], with a total depth of 10 [mm]. An advantage of this design compared with the design of series 3.2, is

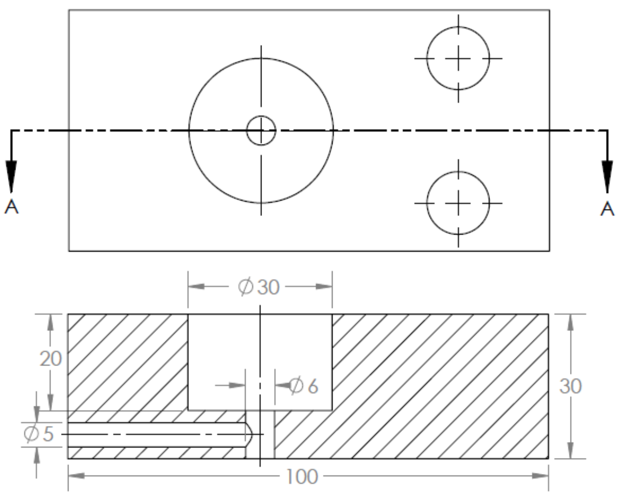

Figure 4.5: Schematic cross section of the support block 3a.

the clamping of the cladding pin. This clamping prevents slip of the cladding pin due to the sideways force of the material supply on the cladding pin.

The support block 3b prevents the possibility of bending the cladding pin by supplying the clad material on the clamping tool, see figure 4.6. This is a combination of design 2 with design 4 of section 4.2.2. To accommodate the heat and force build-up, the block is specified to just fit the in the support block. The aluminum is heated between the clamping tool and the support block, while the cladding pin has a thread to transport the AA1050 to the plate.

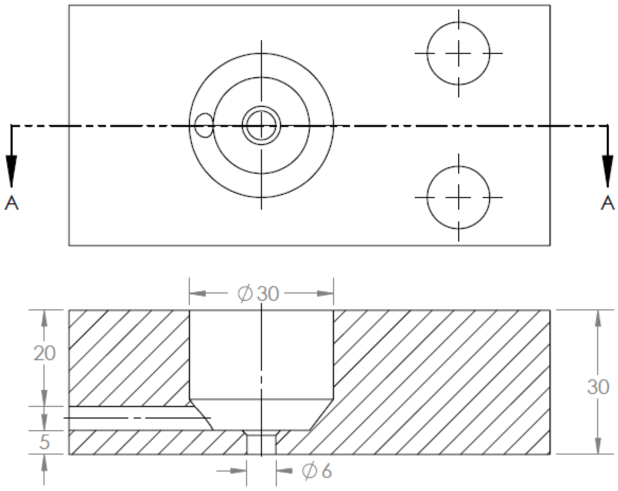

Figure 4.6: Schematic cross section of the support block 3b.

4.3.3 Experimental setup

Experiment series with the different pins and support blocks are performed with the planar machine. Before fixing the block, the tool and cladding pin is lowered into the support block to ensure a good placement. The support block is fixed to the table with clamping bolts. Under the block a AA2024 substrate is placed. The material is supplied from the side and is regulated with a hydraulic jack. The jack delivers enough force to slowly drive the aluminum in the block, see figure 4.7.

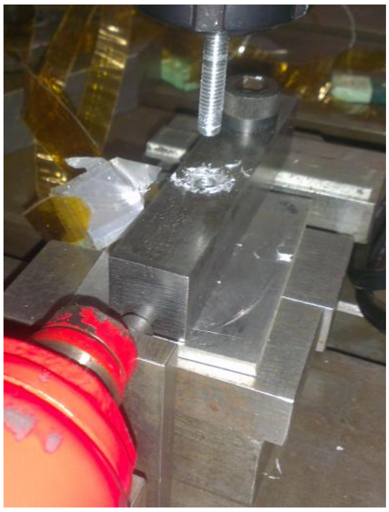

Figure 4.7: Test setup of the print series 2 block.

Each support block will have four K-type thermocouples to monitor the temperature. An example of thermocouple placement in the support block of experiment series 3.2 is in figure 4.8. The first thermocouple (1) is at the outflow point of the aluminum close to the substrate and the second thermocouple (2) is about 5 [mm] above that point. The third thermocouple (3) is placed where the supply material comes in contact with the cladding rod. The fourth thermocouple (4) is placed at the supply channel of the aluminum, at 10 [mm] form the vertical hole of the cladding pin. The fourth thermocouple is to monitor the general temperature of the block during the process.

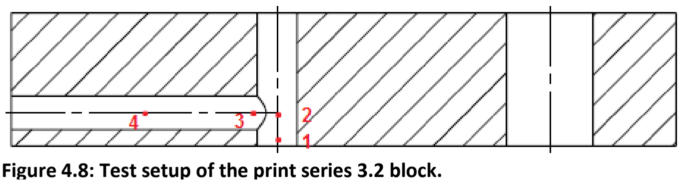

Figure 4.8: Test setup of the print series 3.2 block.

4.4 Results and discussion

The chapter is divided in three sections, each reviewing a experiment series. The series are described in chapter 4.3. The review is performed by evaluating temperature, force, cross sections and the general behavior of the experiments regarding AM.

4.4.1 Results of experiment series 3.1

The first experiment series consist of 4 tests. The tests are performed with a support block of 80*25*25 [mm] and the supply material is AA6262. In total there are four cladding attempts in this section with three different support blocks. The cross sections are visible in figure 4.9-4.11. A toped drill of Ø6 [mm], figure 4.2-A, is used as cladding pin for experiment 3.1.1, 3.1.2 and 3.1.3. The fourth experiment also uses a topped drill, but with a Ø10 [mm]. The cladding pins are mounted with a collet. The temperatures of all experiment are in appendix N.


Figure 4.9: Experiment 1 + 2.


Figure 4.10: Experiment 3.

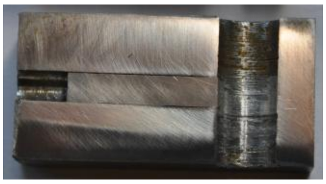
Figure 4.11 Experiment 4.

Test 3.1.1

The first experiment uses a Ø6 [mm] vertical hole, without widening in the lower part. The cladding pin rotates at a rotation speed of 600 [rpm], while the material is slowly added from the side. The bottom side of the support block is without a substrate to check the material transport. An increase in temperature to 40 [°C] occurs at the moment when the supply material is added. The splinters material fals out at the bottom, so the drill cuts the material and transports it downwards.

Test 3.1.2

The second test is the same as the first one. However, a substrate is placed under the support block. When the supply material is added, the heat increases to a maximum of 100 [°C]. This heat increase is both at the supply point of the aluminum and at the cladding point just above the substrate. The experiment ends because the drill is welded to the block (figure 4.9) and the pin starts to slip in the collet. This slip heats the collet to a high temperature till the collet breaks, see figure 4.12. The supply AA6262 is welded between the block and the drill and the space inside the drill is filled with AA6262 splinters. The process has a relative low pressure and temperature, but there is still some material welded to the support block. Most welded material is close to the supply point, which is higher than intended. The material should be welded material should to the substrate.


Figure 4.12. The broken collet.

Test 3.1.3

Test 3.1.3 uses a different support block than test 3.1.1 and 3.1.2. The outer diameter of the lower part of the cladding gap is Ø7 [mm]. This means a gap of 0.5 [mm] between the cladding pin and the surface of the support block, which allows for more supply aluminum inside the support block. The tool rotates at 600 [rpm]. The AA6262 is supplied at a slow pace while the tool moves slowly upwards. Force build-up is thus avoided. The gradual approach results in a temperature over 300 [°C] in the support block. The sideway force of the supply aluminum bends the pin during the process, which makes the cladding pin touch the side of the block. This contact breaks the cladding pin, so the experiment stops. The high temperature did weld clad material to the pin and the

Figure 4.13: The cladding pins of experiment 3 and 4.

support block, which is visible in figure 4.10 and 4.13-A. Welded material is visible in both the intended downward and in the unintended upward direction, which is negative for the usability of the topped drill as a cladding pin.

Test 3.1.4

The fourth uses a Ø10 [mm] topped drill (figure 4.13-B) and the corresponding support block. To compensate for the larger diameter the rotation speed is lowered to 450 [rpm]. The experiment starts with a temperature build-up to 150 [°C] when material is supplied. At the moment when the temperature goes over 150 [°C], the drill contacts the side of the support block. In this setup the drill is stronger than the clamps of the support block, so the block starts rotating and breaks the setup. Therefore, the fixing of the support blocks should be improved to increase the safety.

4.4.2 Results of experiment series 3.2

The second experiment series consists of seven tests. The setup has an updated support block based on the results of the first experiment series. The dimensions of the block are 100*20*20 [mm]. The supply channel for aluminum is lowered, to place the heat generation and supply material closer to the clad surface. Furthermore a hole for fixing the block is added, which prevents the rotation of the support block. In this series seven experiments are performed with four cladding blocks. All blocks have the same geometry, the variation is between the experiments is in the cladding pin geometries and the rotation speed of the pin. A collet is used to clamp the cladding pin. The temperature and force measurements of all experiments are in appendix O.

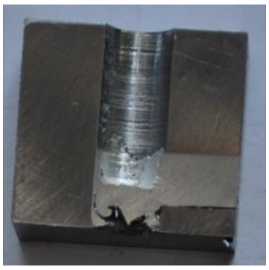

Figure 4.14: Experiment 1, 2.

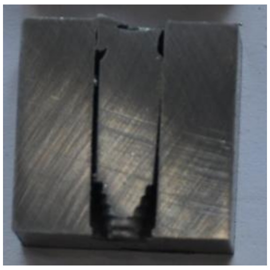

Figure 4.15: Experiment 3.

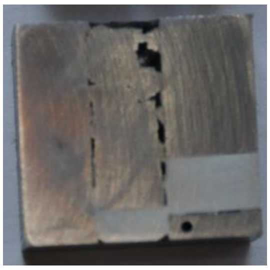

Figure 4.16: Experiment 4

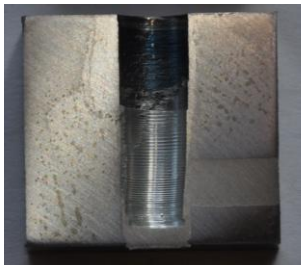

Figure 4.17: Experiment 5 ,6, 7

Test 3.2.1

The first test of the series starts with a bolt as cladding pin, see figure 4.2-B. The thread of the bolt is used to transport the aluminum. When the experiment starts and heats up, the hydraulic jack is on a small angle with the pushing pin to the supply AA6262. Due to this the pushing pin deforms and the process has to be stopped. The experiment shows the importance of proper outlining of the setup.

Test 3.2.2

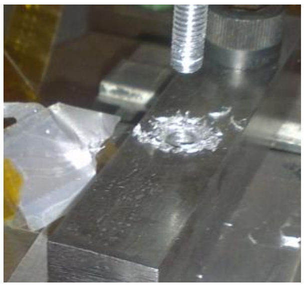

Figure 4.18 The transported aluminum.

Test 3.2.2 uses the same block as the first test of this series. The test starts with a counter-rotating pin at 450 [rpm]. This means the pin will transport the aluminum upwards instead of downwards. During the test the temperature rose to 80 [°C]. AA6262 splinters are moved up, as depicted in figure 4.18. As the transport mechanism is proven, the rotation direction is set back to standard rotating direction. More supply material is inserted from the side to fill the support block. The pin is slowly lowered on top of the supply material. A force of 2.5 [kN] is reached with a temperature of 90 [°C]. The AA6262 is moved down to the substrate and welded inside the support block, as visible in figure 4.14. There is aluminum sticking in the lower part of vertical hole, but there is no sticking above the supply point. This implies the thread of the bolt is working well for transport, even with the high force and resulting pressures. The lower part of the thread is also covered with aluminum, which is shown in figure 4.19-A. The flow pattern of the aluminum indicated that the thread of a bolt is a better transport mechanism for AM than the topped drill used in experiment series 3.1.

Test 3.2.3

The third test uses a new cladding block and different cladding pin. The cladding pin is rotating at 450 [rpm] and has a pointed shape, see figure 4.2-C. The concept of this pointed end is to give the supply material more place to accumulate. As soon as the supply of AA6262 starts, the pin touches the side of the support block. Due to the contact the cladding pin breaks, as visible in figure 4.15 and figure 4.19-B.

Test 3.2.4

Test 3.2.4 uses a flat round cladding pin (figure 4.2-D) in a new support block. To prevent the breaking of the pin and increase the heat generation the rotation speed is increased to 1000 [rpm]. Furthermore the supply material is added before the cladding pin is lowered, so the pin rotates down through the supply material. This reduces the risk of the cladding pin touching the side of the support block due to the sideway force of the supply material. The temperature rises slowly to a maximum temperature of 200 [°C], with force peaks over 4 [kN]. The pin is raised to check the condition in the middle of the test and the condition of the pin appears fine on visual inspection. After the inspection, the pin is moved back into the block. However, as soon as some extra material is supplied from the side, the pin breaks. The pin and welded aluminum are in figure 4.16 and 4.19-C.

Test 3.2.5

The fifth test continues with the flat and round drill. The drill works well for the heat generation and force build-up in test 3.2.4, but it tends to break. A toped drill (figure 4.2-A) is mounted in the collet up-side down to get a flat round cladding pin (figure 4.2-D) of better quality. The pin rotates at 1000 [rpm]. Clad material is supplied before lowering the cladding pin to avoid the cladding pin touching the support block. The pin is lowered through the supply material. The block heats up to over 400 [°C] with force peaks of up to 4 [kN]. These forces are values close to the cladding conditions in chapter 2. The test stops because of a deformed supply pin, which stopped the material supply. The lowest point the pin reached is 2 [mm] above the substrate. The temperature and force appear to be in the cladding range, but the cladding pin is probably still too high above the substrate for a weld. This assumption is tested in the next tests.

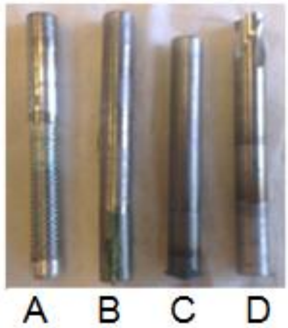

Figure 4.19 The used cladding-pins .

Test 3.2.6

Test 3.2.6 continuous where the fifth test stopped. The sixth test aims to achieve higher temperature and force build-up by supplying more material and moving the cladding pin closer to the substrate. The tool rotates again at 1000 [rpm] and is slowly lowered into the block to allow the force and temperature build-up. The tool is lowered till 0.8 [mm] above the substrate, and then moved back up again. Temperature increased to over 400 [°C] in the support block and the force is between 2 and 4 [kN]. This is again enough for cladding aluminum, though the force is still relative low compared with the force in section 1 and 2. There are also no traces of bonding between the clad material and the substrate.

Test 3.2.7

The last test of the series places the cladding block 0.25 [mm] above the substrate. This gap between substrate and support block allows for some pressure release and should help the build-up of a cladding point. The support block is still the same block as used in test 3.2.5 and 3.2.6. The cladding pin is rotating at 1000 [rpm]. The pin is slowly lowered to the same position as in test 3.2.6. AA6262 is slowly supplied. Temperature increases to a level above 400 [°C] with peaks over 500 [°C]. The force remains low at an average value of 1 [kN]. Peaks in temperature and force are visible at the moment material when the material is supplied. The test works well for the temperature, but the force is relative low for cladding. There is also no cladding of A6868 onto the substrate. The pin used for the test is shown in figure 4.22-D. Reviewing the cross section of the block in figure 4.17, the aluminum moved both in the upward and in the downward direction, so the flat round pin works less well for the material flow than the threaded pin. All in all both tests with a cladding pin at 0.8 [mm] did not produces a weld, albeit temperature and force where close to the cladding range.

4.4.3 Results of experiment series 3.3

The third experiment series consist of 3 tests. The setup uses a different clamping tool for the cladding pin, thus another support block is required. The different clamping tool uses a hole of Ø6 [mm] for the cladding pin and a set screw to fix the pin to prevent slip. For the test two different support blocks of 100*50*30 [mm] are prepared. The first support block repeats test 3.2.2. The second block supplies the clad material on the clamping tool edge, thus entirely eliminating the risk of breaking the cladding pin. Due to the possible larger force, two security holes are added to fix the block. The test of the third series are with AA1050 supply material. The results of temperature and force during experiment series 3.3 are in appendix O.

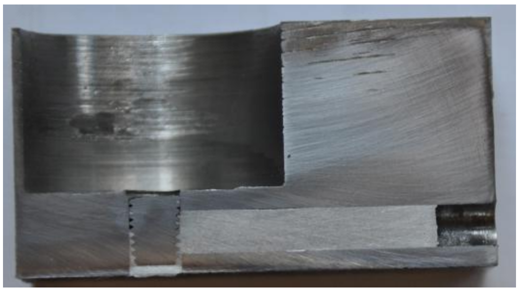

Figure 4.20: Experiment 3.3.1 and 3.3.2.

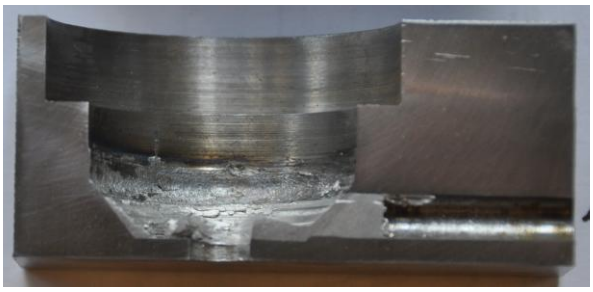

Figure 4.21: Experiment 3.3.3.

Test 3.3.1

The first test is a re-examination of test 3.2.2 with a different tool and supply material. The rotation speed is set at 600 [rpm] and there is no substrate under support block 3a. The removal of the substrate is to test the transport capacity of the bolt thread. The AA1050 is supplied slowly from the side. During the test there are small force and temperature fluctuations, due to the irregular supply of aluminum. Added aluminum is transported down and falls out, see figure 4.22. The process is stopped to check the transported material.

Figure 4.22: The deposited AA1050 under the support block.

Test 3.3.2

A substrate is placed under support block 3a for the second test. This enables accumulation of material and force build-up. The tool rotates at 600 [rpm]. The pin is lowered to 0.8 [mm] above the substrate before the AA1050 is supplied. As soon as there is material supply, the temperature starts to rise slowly. Simultaneously the force is increasing. When the material is supplied, the force rapidly increases to a peak of 12 [kN], while the temperature reaches 100 [°C]. Due to the large force the cladding pin breaks. Reviewing the process for AM based on figure 4.20, it is visible that the screw works well for building force and transporting aluminum. Above the supply channel there are no traces of aluminum, so all the material supply goes downward. The temperature will increase with a longer process time, bigger cladding pin diameter or a higher rotation speed. Placing the support block above the substrate should allow for force relieve, just as in test 3.2.6.

Test 3.3.3

Support block 3b is used in the final test 3.3.3. The block is designed to deliver the supply material on the clamping tool, instead of on the cladding pin. The tool is lowered in place while rotating at 600 [rpm]. The AA1050 is delivered slowly onto the clamping tool. The support block heats up quickly, to a top temperature of 430 [°C] and the temperature is probably higher at the tool surface, as visible in figure 4.23. The force meanwhile remained stable around the 2 [kN]. When the supply of the material stopped, the clamping tool locked inside the support block. Reviewing the support block in figure 4.21, the supply aluminum is at the outside. The cladding hole is not filled. Temperature in the design is high enough, but the transportation and force towards the substrate are insufficient.

Figure 4.23: The used cladding-tool + pin.

4.5 Simulation Model

A computer model is built for more insight in the behavior of the supply aluminum in the support block. First the setup and geometry of the model is explained. The results of this model are then compared with the experimental data in section 4.4. Both support blocks of experiment series 3.3 are analyzed and compared. The model is built in COMSOL Multiphysics 4.4.

4.5.1 Preparation and assumptions

The material of the cladding pin and support block are assumed constant during a simulation, while the material properties of the aluminum vary depending on the temperature and shear rate. The cladding pin and support block use the standard steel properties in COMSOL. The material properties of the substrate beneath the tool are depending on the temperature and determined in by Li[23] and the plots are available in appendix Q. The AA1050 supply material is modeled as a fluid with a high viscosity, while the other properties are held constant. The modeled material properties are in table 4.3.

Table 4.3: Properties of the materials in simulation.

		Steel	AA2024	AA1050 fluid
Thermal conductivity	[W/(m*K)]	45	164 – 217*	190
Heat capacity at constant pressure	[J/(kg*K)]	500	880 – 1150*	900
Density	[kg/m^3]	7800	2780	2700
Dynamic viscosity				η

* interpolated values based various date points, the plots with the data are in appendix Q.

The dynamic viscosity (η) depends on the temperature and the shear rate ($\dot{\gamma}$) and is simulated with a Zener-Holloman parameter(equation 4.1) in a hyperbolic sinusoidal type equation (equation 4.2). In this manner the flow behavior is approached in a relative straight forward way, while compensating for both temperature and shear rate. This is a comparable approach as in the COMSOL tutorial and the paper of Asthiani et al[22] about the flow behavior of the commercially pure aluminum alloy AA1070. The values used for the Zener-Holloman parameter are based on these two sources and are in table 4.4.

The Zener-Holloman parameter is defined as:

$$Z = \frac{1}{\sqrt{3}}\dot{\gamma}e^{\left(\frac{Q}{RT}\right)} \quad (4.1)$$

Which is used to calculate the dynamic viscosity by:

$$\eta = \frac{ashinh\left(\left(\frac{Z}{A}\right)^{\frac{1}{n}}\right)}{\sqrt{3}a\dot{\gamma}} \quad (4.2)$$

In this functions $\dot{\gamma}$ is the shear rate and T the temperature. Multiplying of the formula with $\sqrt{3}$ is to compensate for the difference in von Mises stress in the formula en the definition in COMSOL. To prevent viscous heating above the melting temperature, the dynamic viscosity reduced to zero at 502 [°C] by a steep ramp function.

The model uses conjugate heat transfer model of COMSOL and a time dependent solver. The heat generation is simulated by viscose heating. The solving of the model is with a triangular mesh and a direct PARDISO solver and the time steps are 0.1 [s] with a total analysis time of 30 [s].

Table 4.4: Variables and input values of the Zener Holloman equation

Variables	Value	Unit	Description
T	Calculated by the model	[K]	Temperature at the node
$\dot{\gamma}$	Calculated by the model	[1/s]	Shear rate at the node
Z	Determined by equation 4.1	[1/s]	Zener-Holloman parameter
η	Determined by equation 4.2	[Pa*s]	Dynamic viscosity
Constants			
Q	150.000	[J/mol]	Activation energy of the process
n	2.97	[-]	Experimental determined material constant
A	2.39e8	[1/s]	Experimental determined material constant
α	0.0521	[1/MPa]	Experimental determined material constant
R	8.31	[J/(K*mol)]	Gas constant

4.5.2 Model geometry

The model of both test of experiment series 3.3 is built as a 2D axisymetric model. In figure 4.24 and 4.25 the models are shown. The center line of the cladding pin is assumed as the symmetry axis, at the left in both figures. The pin & clamping tool (E) and clad material (blue) are axi-symmetric in the concept. These can be used with the original settings. The support block (F), aluminum substrate (G) and backing table (H) are not circular, hence these are changed to axi-symmetric. The support block (F) has a height of 30 [mm] and an assumed diameter of Ø60 [mm]. The diameter is thus a bit longer than the width and a bit shorter than the length. The 4 [mm] thick aluminum substrate (G) is modeled as a cylinder of Ø80 [mm]. The table (H) is modeled as a Ø100 [mm] cylinder with a height of 30 [mm].

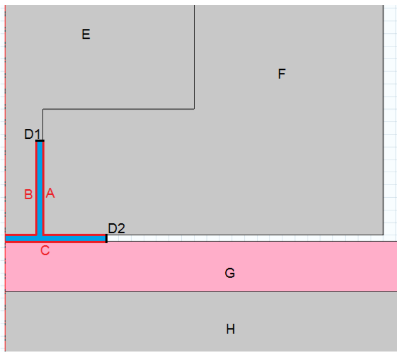

Figure 4.24: The COMSOL model of experiment 3.3.2, the blue part is the fluid AA1050, the pink part (G) the substrate, the grey parts are steel.

The boundaries which interact with the clad material are marked with red in figure 4.24 and 4.25. The walls of the support block (A) are modeled as a stationary wall with a no slip condition. The wall between the AA1050 and the substrate (C) is also seen as a stationary wall without slip. All exterior walls are assumed to radiate heat to an environment of 20 [°C] and the bottom of the table (H) has a constant temperature of 20 [°C].

The wall between the AA1050 and the pin & clamping tool (B) is modeled as a moving wall. The movement of the wall (v_{wall}) is in the direction of the tool rotation and determined by multiplying the rotation speed (ω, 600 [rpm]) with the radius(r):

$$v_{wall} = r * \omega \quad (4.3)$$

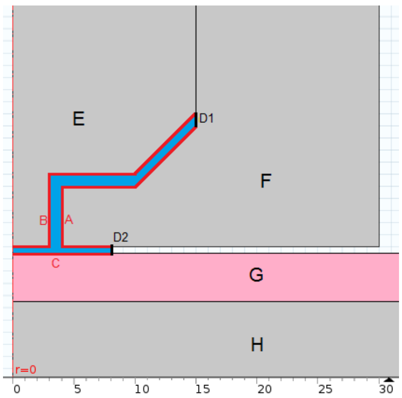

Figure 4.25: The COMSOL model of experiment 3.3.3, the blue part is the fluid AA1050, the pink part (G) the substrate, the grey parts are steel.

To simulate the thread, a wall movement alongside the wall is simulated by multiplying the pitch (n, 1 [mm]) with the rotation speed (ω, 600 [rpm]):

$$v_{tread} = n * \omega \quad (4.4)$$

The supply is modeled as an inward flow of aluminum at the top of the clad material layer (D1). The inward flow is 1 [mm/s] and the inflow is in the normal direction. The outflow (D2) is free with no pressure (p=0) at the outflow boundary.

4.5.3 Parameter review

The model of test 3.3.2 is used for a parameter analysis to review the model and see the influence of changing parameters. The clad layer width, the rotation speed and the supply are varied to test the model. Each comparison has a reference plot and a second changed plot. The comparisons are based on the pressure, temperature and velocity profile.

The first comparison shows the influence of the clad layer width in figure 4.26. The wide clad layer has a radius of 8 [mm]. The small clad layer has a 3.1 [mm] radius, just a bit wider than the radius of the supply material. The wide clad layer has a peak pressure over 2.5 [GPa], while the smaller clad layer stays under 250 [MPa]. The difference in pressure is explained by no slip boundary conditions on the walls (figure 4.24-A + C). The pressure required to let the material flow between these non-moving walls raises the pressure in the entire model. This effect eliminates any visible pressure difference close to the cladding pin in the wide clad layer model. Reviewing the model with the small clad layer the pressure increases when the material flows downward. This increase is probably due to the thread of the moving wall. The pressure peak is at the place where the cladding pin ends. As the small clad layer model delivers clearer pressure results, this model is used further on.

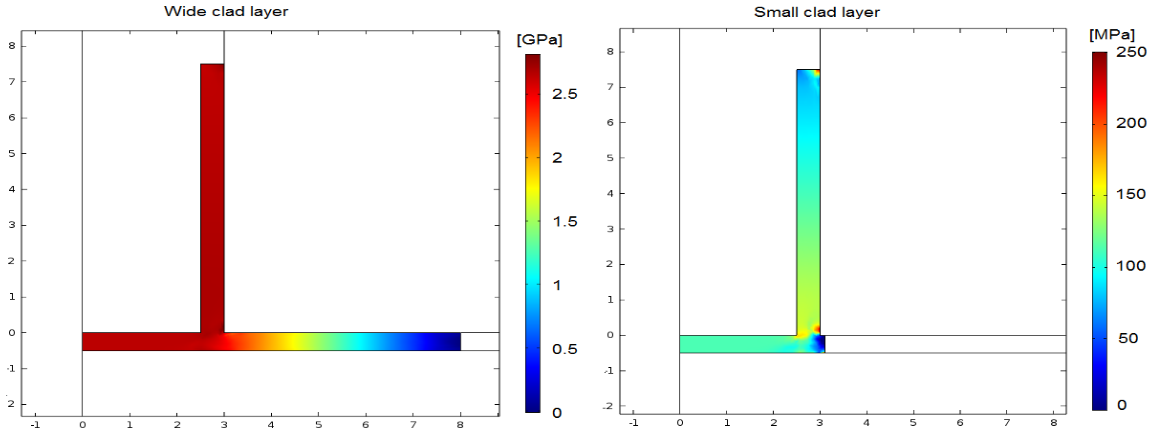

Figure 4.26: Pressure plots of the simulation of experiment 3.3.2 with two different clad layer widths. The wide layer has a width of 8 [mm] and the small layer has a width of 3.1 [mm], just 0.1 [mm] wider than the gap in the support block.

In figure 4.27 the influence of the supply rate is reviewed. The left model has a normal inflow of 1 [mm/s] in the vertical direction while the right model has an inflow of 0.5 [mm/s]. The pressure in the horizontal part under the cladding pin is comparable. The vertical supply direction has however a reduction in pressure, the pressure of the higher inflow is about 150 [MPa], while the slower inflow has a peak around 100 [MPa]. The 50% lower material inflow results in a ~30% lower pressure. This influence of the supply inflow is also visible in the experiments series in chapter 4 by force and temperature peaks.

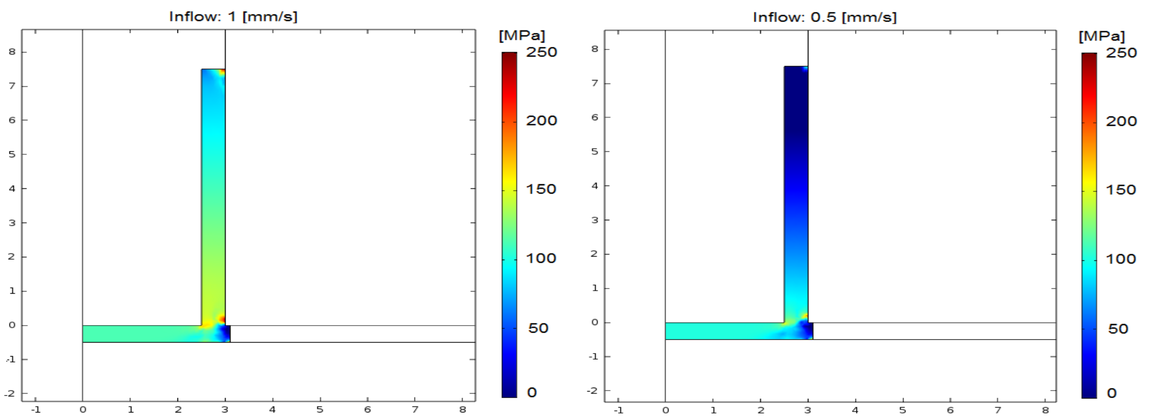

Figure 4.27: Pressure plots of the simulation of experiment 3.3.2 with two different supply rates. The left model has a supply rate of 1 [mm/s] and right model has a supply rate of 0.5 [mm].

The influence of the rotation speed is reviewed in figure 4.28. The model at the right uses a rotation speed of 600 [rpm], while the left model has a rotation speed of 300 [rpm]. The velocity profiles of both models show a similar pattern, but the velocities close to the cladding pin are much higher in the 600 [rpm] model. Most of the material in both models is slow moving. The temperature profile of both simulations are quite different. As heat is generated by viscose heating, the difference in rotation speed results in much higher heat generation for the 600 [rpm] model. The 600 [rpm] model has a temperature over 450 [°C], while the temperature of the 300 [rpm] model stays under 350 [°C]. The highest temperature is located halfway the vertical transport.

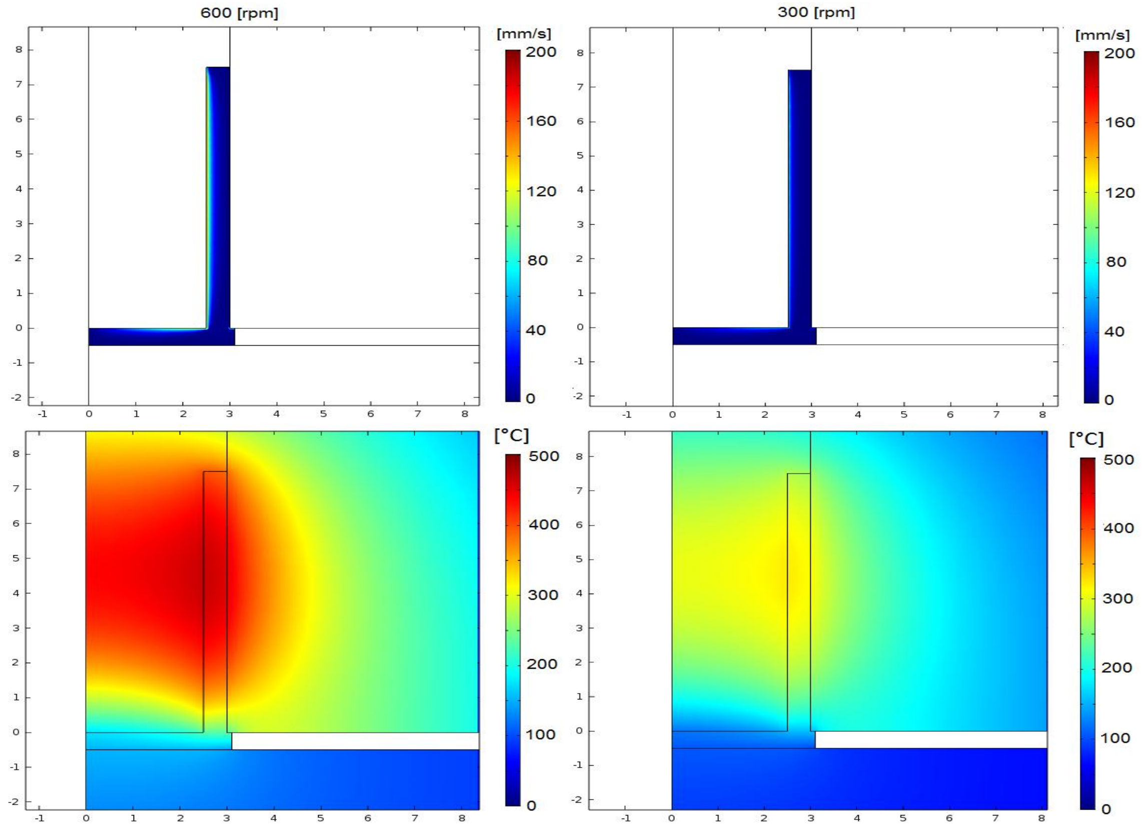

Figure 4.28: Temperature and velocity plots of the simulation of experiment 3.3.2 with two different rotation rate. (A) has a rotation rate of 600 [rpm] and while (B) has a rotation rate of 300 [rpm].

4.5.4 Simulation of test 3.3.2

The geometry and parameters of the model are based on test 3.3.2. Two simulations are compared, one with a threaded cladding to transport aluminum and one without a thread. The model with the thread is comparable to test 3.3.2. The model without a thread is comparable to test 3.2.5 with a different geometry of the support block. The tool is rotating at a speed of 600 [rpm] and the heat is generated by viscose heating. The thread is modeled as a downward velocity of the pin wall. A material uniform inflow of 1 [mm/s] at the top is chosen as the supply speed. At the start of the simulation the temperature of the entire model is 20 [°C] and the test runs for 30 [s]. For the comparison of the models the temperature, flow speed and pressure are reviewed.

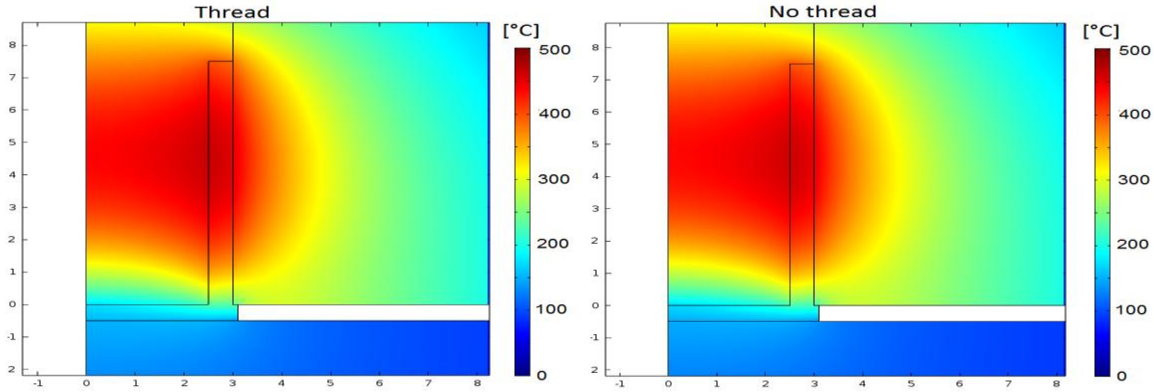

Figure 4.29: Temperature in [°C] of the threaded and not threaded pin.

The use of a threaded cladding pin minorly influences heat generation as shown in figure 4.29. The thread model has a top temperature of 464 [°C] while the no thread model has a peak temperature of 462 [°C]. Most of the heat is concentrated in the support block. At the cladding point above the substrate the temperature is to low (~150 [°C]) for cladding in both simulations. This correspondents with the lack of temperature of test 3.3.2 and the lack of a clad layer in experiment series 3.1, 3.2 and 3.3. More heat can be produced by an increased rotation speed, as simulation in figure 4.28. Other possibilities to increase the heat generation are a wider cladding pin or a heating element in the support block.

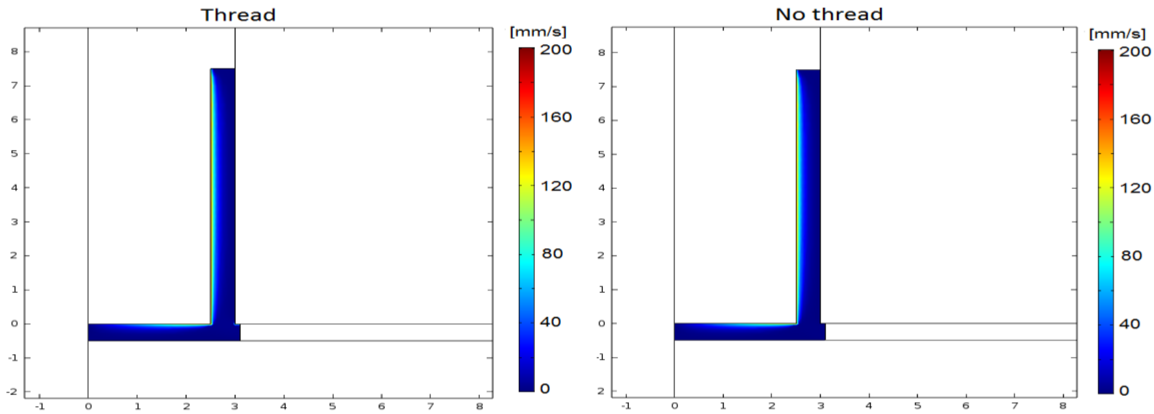

Figure 4.30 : Flow speed of the AA1050 in m/s round the cladding pin.

In figure 4.30 the difference of velocity speed profile of both models is shown. The patterns appear similar as the radial speed is dominant in the velocity profile. The thread model has a maximum velocity of 190 [mm/s], while the no thread model has a velocity of 160 [mm/s]. The maximum velocity is alongside the cladding pin and under the cladding pin there is also a small visible material flow. The rest of the material has a relative slow flow. The velocity is 40 [mm/s] 0.1 [mm] under the tool and 1 [mm/s] 0.1 [mm] above the substrate in both models.

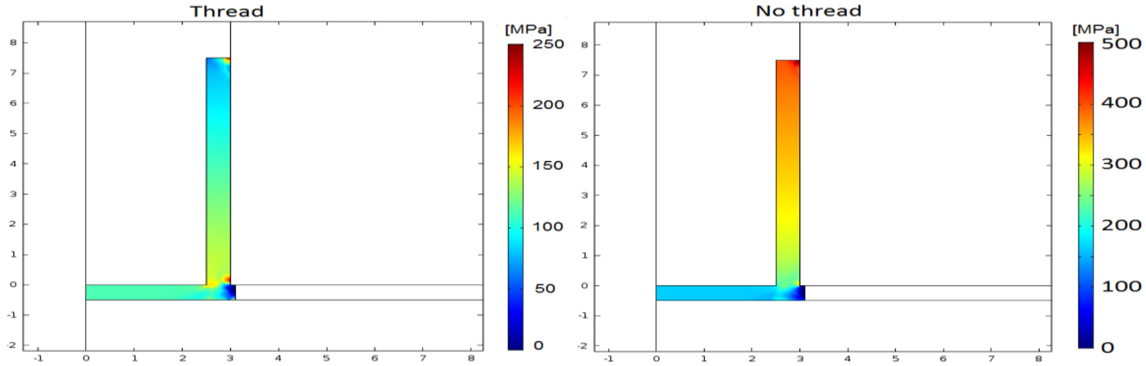

Figure 4.31 : Pressure comparison in [Pa] between a threaded and non-threaded pin.

The pressure distribution of the two models shows a clear difference in figure 4.31. The thread model has a peak pressure of 263 [MPa] while the no thread model has a pressure peak of 529 [MPa]. The pressure distribution of the threaded model is better for AM. The pressure increases to the bottom and is around 125 [MPa] under the tool. The no thread model pressure distribution peaks at the material inflow, and reduces towards the outflow. The pressure is higher under the tool and remains around 200 [MPa]. The height of the peak pressure is in line with the breaking of the pin in several tests in experiment series 3.1 and 3.2.

4.5.5 Simulation of test 3.3.3

The second model is based on the geometry and parameters of the test 3.3.3. The original set-up does not have a thread to facilitate the transportation of aluminum. To further investigate the setup, the original model is compared with a threaded model. The tool is rotating at a speed of 600 [rpm]. The transporting screw is simulated as a moving wall with the same velocity as the thread and is directed alongside the wall. An uniform supply inflow of 1 [mm/s] is chosen as the supply rate. The model starts at a temperature of 20 [°C] and runs for 30 [s]. The temperature, velocity and pressure of the simulations are reviewed.

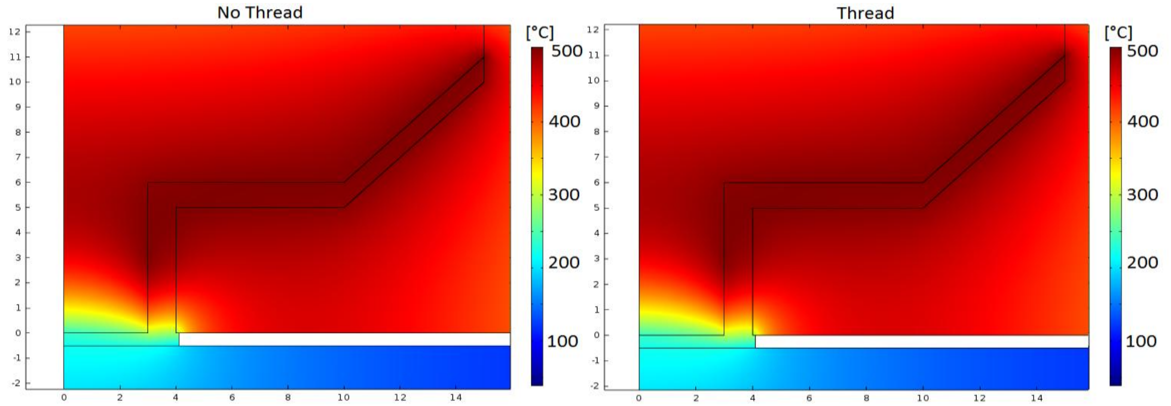

Figure 4.32: Temperature in [°C] of the threaded and not threaded pin.

The temperature distribution in both models is roughly the same, as visible in figure 4.32. Both models reach the aluminum melting temperature of 502 [°C]. The tool generates much heat due to the large diameter. This is also seen in the test 3.3.2. However, the temperature above the clad layer is 225 [°C]. This is still a relative low temperature for the cladding process.

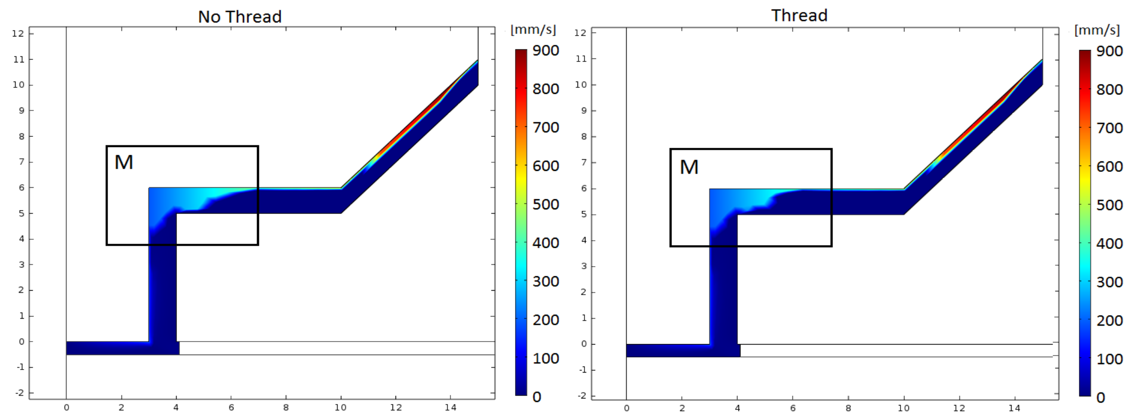

Figure 4.33 : Flow speed of the AA1050 in m/s round the cladding pin.

The velocity profile in figure 4.33 of the both simulations is similar. The relationship between radius and velocity is well visible, hence the speed decreases with the reducing radius. The influence of the thread is small. Only in the corner in the center of the graph (M) a small difference is visible. The higher velocity in this corner is due to the reduced influence of the no slip wall standing wall, so the material can flow well. Above the substrate surface the velocity is lower again. The velocity is 60 [mm/s] 0.1 [mm] under the cladding pin and 2 [mm/s] 0.1 [mm] above the substrate.

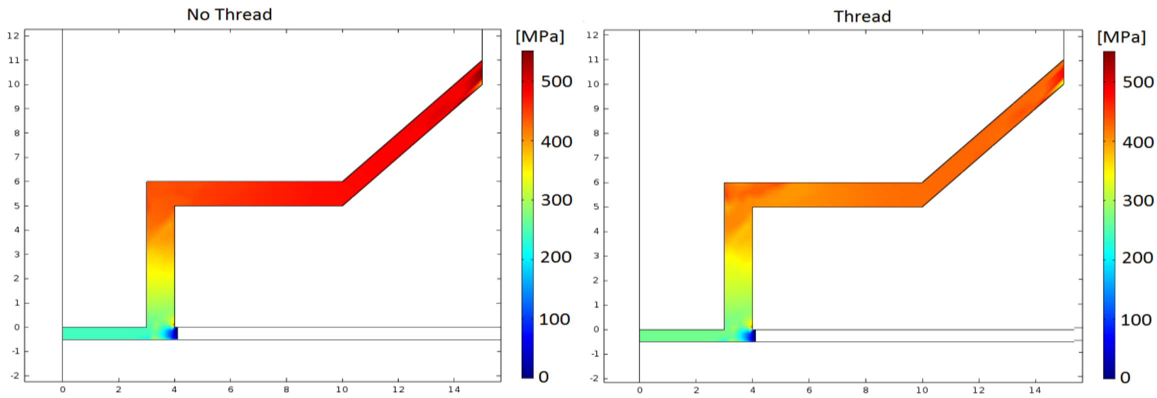

Figure 4.34 : Pressure comparison in [Pa] between a threaded and non-threaded pin.

The difference in pressure between the threaded and non-threaded pin is especially clear at the supply point, as visible in figure 4.34. The pressure of the non-threaded model has a peak pressure of 545 [MPa], while the threaded version has a peak pressure of 482 [MPa]. The positive effect of the thread already recognized in the previous model reappears. The pressure distribution in the thread model is more evenly spread and the entrance pressure is lower. The model of the non-threaded version explains a problem with test 3.3.3. There is no inward flow if the high pressure required for the downward flow is not reached. The pressure in the clad layer is in both cases again around ~250 [MPa]. At the bottom of the support block the pressure drops again, which is a disadvantage for the AM tool.

4.6 Conclusion

Reviewing the design process and the results of the experiment series, the production of a continuous cladding tool for aluminum is difficult. It has not been possible yet to clad aluminum on a substrate during experiment series. A cladding pin which delivers heat, transportation and pressure works relative well inside a support block. The experiment series show it is possible to acquire enough force, temperature and transport. The combining of these factors on substrate for a clad layer remains challenging however.

A cladding pin with a thread like a Ø6 [mm] bolt works well inside the support block. The thread avoids the problems with drills touching the side and breaking due to this contact, while also the transportation is better. The breaking risk of the pin is increased by the sideways inflow force of the supply aluminum. The transport and force build-up with the thread work well. This is supported by the modeling of the experiment series 3.3. The model shows that the thread makes the pressure distribution much more favorable towards the substrate. Force build-up becomes a problem if it exceeds certain limits. The high pressure breaks the cladding pin by clamping it. A relative small pin performed less well on heat generation, but a bigger pin or a higher rotation speed would compensate this. Another solution could be a heat element in the tool or a smaller support block. Both these solutions require less heat generation from the cladding pin.

The biggest challenge is in forming the clad layer in the space between the support block and the substrate. Difficulties are with the stationary edge of the support block and the temperature just above the substrate. Between the stationary support block and the stationary substrate the aluminum stops flowing and the pressure increases strongly if the layer becomes wider, as demonstrated by the COMSOL model. The heat generation in the continues cladding setup is different compared to the FSC process in chapter 2 and 3. Most heat is generated inside the support block, instead of close to the substrate surface where it is needed. This results in a lower temperature at the substrate clad layer interface. Both these effects impede the forming of a clad layer.

Figure 4.35 and 4.36 show two possible solutions to prevent this problem with the heat generation and stationary parts. Figure 4.35 combines design three and four. Moving the tool over the deposited material will generate the heat closer to the substrate and clad the layer. The concept can further be enhanced by an involute grove pattern at the bottom of the cladding pin. The second suggested solution is a combination of design four and five, as shown in figure 4.36. By rotating the edge of the support block, extra heat and movement are generated just above the substrate. This rotating edge works well with the current setup, but will make the proposed printing block more complex.

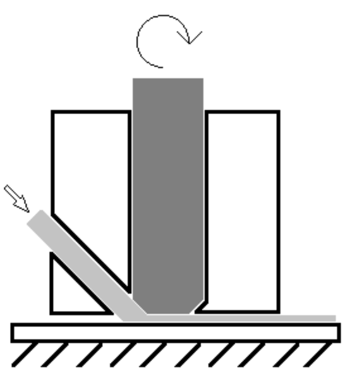

Figure 4.35: A proposed design solution. The stationary parts are in white, clad material is light grey and the moving parts are dark grey.

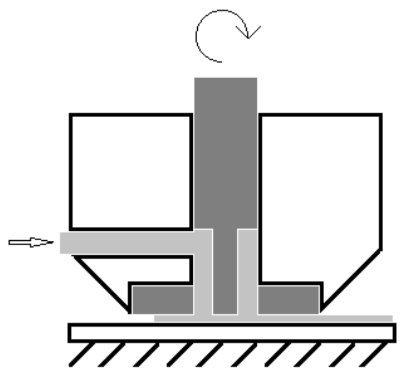

Figure 4.36: A proposed design solution. The stationary parts are in white, clad material is light grey and the moving parts are dark grey.

5 General conclusion

The use of friction surface cladding (FSC) as an additive manufacturing (AM) process appears promising. The FSC has a stable performance for AA2024 on AA2024 within certain window. The layers are smooth, regular and there are no problems with building overlapping layers. Multiple cladding works for both parallel and stacked layers, so building structures is possible. There is a reduction in hardness and strength in the substrate material due to the heating. A heat treatment could solve this reduction of hardness.

Based on the tests with AA1050 the process appears to have the possibility to cope with small irregular surface geometries. The small ridge detectable between two overlapping layers of AA2024 can be repaired based on experiments of parallel cladding and cladding over an edge. To avoid voids and other problems in the overlapping layers, it is preferable to clad the irregularities or overlap at the retreating side and at high temperatures (>400[°C]). High temperature can cause intermixing between layers, but this is not a fundamental problem for the AM. The cladding process over bigger irregularities is more problematic. The filling quality of bigger irregularities is not as good as that of smaller irregularities. With bigger irregularities there are voids in holes and under the layers. However, this can be mostly solved if more material is supplied at higher temperatures. Bigger irregularities have the risk of destabilizing process by losing control of force and temperature.

The main challenge of developing the AM method is to design a continuous cladding device. Pressure build-up and heat generation are possible within a support block, but the bonding to the substrate is difficult. For the AA1050 cladding process within the support block, a threaded bolt works well. This threaded bolt delivers transportation, heat and force. The use of AA2024 in the tool instead of AA1050 will generate more difficulties with the force build-up within the support block, because a harder material will increases the risk of breaking the pin. The problems can be reduced by a heat treatment of the AA2024 and a stronger cladding pin. The main challenge for the process is at the cladding point, as a combination of a stationary support block edge and a low temperature at the substrate/clad layer interface prevents the forming of a clad layer. To clad a layer on the substrate, the tool has to move over the supplied material or the edges of the support block should rotate.

5.1 Recommendations

Based on the research several reconditions for further research are recommended:

- The research of cladding at lower temperatures and higher forces is recommended. In experiment 1.3 there are some problems with the startup, resulting in a low temperature and high forces. The results are good. The substrate has only a 10% decrease in hardness. The current setup is not able to bear much higher forces, with a different setup it would be interesting to investigate even lower temperatures and higher forces.

- More general research on the cladding of AA2024 is recommend, as the process is only proven in a small test window. The parameters are not varied to explore the process window. To better understand the process of cladding AA2024 a more thorough research with varying temperatures, rotation speeds and layer widths is useful. This can be complemented with research about holes, irregularities and higher stacked geometries. This will greatly help to understand the process and possibilities of the AM method.

- Further research on the creation of deliberant holes in the printed product is recommended. With the current setup it is not possible to create deliberate holes. Bigger holes result in a strong drop in temperature and force, while the hole is partially filled. Possible solutions are in overlap cladding and combinations between friction stir welding and friction surface cladding.

- For the design of the continuous cladding tool the use of the third design with a transporting screw similar to a plastic extrusion process works well for supplying material. However, at the delivery point the supply material requires more movement and heat to create a clad layer. Two possible solutions for further investigation are foreseen:
    - The first solution is to move the cladding pin over a delivered material, similar to combining design 3 and 4. In this way the tool welds the supply material to the substrate. A special involute grove geometry at the bottom of the tool could further improve the cladding. This design is depicted in figure 4.35.
    - The second possibility is a moving outer edge of the support block, similar to a combination of design 4 and 5. In this design it might be possible to avoid a cladding pin by threading the inside of the supply channel. The design with a cladding pin is in figure 4.36.

5.2 References

1. Stelt, A.A.v.d., *Friction Surface Cladding: development of a solid state cladding process*, in *Engineering Technoloy*. 2014, Univeristy of Twente. p. 165.

2. Kruth, J.P., M.C. Leu, and T. Nakagawa, *Progress in Additive Manufacturing and Rapid Prototyping.* CIRP Annals - Manufacturing Technology, 1998. **47**(2): p. 525-540.

3. Squillace, A., et al., *A comparison between FSW and TIG welding techniques: modifications of microstructure and pitting corrosion resistance in AA 2024-T3 butt joints.* Journal of Materials Processing Technology, 2004. **152**(1): p. 97-105.

4. Gandra, J., et al., *Friction surfacing - A review.* Journal of Materials Processing Technology, 2014. **214**(5): p. 1062-1093.

5. Chen, Y.C., J.C. Feng, and H.J. Liu, *Precipitate evolution in friction stir welding of 2219-T6 aluminum alloys.* Materials Characterization, 2009. **60**(6): p. 476-481.

6. Jones, M.J., et al., *Correlation between microstructure and microhardness in a friction stir welded 2024 aluminium alloy.* Scripta Materialia, 2005. **52**(8): p. 693-697.

7. Yadav, D. and R. Bauri, *Effect of friction stir processing on microstructure and mechanical properties of aluminium.* Materials Science and Engineering A, 2012. **539**: p. 85-92.

8. Khodir, S.A., T. Shibayanagi, and M. Naka, *Influence of friction stir welding parameters on microstructure and mechanical properties of AA2024-T3 aluminum alloy*, in *Ceramic Transactions*. 2007. p. 91-96.

9. Genevois, C., et al., *Quantitative investigation of precipitation and mechanical behaviour for AA2024 friction stir welds.* Acta Materialia, 2005. **53**(8): p. 2447-2458.

10. Zhang, P., S.X. Li, and Z.F. Zhang, *General relationship between strength and hardness.* Materials Science and Engineering: A, 2011. **529**(0): p. 62-73.

11. Tiryakioğlu, M., et al., *Hardness–strength relationships in the aluminum alloy 7010.* Materials Science and Engineering: A, 2015. **631**(0): p. 196-200.

12. Krishnan, K.N., *On the formation of onion rings in friction stir welds.* Materials Science and Engineering: A, 2002. **327**(2): p. 246-251.

13. Li, W., et al., *Pinless friction stir welding of AA2024-T3 joint and its failure modes.* Transactions of Tianjin University, 2014. **20**(6): p. 439-443.

14. Gandra, J., et al. *Influence of process parameters in the friction surfacing of AA 6082-T6 over AA 2024-T3*. in *Procedia CIRP*. 2013.

15. Dilip, J.J.S., et al., *Use of friction surfacing for additive manufacturing.* Materials and Manufacturing Processes, 2013. **28**(2): p. 189-194.

16. Koopman, A.J., *Analysis tools for the design of aluminium dies*, in *Applied Mechanics*. 2008, Univeristy of Twente: Enschede. p. 164.

17. Nadan, R., *Computational modeling of heat transfer and visco-plastic flow in friction stir welding*, in *Materials Science and Engineering*. 2008, The Pennsylvania State Univeristy: December 2008. p. 196.

18. *COMSOL Multiphysics* in *Version 4.4*. COMSOL, Inc.: Burlington, MA.

19. COMSOL, i. *Fluid-Structure Interaction in Aluminum Extrusion*. Available from: http://www.comsol.com/model/fluid-structure-interaction-in-aluminum-extrusion-4386.

20. COMSOL, i. *Friction Stir Welding*. Available from: http://www.comsol.com/model/friction-stir-welding-of-an-aluminum-plate-461.

21. M. Schikorra, L.D., L. Tomesani, and A.E. Tekkaya, *The Extrusion Benchmark 2007*, in *Proceedings of the Extrusion Workshop 2007 and 2nd Extrusion Benchmark Conference*. 2007: Bologna, Italy.

22. Rezaei Ashtiani, H.R., M.H. Parsa, and H. Bisadi, *Constitutive equations for elevated temperature flow behavior of commercial purity aluminum.* Materials Science and Engineering: A, 2012. **545**(0): p. 61-67.

23. Li, W., et al., *Numerical Analysis of Joint Temperature Evolution During Friction Stir Welding Based on Sticking Contact.* Journal of Materials Engineering and Performance, 2012. **21**(9): p. 1849-1856.

5.3 Nomenclature

Abbreviations

FS	Friction surfacing
FSW	Friction stir welding
FSC	Friction surface cladding
AM	Additive manufacturing
AA1050	Commercially pure AA1050 aluminum alloy
AA2024	AA2024-T351 aluminum alloy
AA6262	AA6262-T9 aluminum alloy
RS	Retreating side (of a clad layer)
AS	Advancing side (of a clad layer)

Symbols

Process parameters

ϕ	Tilt angle of the cladding tool
Ω	Rotation speed of the cladding tool
h_0	Tool gap between the cladding tool and the substrate
v_f	Clad feet rate
v_t	Substrate translation speed

Zener-Holloman parameter

T	Temperature at the node
$\dot{\gamma}$	Shear rate at the node
Z	Zenner-Holloman parameter
η	Dynamic viscosity
Q	Activation energy of the process
n	Experimental determined material constant
A	Experimental determined material constant
α	Experimental determined material constant
R	Gas constant

6 Appendix

Appendix A: Dimensions of the sample plate

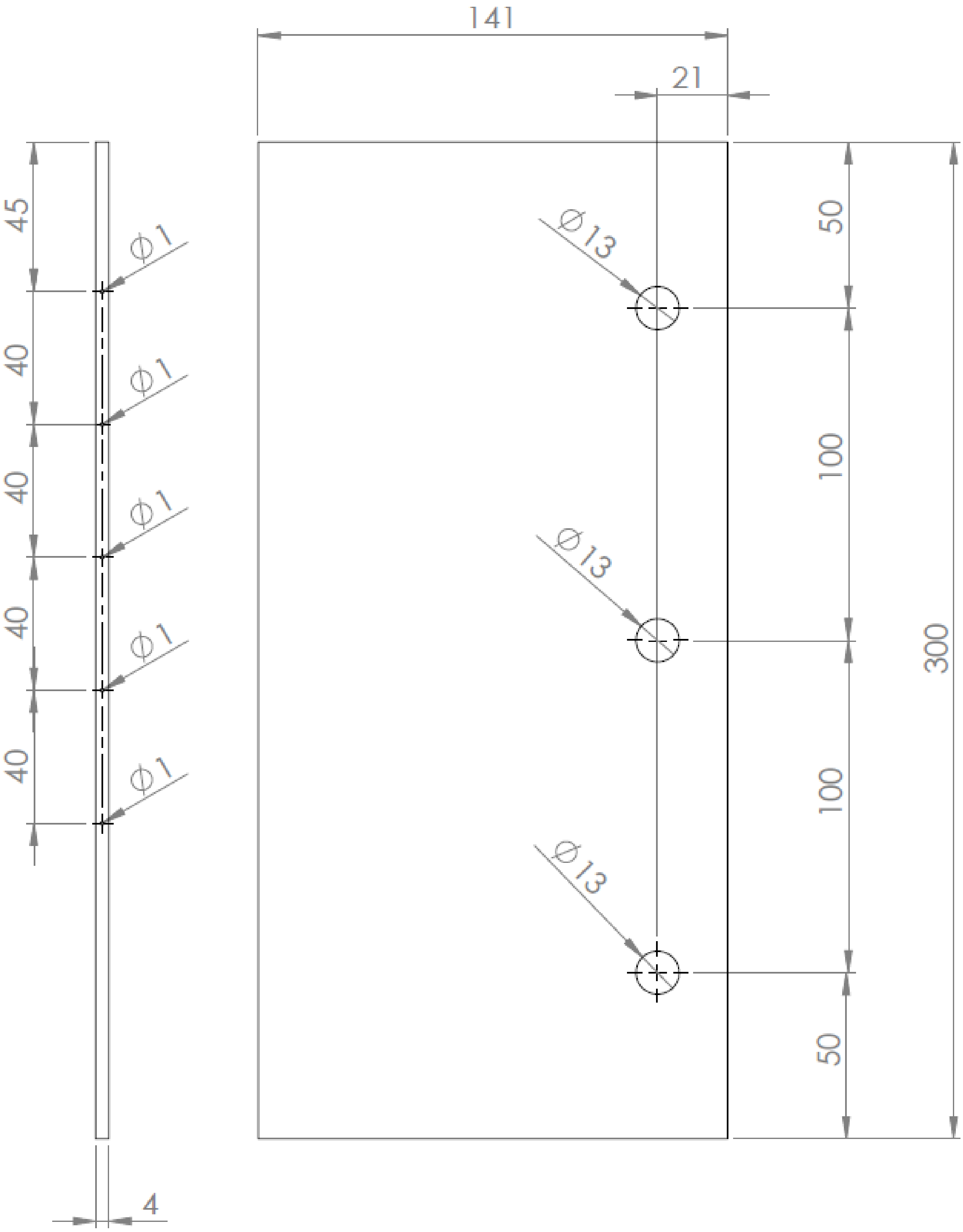

Appendix B: Results of Experiment 0

Experiment 0, the single clad layer

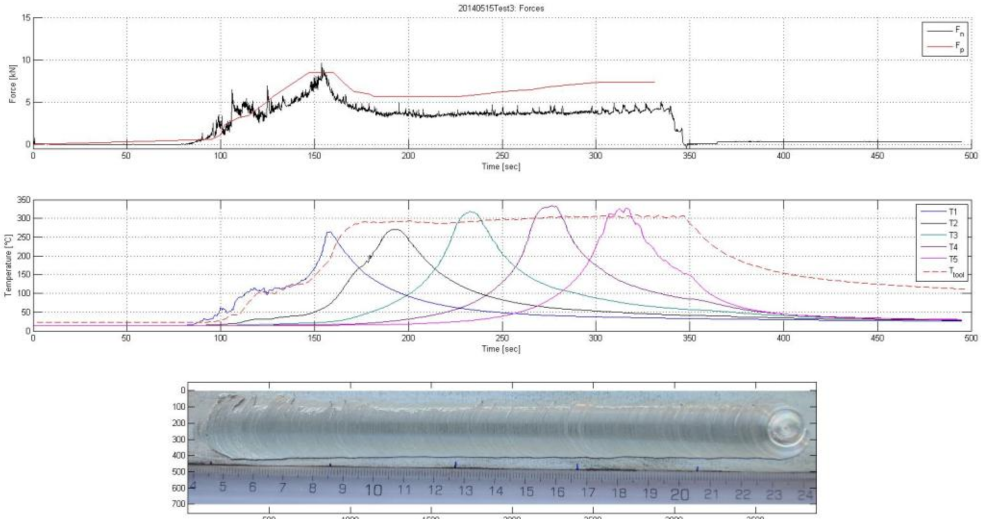

Experiment 0, hardness profile perpendicular to the cladding direction, taken at the point of the third thermocouple:

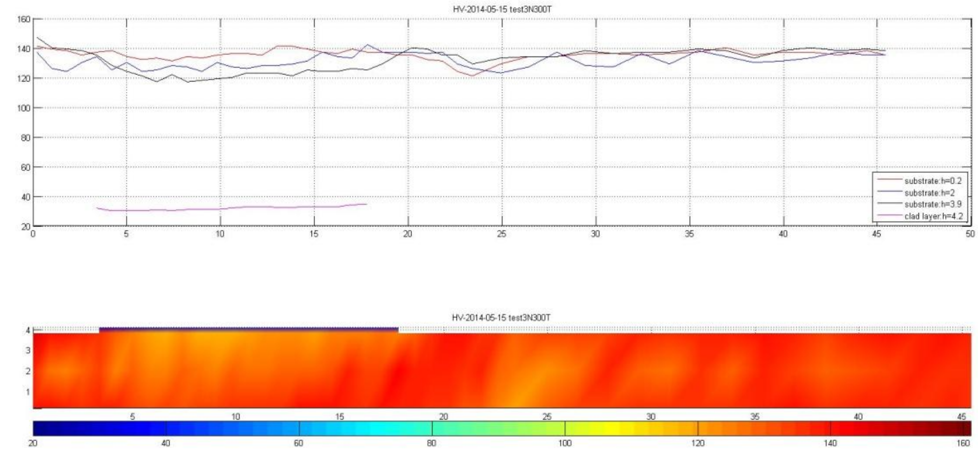

Appendix C: Results of Experiment 1.1

Experiment 1, first cladding row

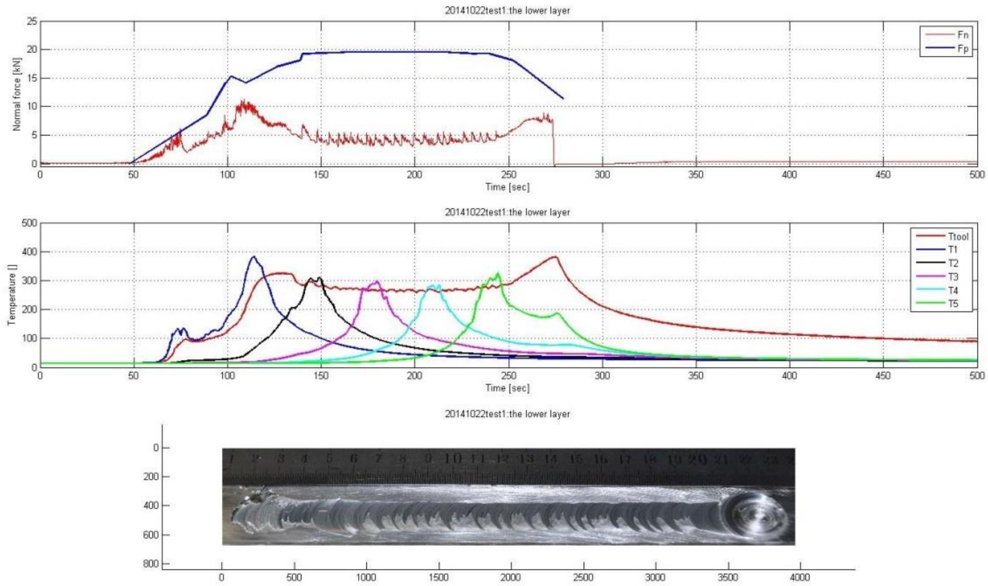

Experiment 1, second cladding row

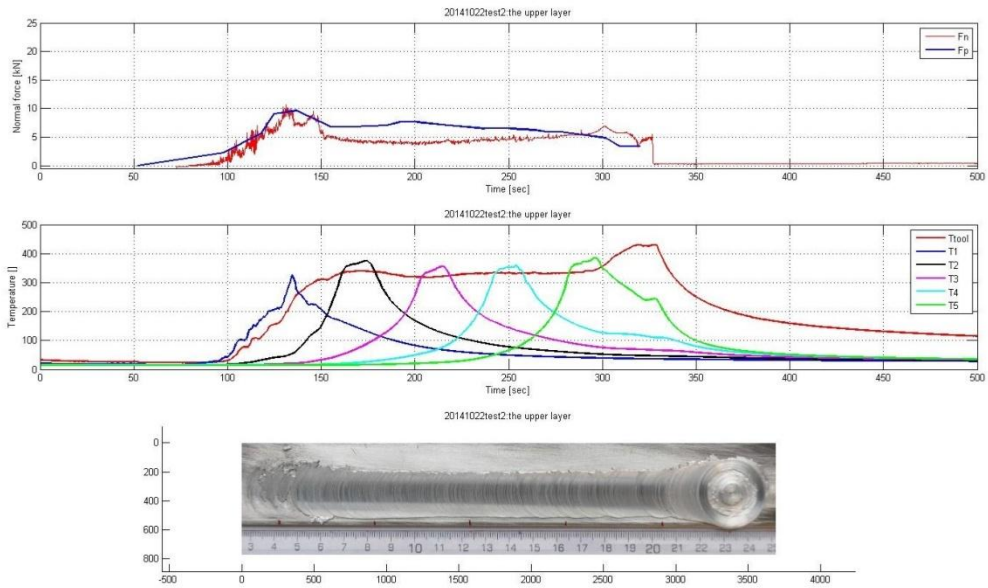

Cutting profile:

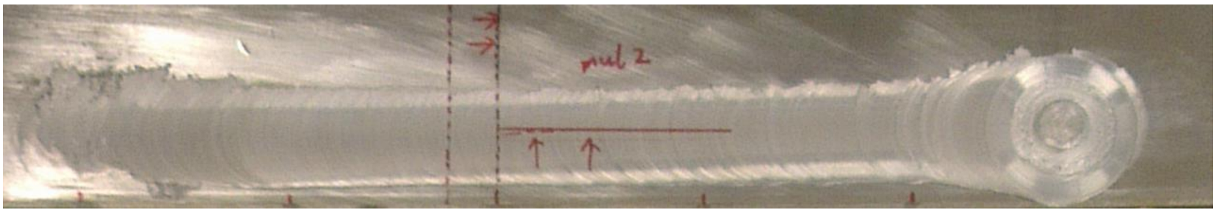

Experiment 1, first harness profile, perpendicular to the cladding direction

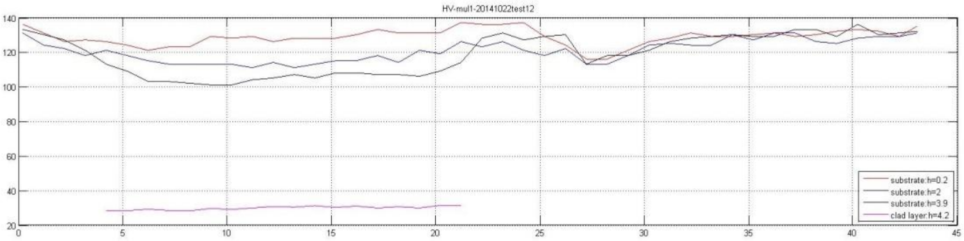

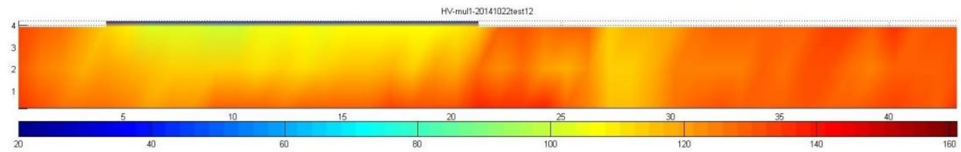

Experiment 1, second hardness profile, alongside the cladding direction

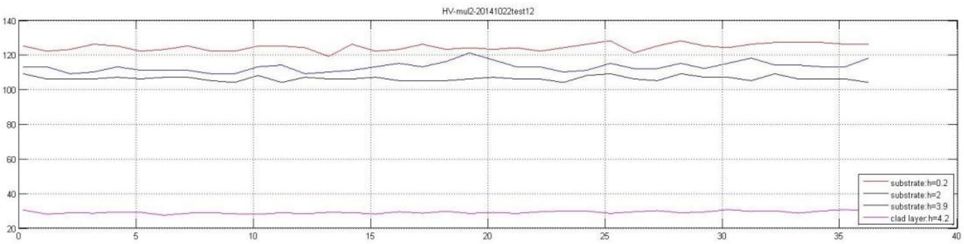

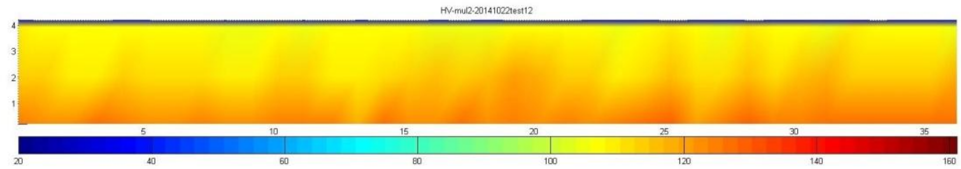

Appendix D: Results of Experiment 1.2

Experiment 2, first cladding row

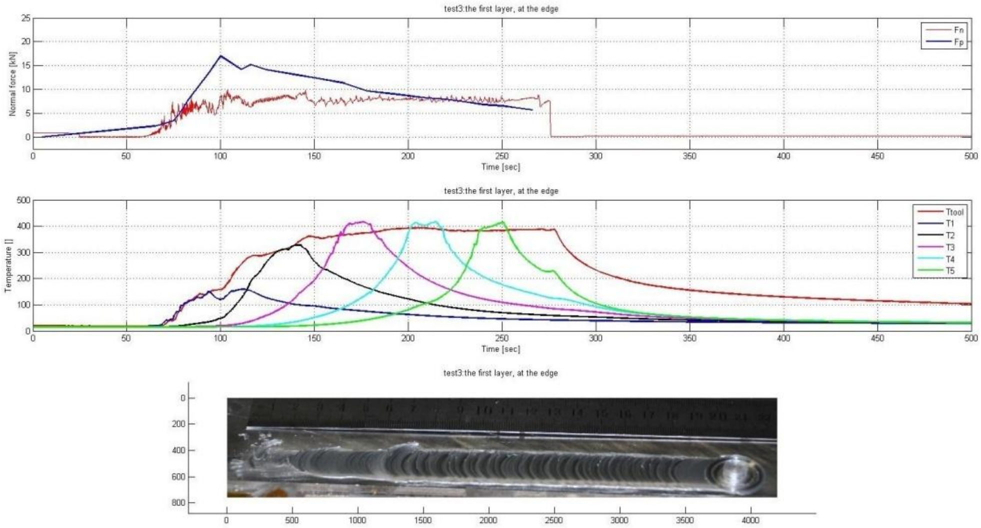

Experiment 2, second cladding row

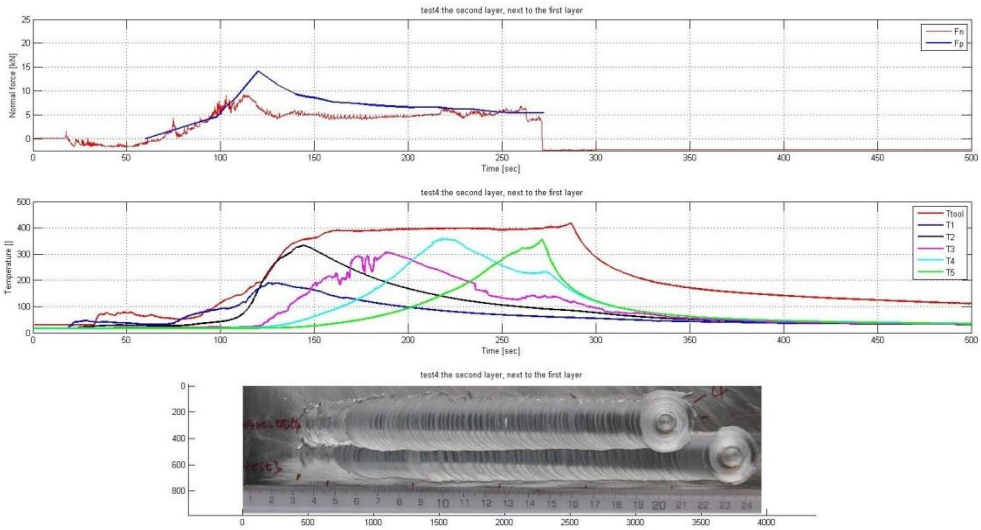

Cutting profile:

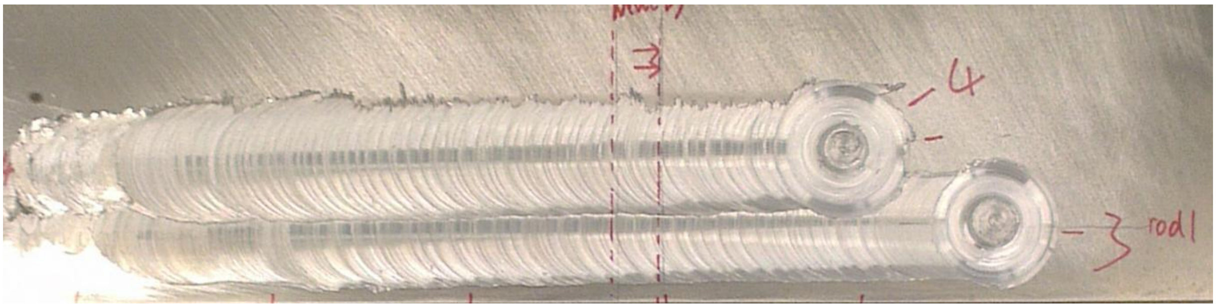

Experiment 2, first harness profile, perpendicular to the cladding direction

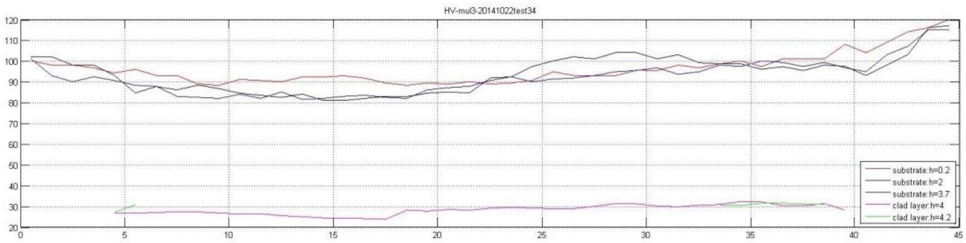

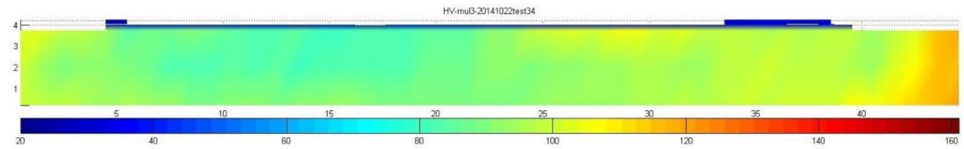

Appendix E: Results of Experiment 1.3

Attempt 1:

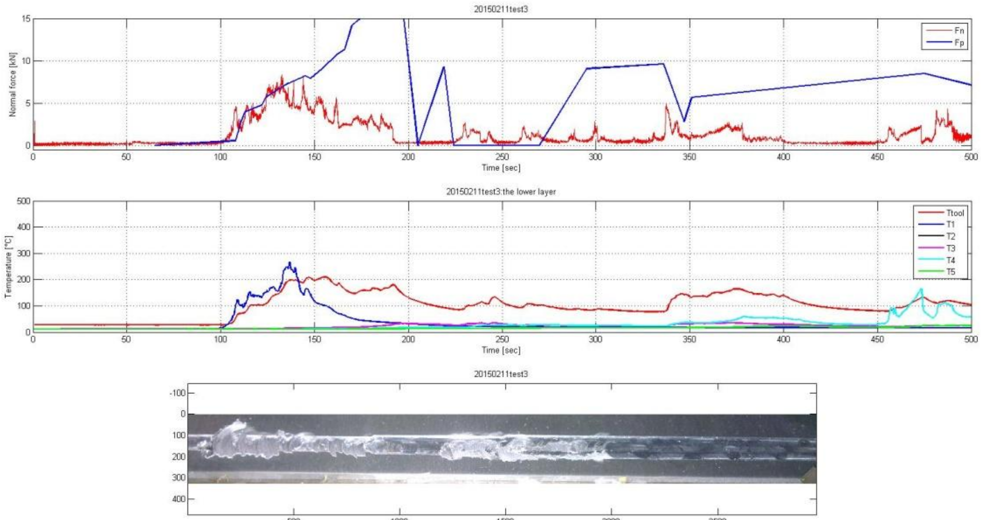

Attempt 2:

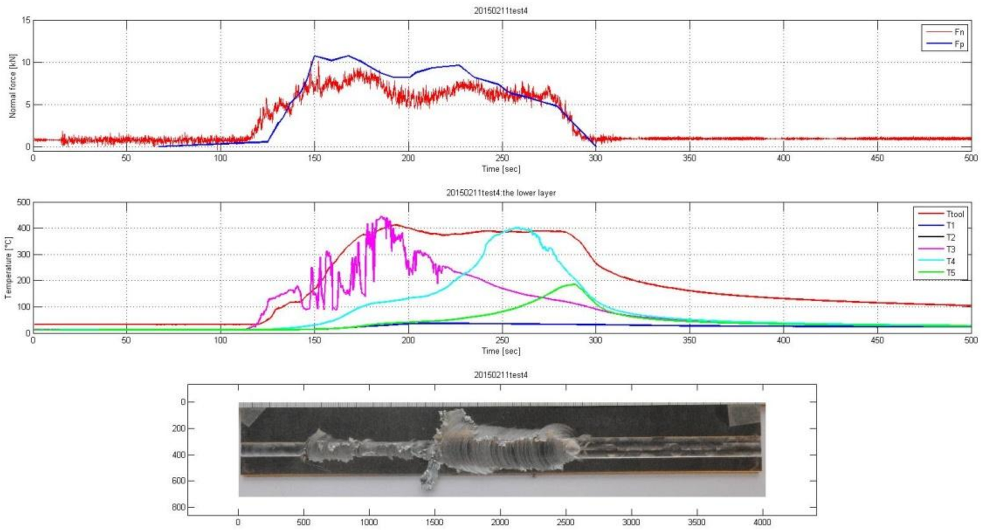

Cutting profile:

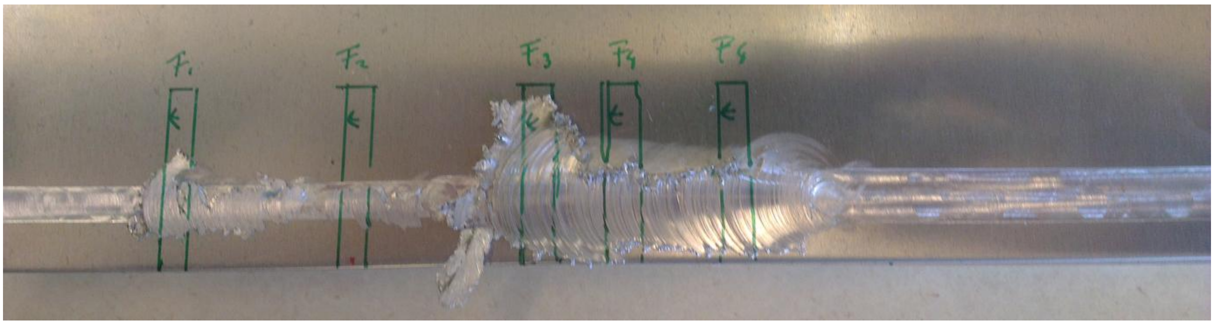

Hardness profile F1:

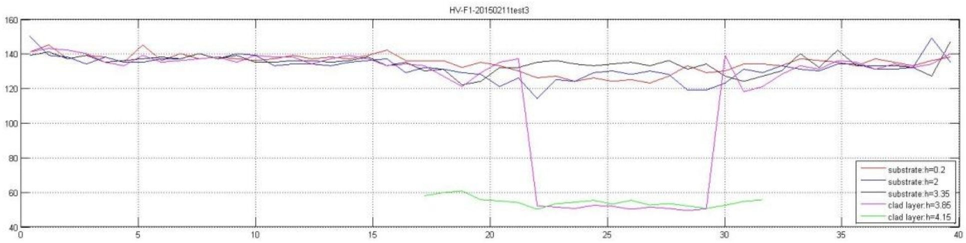

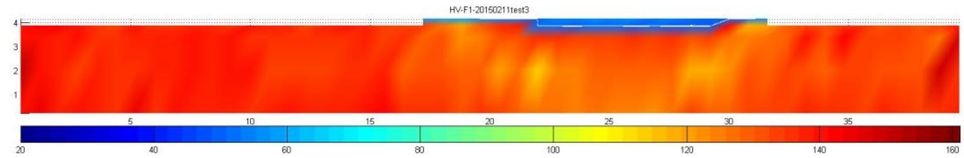

Hardness profile F2:

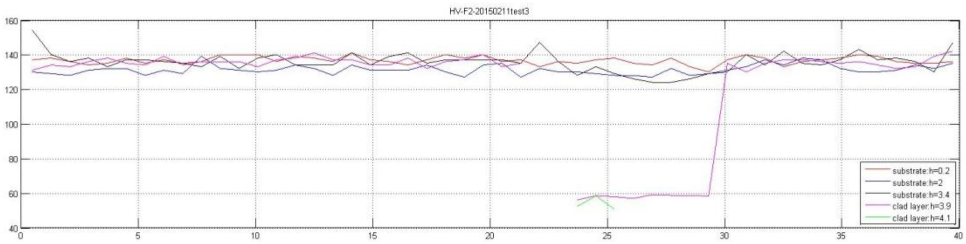

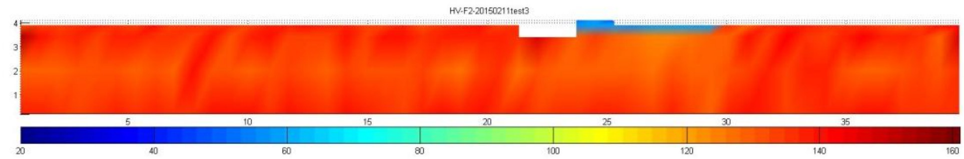

Hardness profile F3:

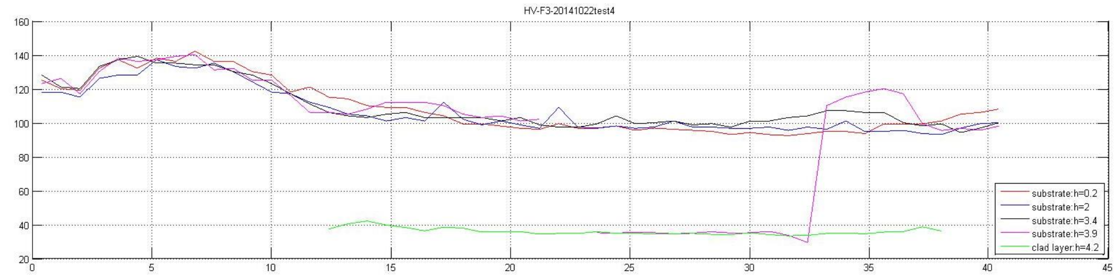

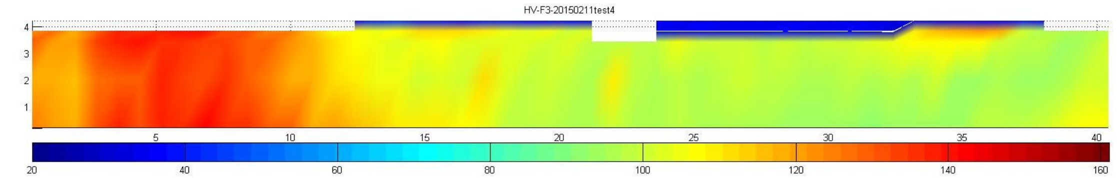

Hardness profile F4:

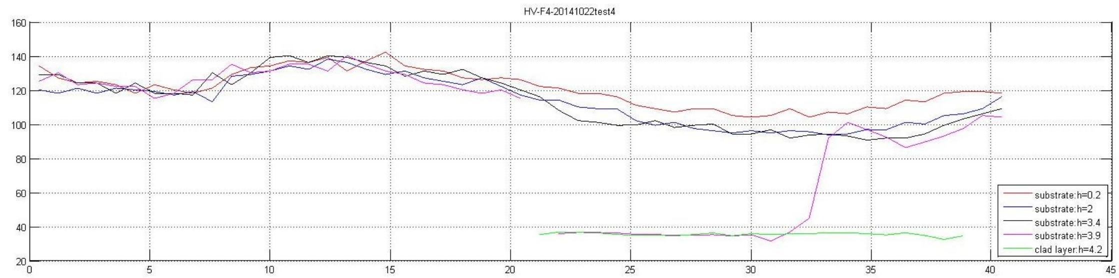

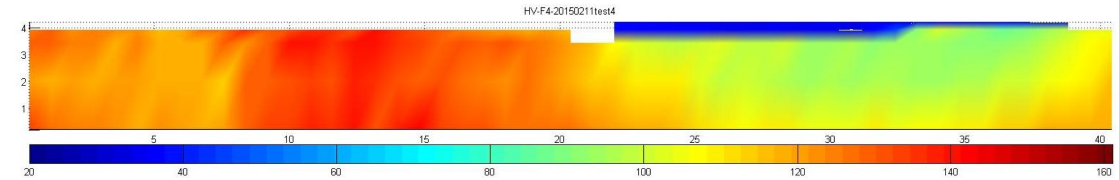

Hardness profile F5:

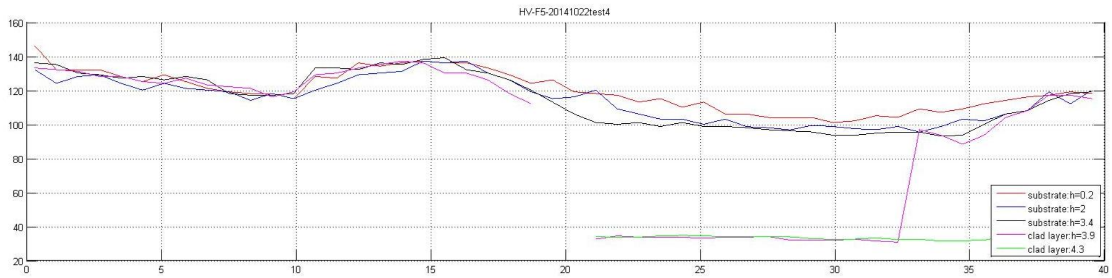

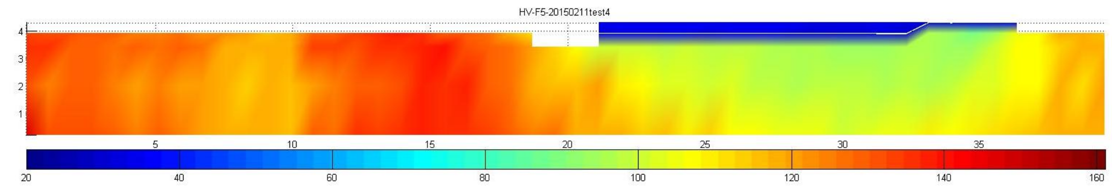

Appendix F: Results of Experiment 1.4

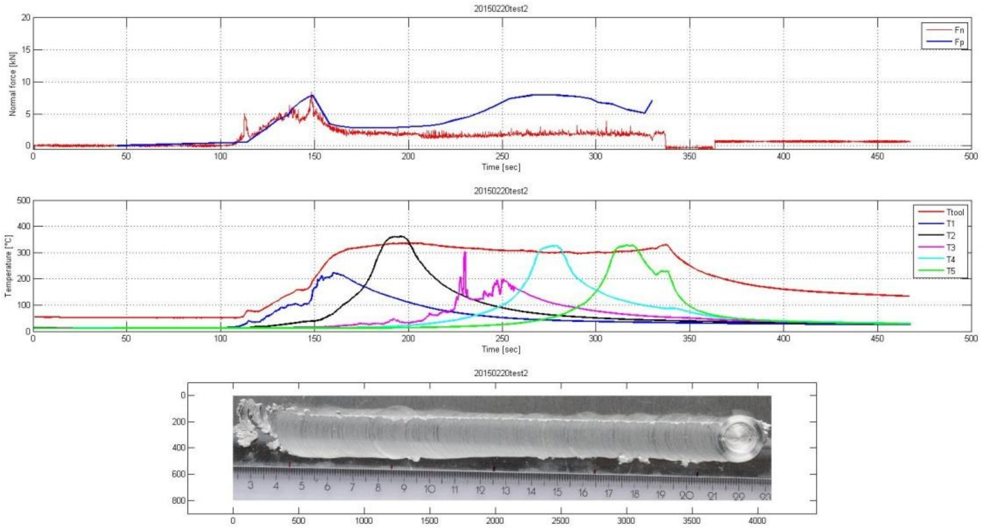

Cutting profile of the cross sections:

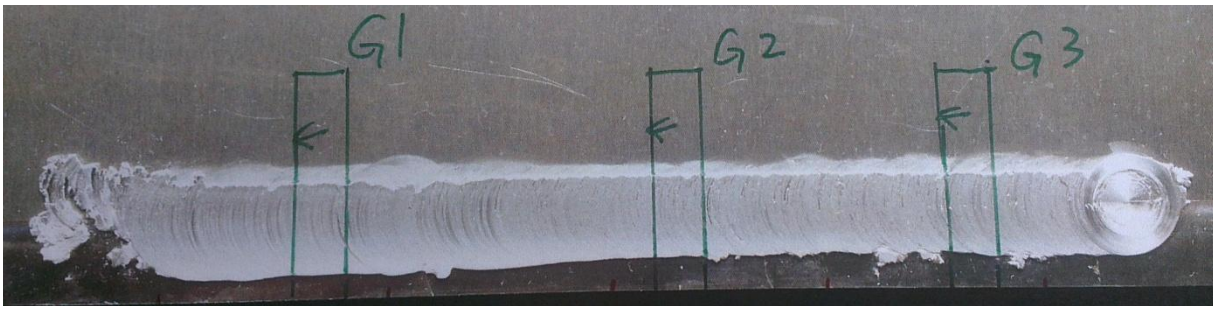

Hardness cross section G1

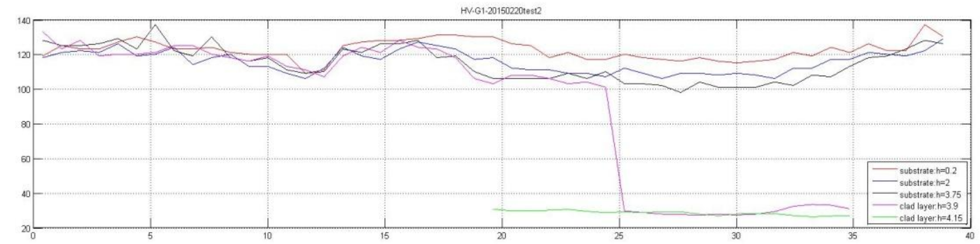

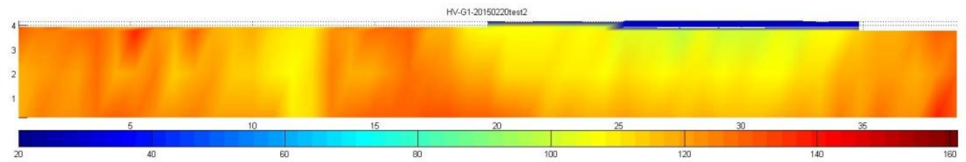

Hardness cross section G2

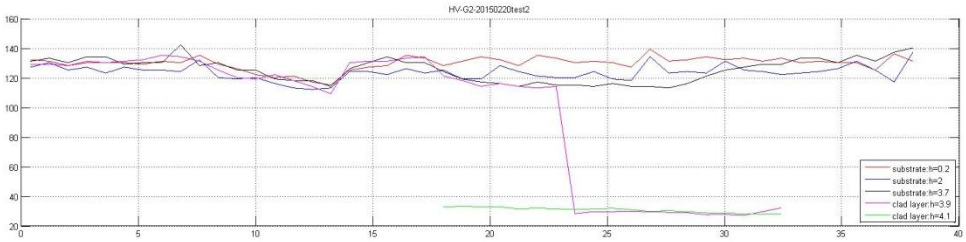

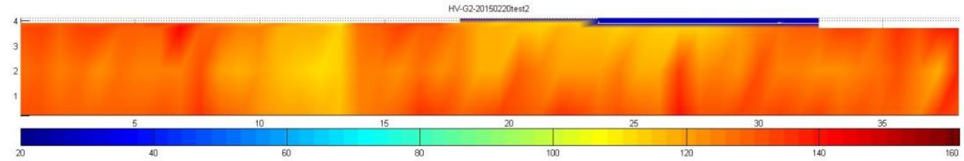

Hardness cross section G3

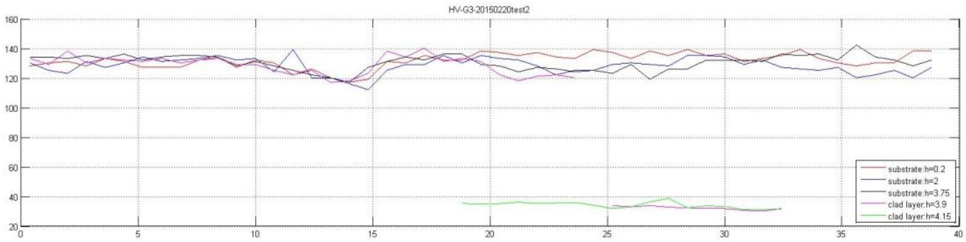

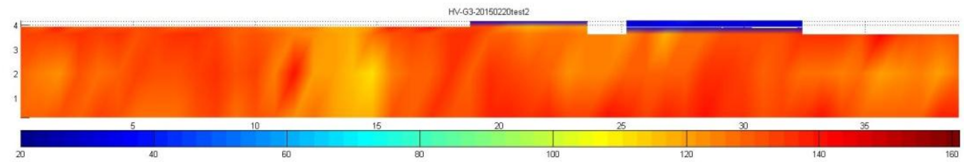

Appendix G: Results of Experiment 1.5

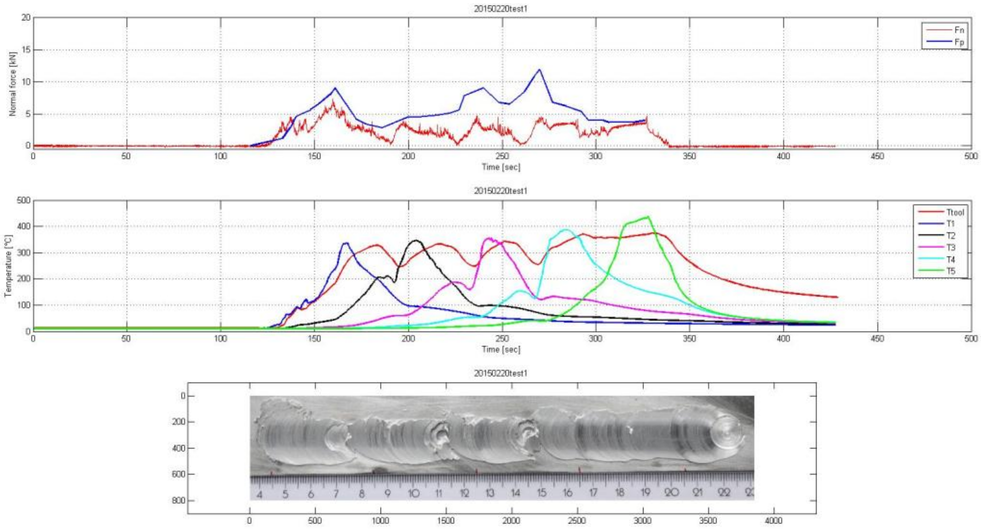

Cutting profile for the cross sections:

Hardness profile H1:

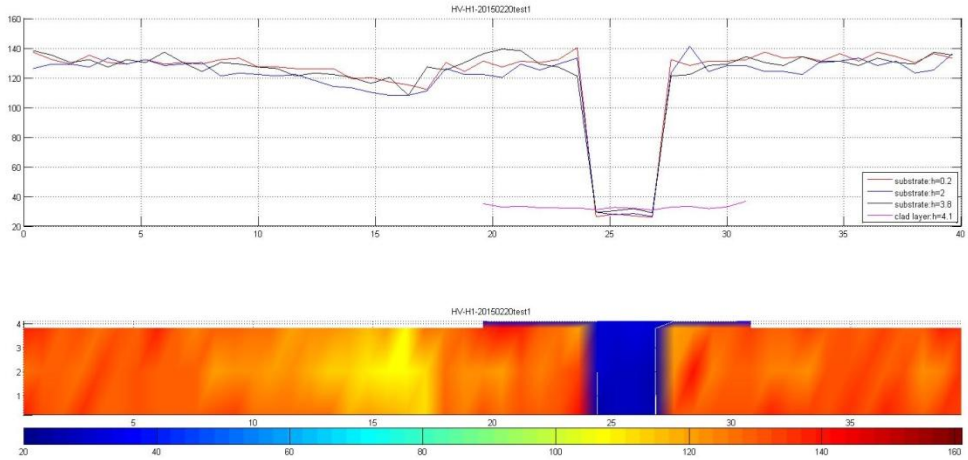

Hardness profile H2:

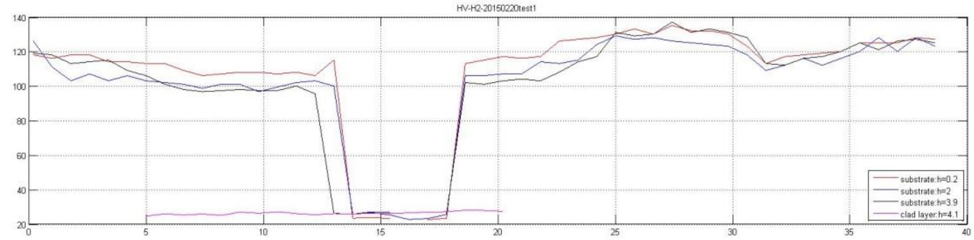

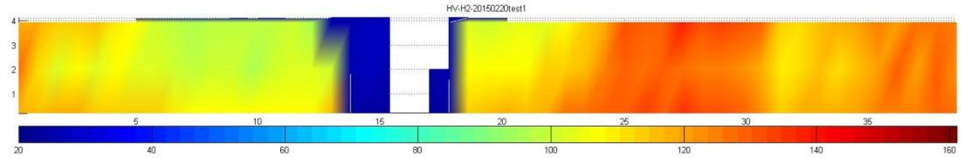

Appendix H: Results of Experiment 1.3-a

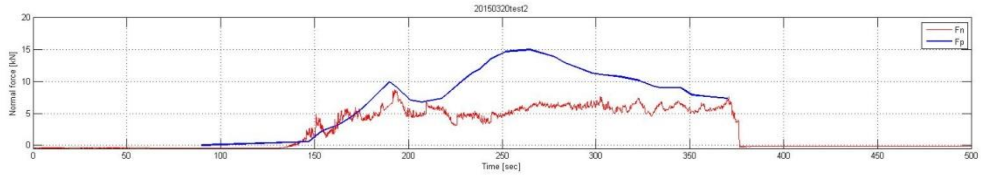

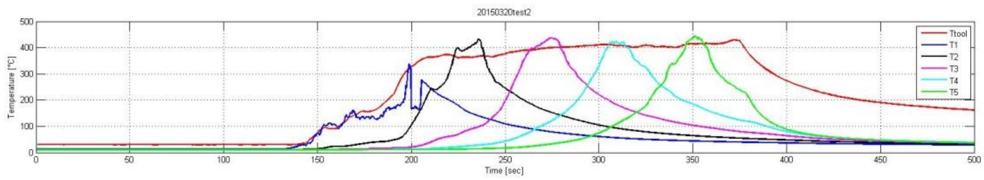

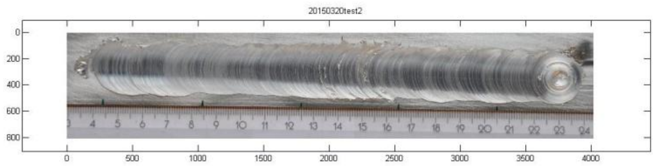

Cutting profile for the cross sections:

Left red line hardness profile

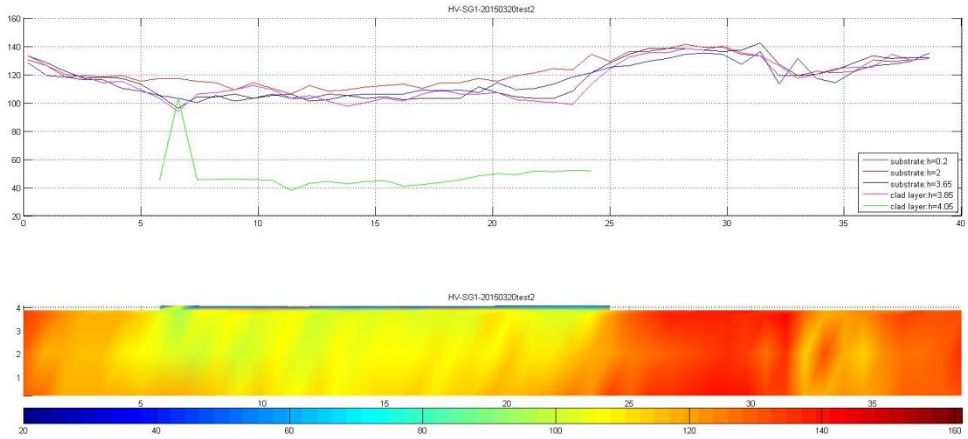

Middle red line hardness profile

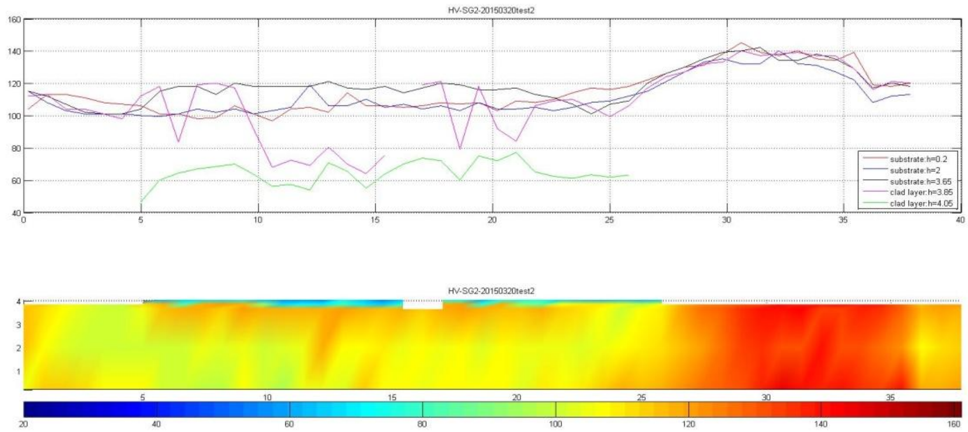

Right red line hardness profile

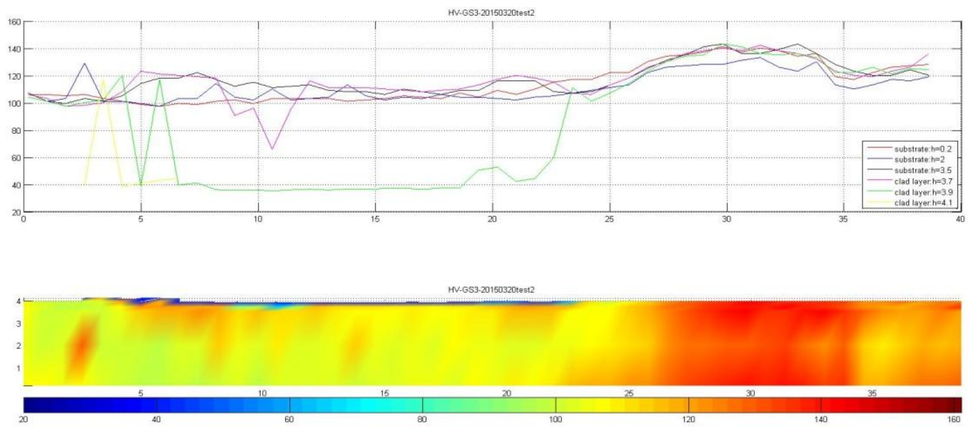

Appendix I: Results of Experiment 1.3-b

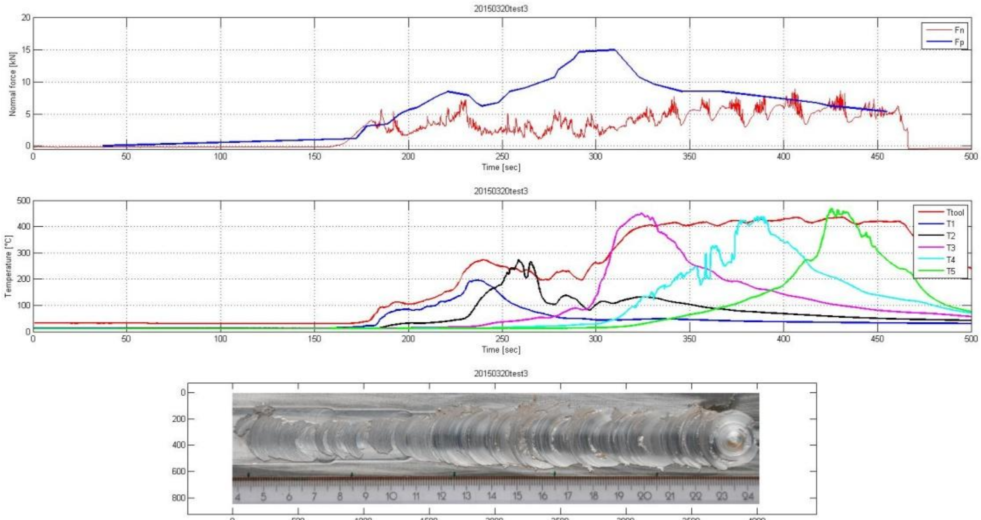

Appendix J: Results of Experiment 1.5-a

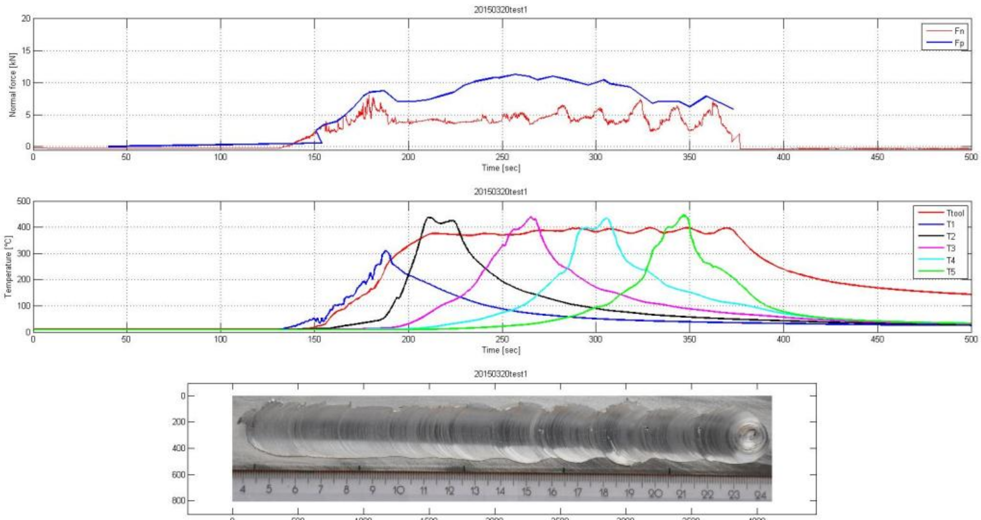

Appendix K: Results of Experiment 2.1

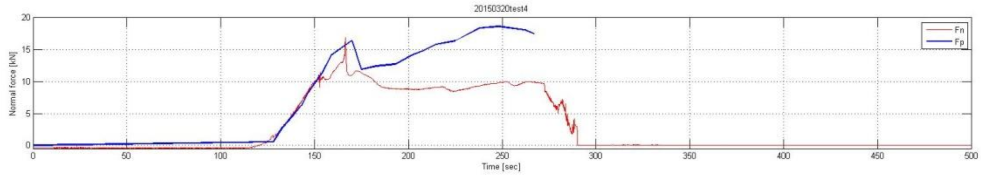

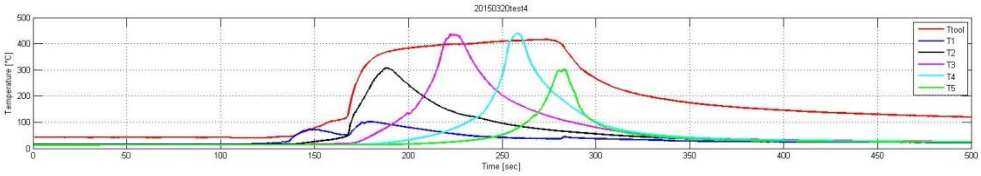

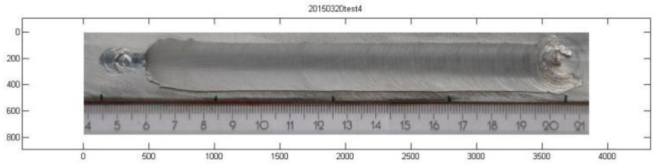

Hardness profile, taken at centimeter 7.5, perpendicular to the cladding direction:

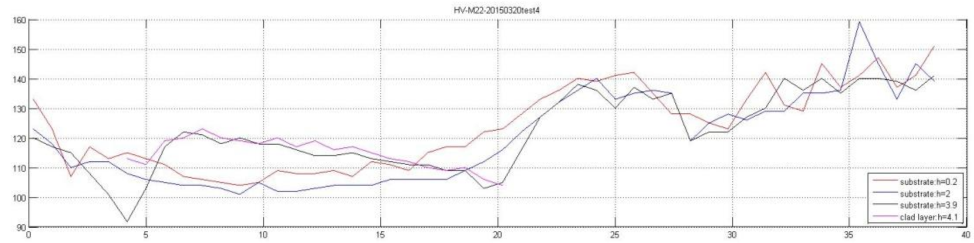

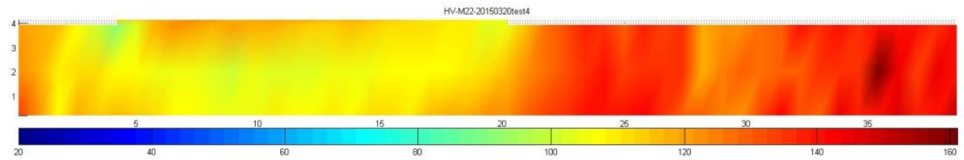

Appendix L: Results of Experiment 2.2

First layer:

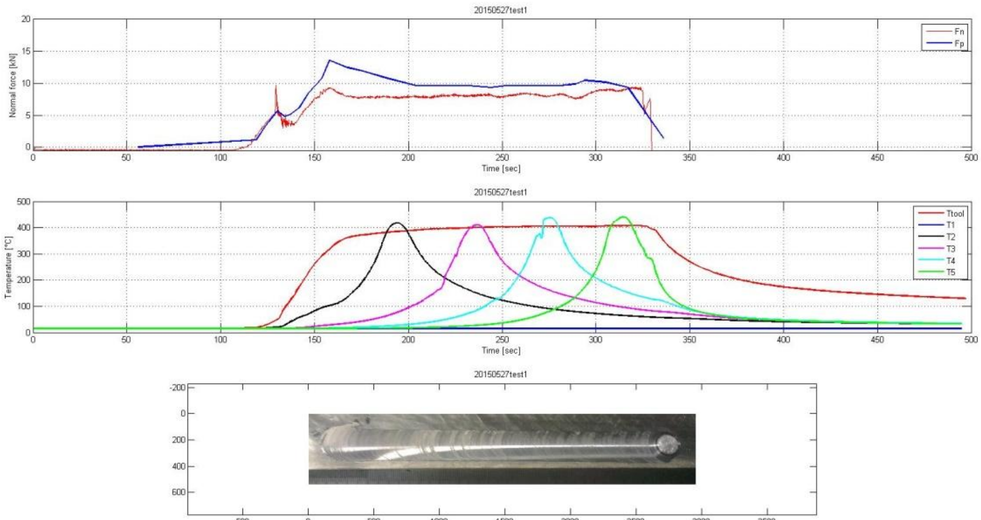

Second layer:

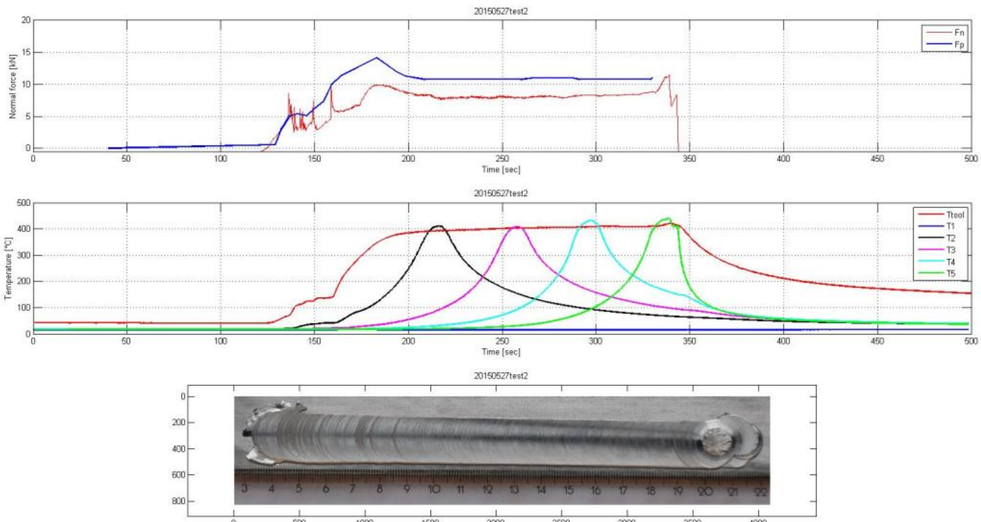

Rotation speed of the first and second run, vertical the rotation speed in [rpm], the horizontal the time in [s]:

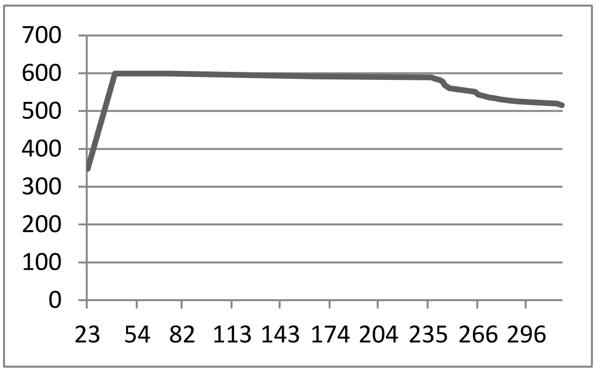

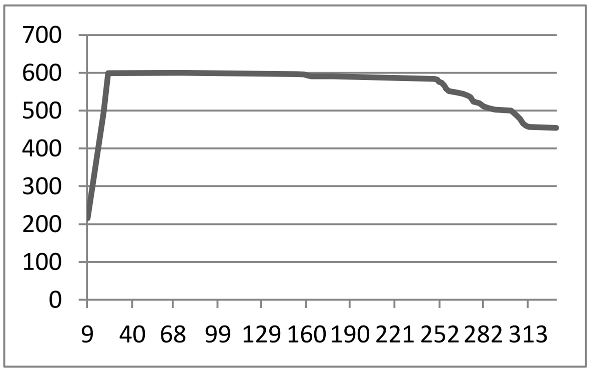

Cutting profile for the cross sections:

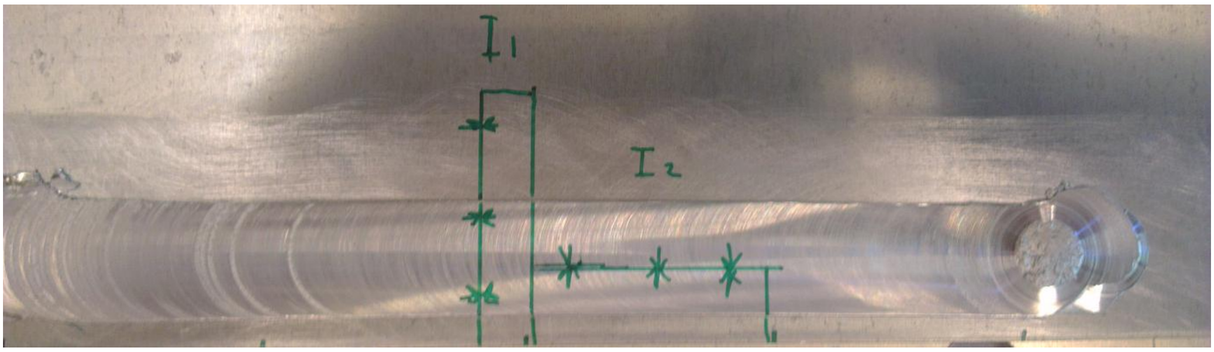

Hardness profile at the cross section I1:

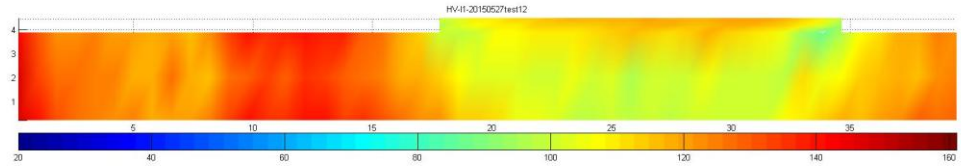

Hardness profile at the cross section I2:

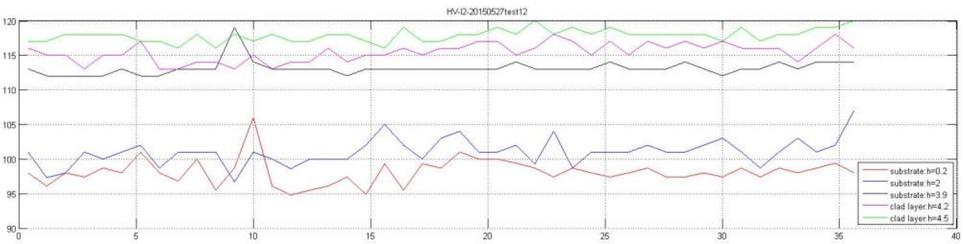

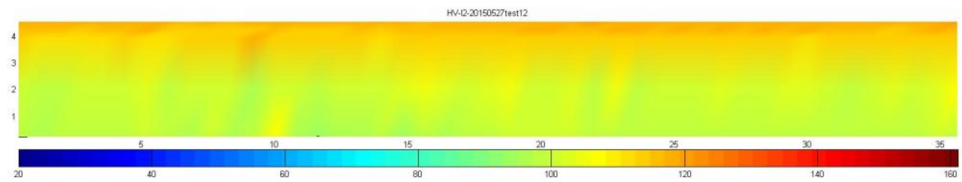

Appendix M: Results of Experiment 2.3

First (bottom) layer:

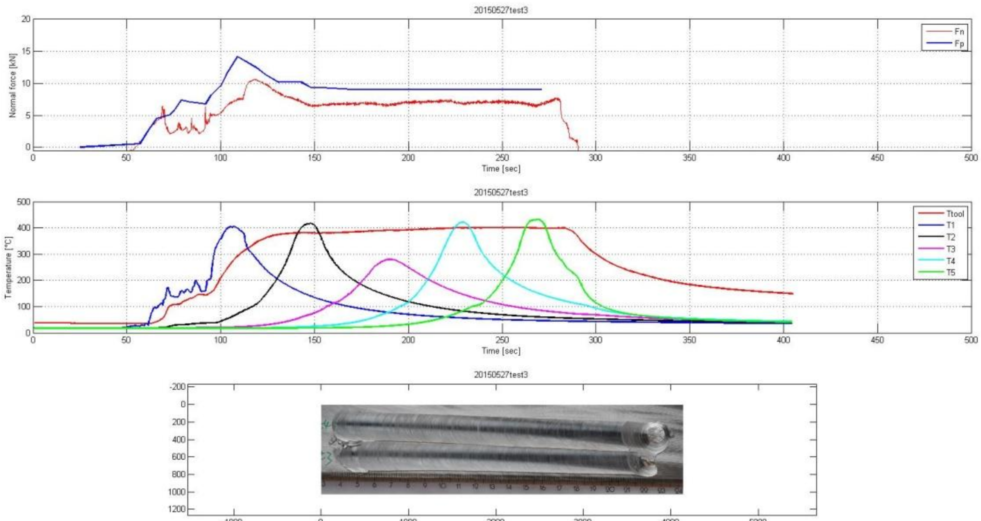

Second (upper) layer:

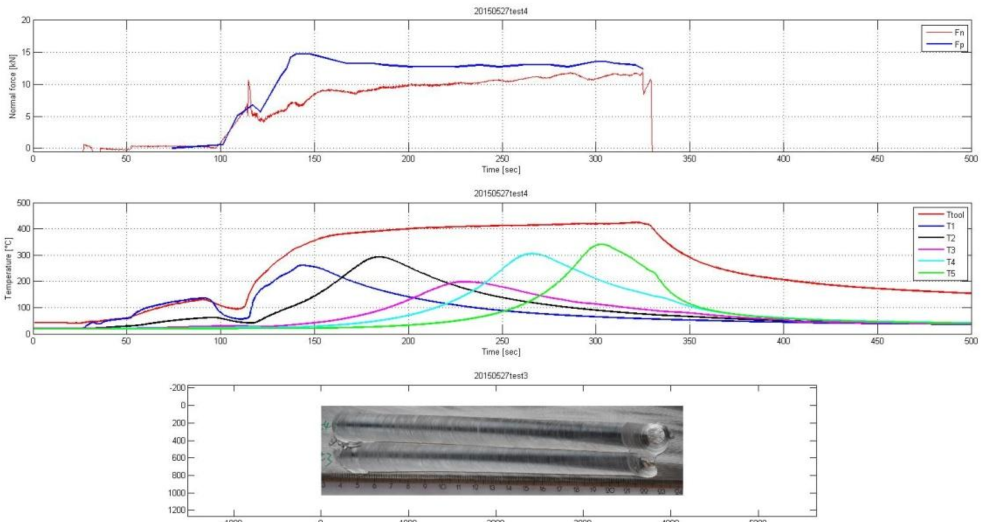

Rotation speed of the first and second run, vertical the rotation speed in [rpm], the horizontal the time in [s]:

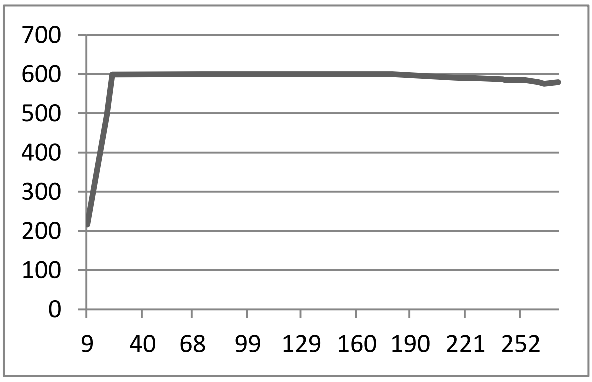

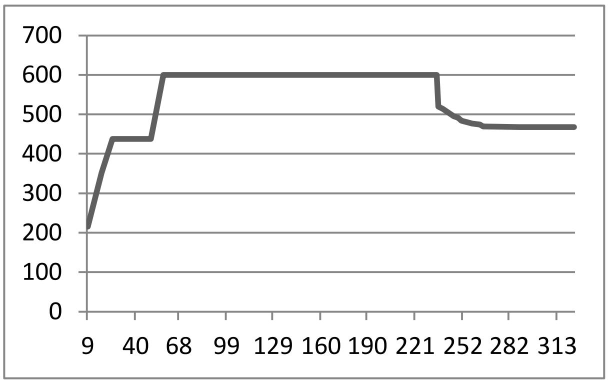

The cutting profile at the cross sections:

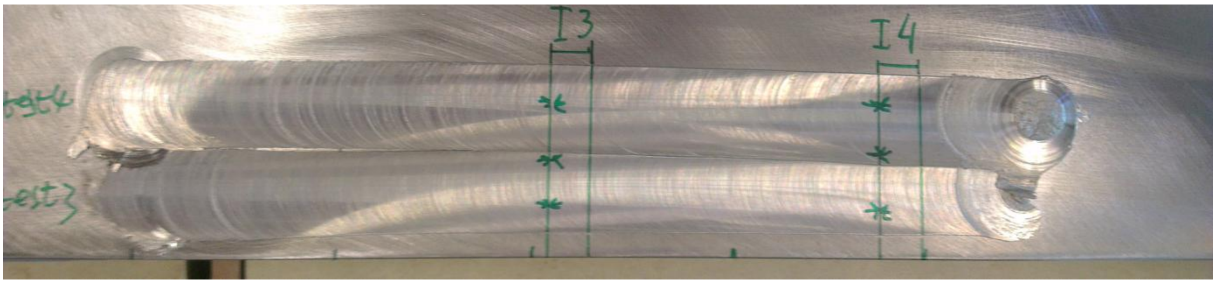

Hardness profile at cross section I3:

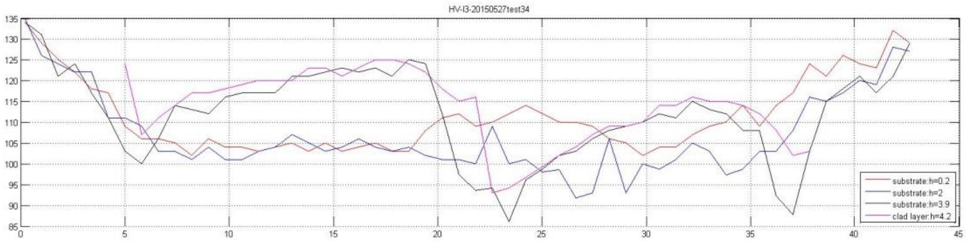

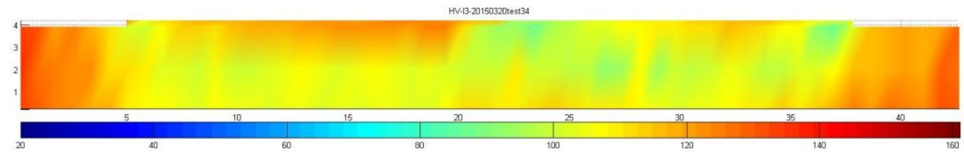

Hardness profile at cross section I4:

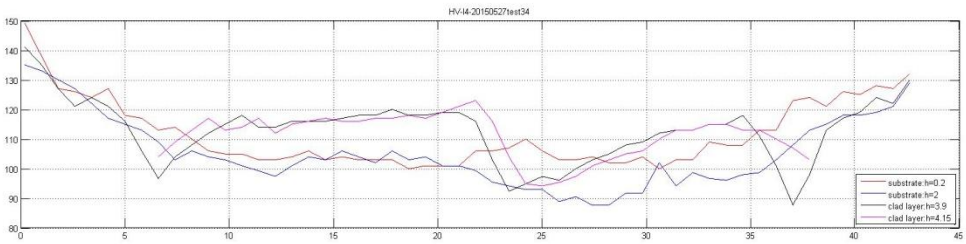

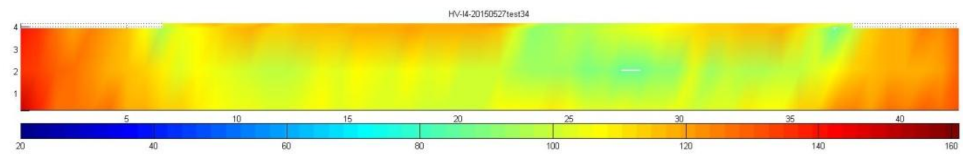

Appendix N: Results of experiments series 3.1

First experiment temperature plot:

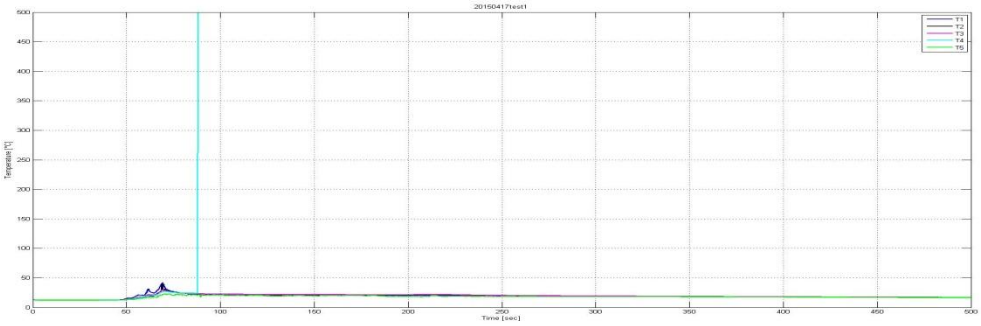

Second experiment temperature plot:

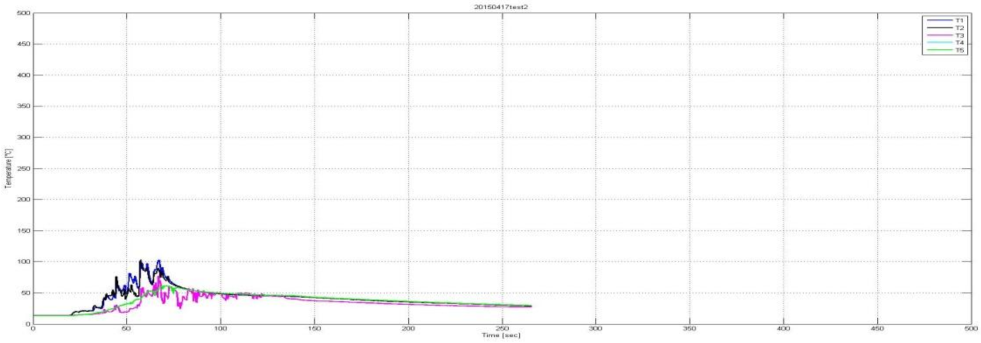

Third experiment temperature plot:

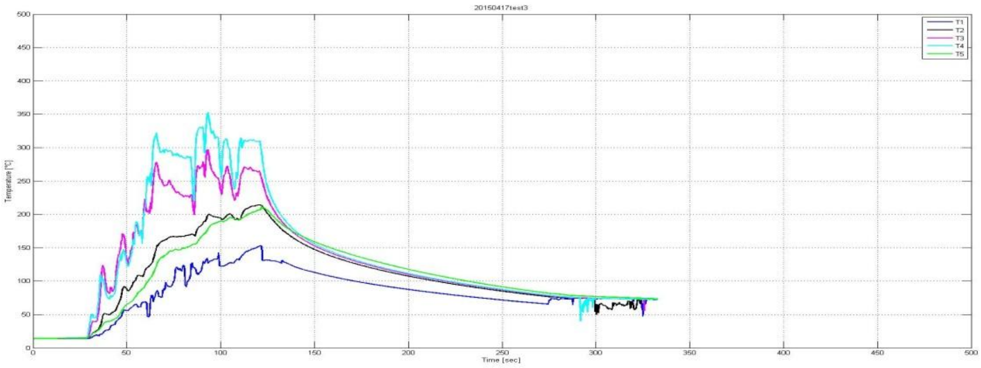

Fourth experiment temperature plot:

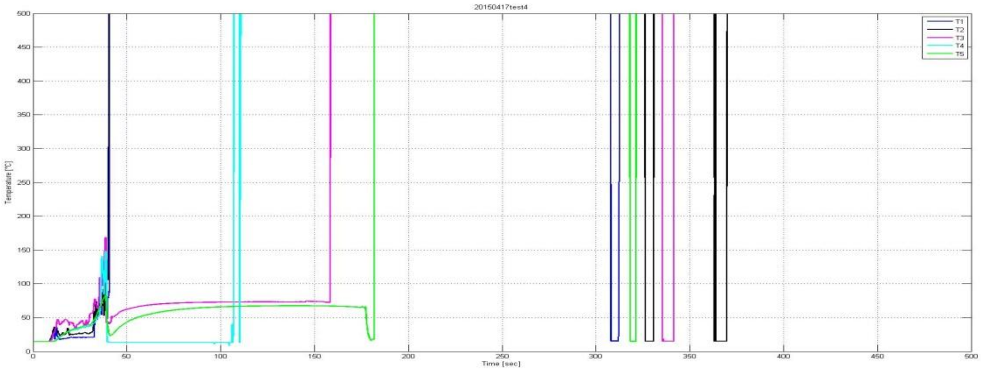

Appendix O: Results of experiments series 3.2

First experiment:

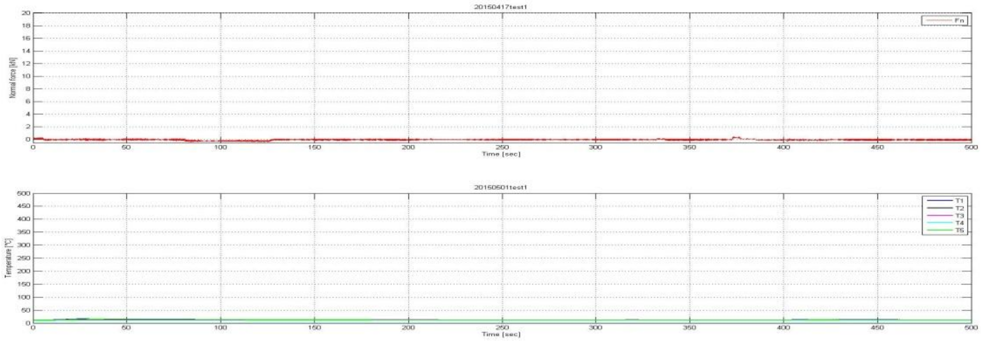

Second experiment:

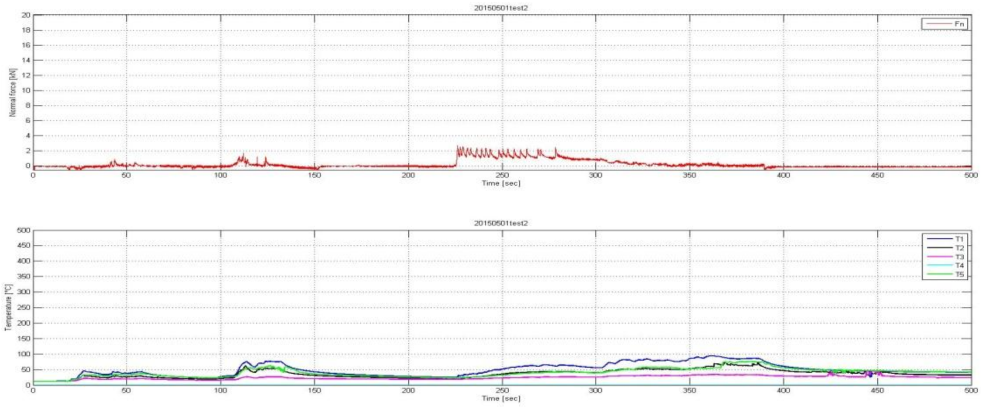

Third experiment:

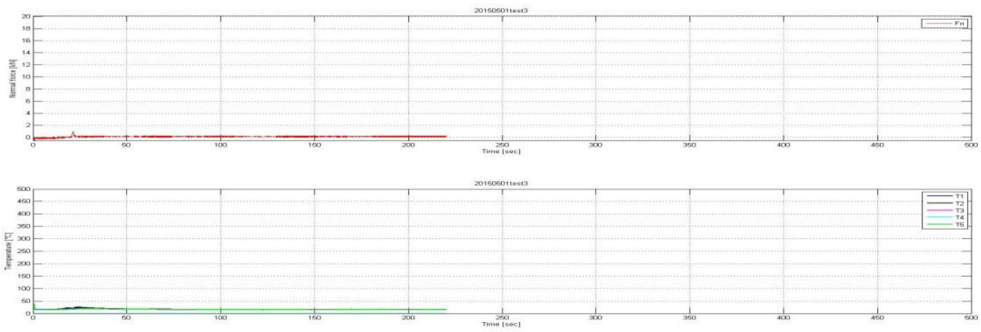

Fourth experiment:

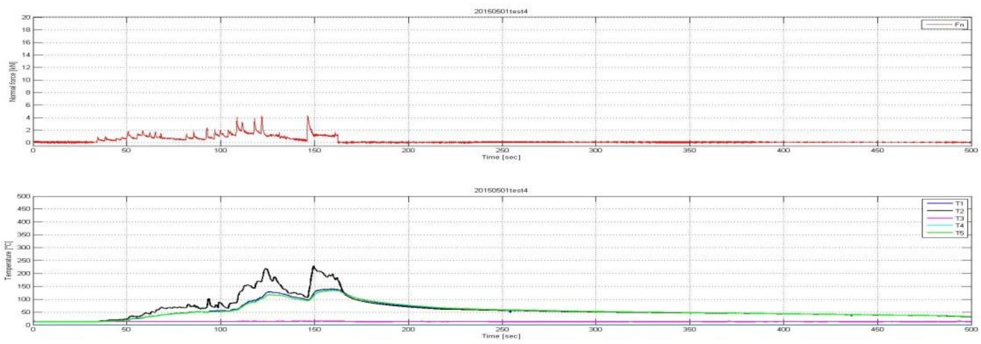

Fifth experiment:

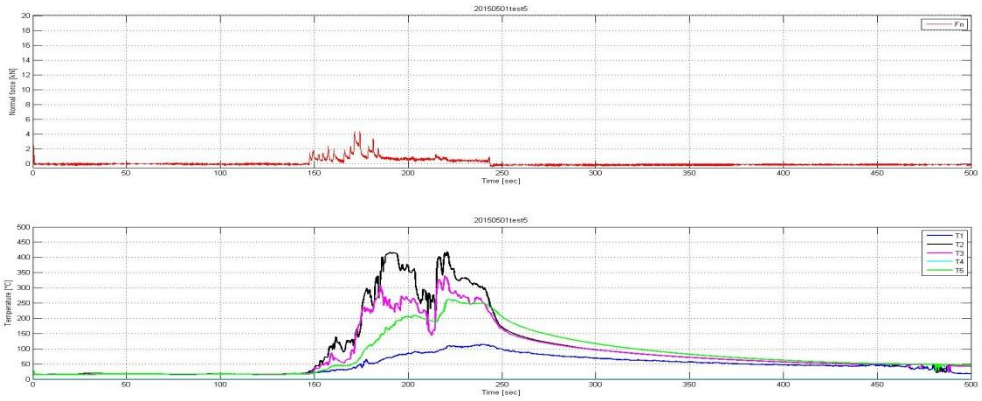

Sixth experiment:

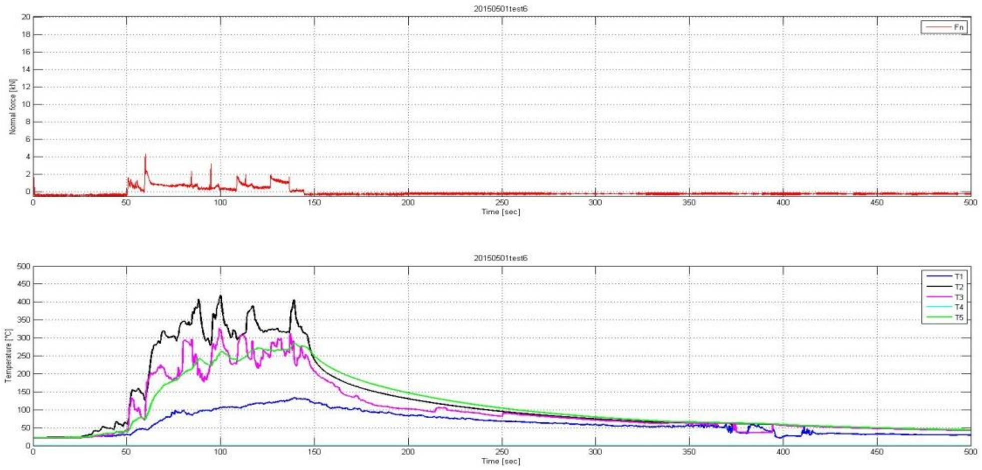

Seventh experiment:

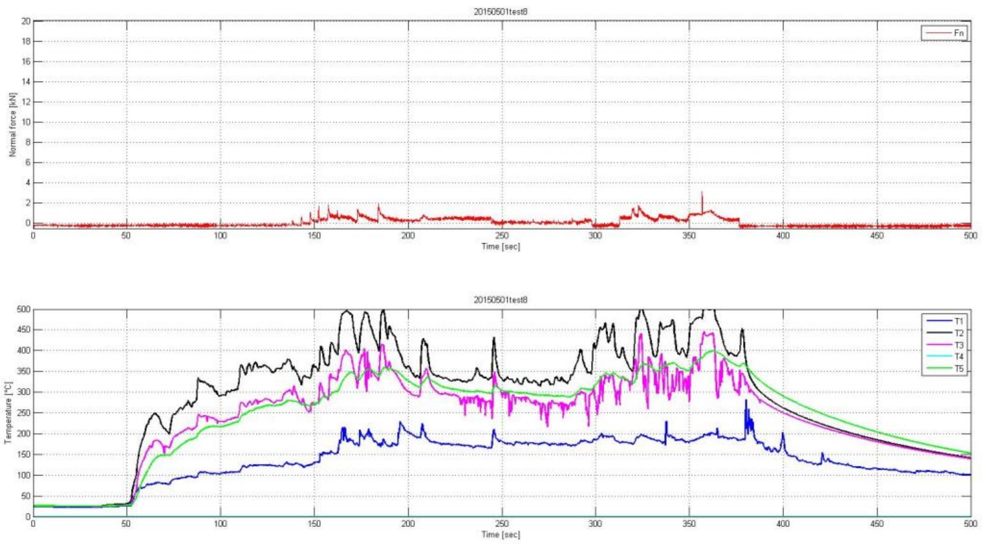

Appendix P: Results of experiments series 3.3

First experiment:

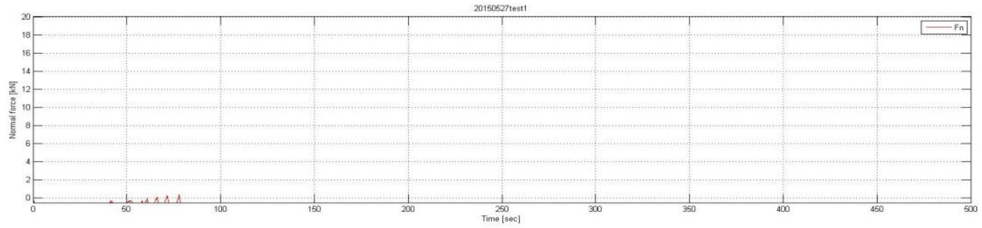

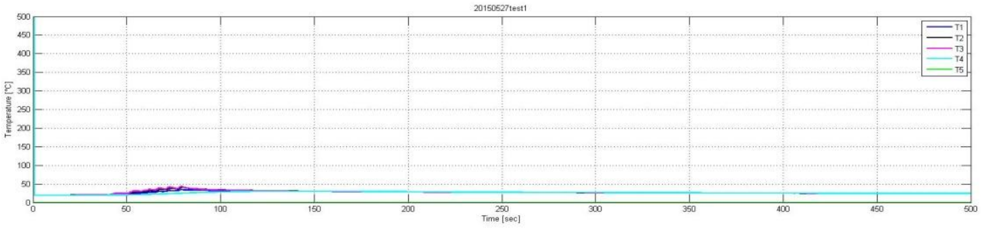

Second experiment:

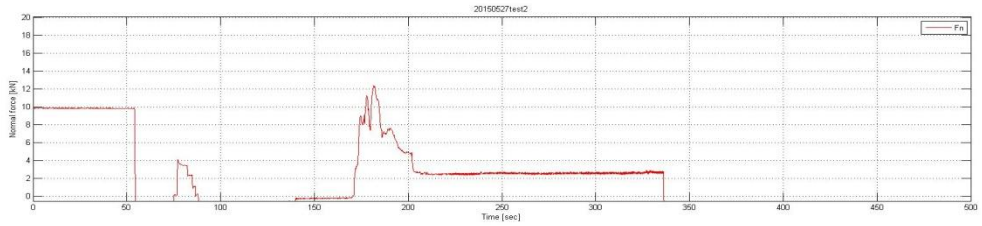

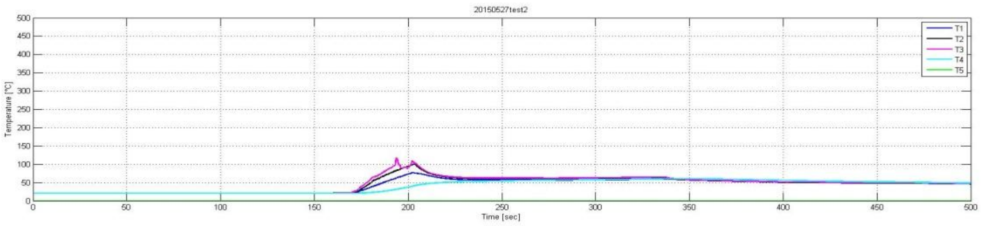

Third experiment:

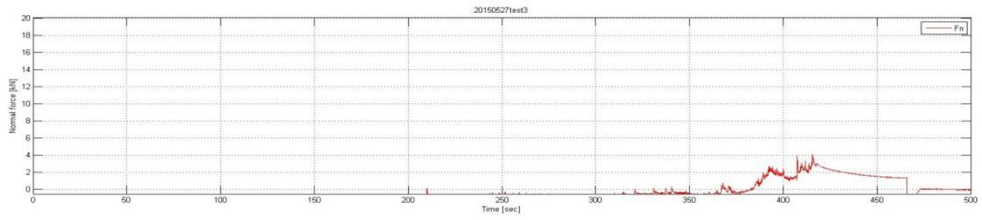

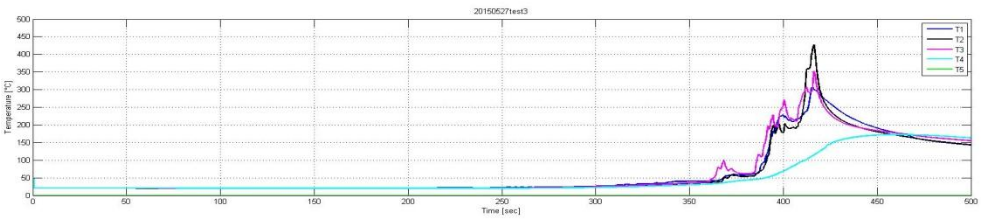

Appendix Q: Comsol interpolations

Cp2024, temperature on the horizontal axis, Cp on the vertical

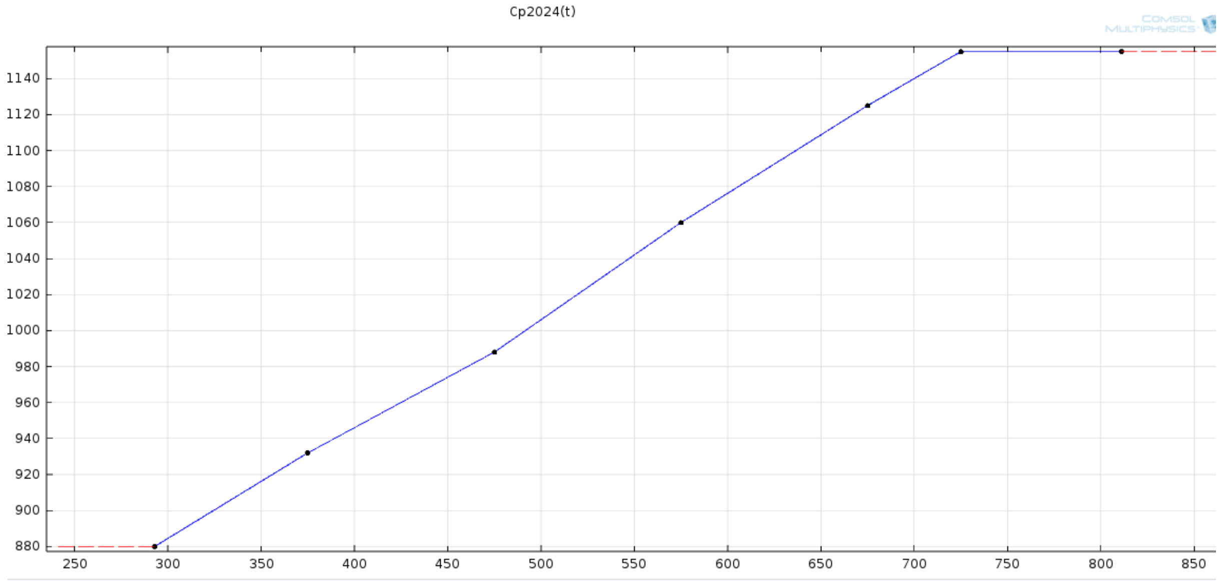

K20242, temperature on the horizontal axis, k on the vertical